Alma Mater Studiorum – Università di Bologna

Dottorato di Ricerca in Scienze Biochimiche e Biotecnologiche

Ciclo XXIX

Settore Concorsuale: 03/D1

Settore Scientifico Disciplinare: CHIM/11

Saccharomyces cerevisiae as anodic biocatalyst in microbial fuel cell: influence of redox mediator and operative conditions.

Presentata da:

Ruggero Rossi

Coordinatore Dottorato:

Chiar.mo Prof.

Santi Mario Spampinato

Relatore:

Leonardo Setti, Ph. D.

Esame finale anno 2016/2017

Abstract

Microbial fuel cells (MFCs) can generate electricity by oxidizing the organic substrates in domestic or industrial wastewater, using microorganisms as biocatalysts. The wastewater streams from the food industry based on yeasts could be directly purified and contemporary produce electricity in MFCs. However, the electron transfer mechanism between yeasts and electrodes has not been positively identified. *Saccharomyces cerevisiae* was implemented as biocatalyst in the anaerobic anodic compartment of an MFC using glucose as carbon source and methylene blue as electron mediator. Our findings showed the effect of the methylene blue on the microbial metabolism and the reversibility of the redox reaction of the shuttle mediator in the presence and the absence of a carbon source. The implementation of this reaction in an yeast catalyzed MFC showed a fast substrate consumption and a power generation up to 96 μW after 22 h of incubation was produced using oxygen as electron acceptor in the cathodic compartment. The different contribute to the cell output of the mediator concentration in the anodic compartment and of the hydrogen peroxide concentration as electron acceptor in the cathodic compartment have been studied. The biopower generation of the MFC were linked to the yeast adsorption onto the electrode surface and growing cells of *S. cerevisiae* were immobilized by inclusion techniques in cellulose acetate membrane on the surface of a graphite electrode. The rate of substrate consumption of the functionalized electrode indicated that *S. cerevisiae*, also immobilized, had a huge potential to generate electrons. Our results showed that the current and voltage output of an *S. cerevisiae* based MFC were directly correlated to the cells on the micro–environment of the electrode and to the presence of methylene blue as electron mediator. Cyclic voltammetry showed that methylene blue, after the reduction, was entrapped into the cells, enhancing the electron transfer to the electrode as an internal mediator of the cellular metabolism. The influence of the ferric reductase enzyme complex in direct electron transfer in yeast fuel cell has

been identified both in the presence and in the absence of methylene blue. *Saccharomyces cerevisiae* reduced iron outside of the cells and showed high activity in the iron(III)–EDTA reduction in anaerobic conditions. These activities disappeared upon exposure to an inhibitor of the ferric–reductase complex and the power density produced decreased by 70% from 15.3 mW m^{-2} to 4.49 mW m^{-2} after the inhibition in mediatorless microbial fuel cells. Adding methylene blue as electron mediator overcomes the inhibition and the power density of the MFC slightly decreases of 7% from 46.7 mW m^{-2} to 43.8 mW m^{-2}.

Keywords

Microbial fuel cell, *Saccharomyces cerevisiae*, glucose, methylene blue, graphite electrode, power generation, open circuit voltage, oxygen, hydrogen peroxide, iron reduction, CCCP.

Table of contents

List of figures

List of tables

Introduction

Chapter 1

1.1 Research and development for a low carbon future

The current economic crisis, the uncertainties related to the cost and supply of energy, the increasing level of emissions and the risks of climate changes, casts serious doubts on the sustainability of the worldwide economic and productive system. The priority actions to be taken, globally, to address these issues, concern primarily about the spread of the technologies and the behaviors for a rational use of energy. But if the acts on efficiency, particularly in end use efficiency, are a necessary precondition for meeting the challenges of energy and climate, a long–term perspective can not be tackled unless accelerating the research efforts and in the development of technologies, which enables on the one hand a clean use of the fossil fuels, and on the other hand encourage a full use of the renewable sources. The definition of a long–term strategy regarding the energy supplying, particularly in the renewables, is a necessary precondition for reducing the many barriers that hamper their development. The policies that will be adopted should achieve the necessary balance between the tools for creating an adequate demand for renewable technologies, and tools for stimulating innovation and technological development. On the pursuit of these objectives will weigh the rate of investments, both public and private, which will be earmarked for the development and industrialization of innovative technological systems and, above all, the ability to focus on priority technological options these investments, in a spirit of cooperation between research and industrial system. In this view, the European community target assigned to Italy in 2020, which provides a coverage of 17% of the final consumption with energy from renewable sources, represents a stimulus to the development and diffusion of new technologies, responding to important and urgent questions facing

today's energy and environmental plan, may be able to promote growth and economical sustainability, to the country.

1.2 Competitive technologies in the development of renewable energy sources

The growing attention by the governments of the major economies to the use of renewable energy sources for the energy security and environmental protection, foreshadows a fundamental shift in the economic development in the sign of a renewed technological dynamism. The development of technologies for renewable energy production affects the capability of industrialized countries to meet the standards of energy and environmental sustainability, however, not less significant are the effects on the economic and social sustainability, given by the importance of the productive transformations induced with them and the emersion of a new balance between the supply and the demand of the national economic resources. So not a case if the reflection on possible developments of these technologies has been gradually extended from the initial assessments on the cost and effectiveness of individual measures, to a more detailed consideration on the size of the structural change. In this sense, the "bet" of those countries that have firstly promoted the development of renewable energy has been soon translated into targeted actions to encourage independent national paths of technological development. The increasing attention, attracted by the energy security and climate change issues, has indeed given reason to these views and that is why it is not possible to ignore the position of the European Union to ratify the lines of the policies initiated in the Kyoto Protocol. This is the sense of the SET–plan, with which at the end of 2007 the actions to promote clean energy technologies in the member states have been outlined, and to follow, just an year later, the launch of the "climate package" which assigned to the renewable energy sources a prominent role in fighting climate changes.

1.3 Energy–climate package

The European Commission proposed on January 10th, 2007 a comprehensive package of measures to establish a new energy policy for Europe, which aims to fight climate change and boost energy security and competitiveness of the European Union. The package of proposals set a series of ambitious targets on greenhouse gas emissions and renewable energy consumption and aim to create a true internal market in making the effective regulation. As part of this package, the Commission presented its communication "Limiting Global Climate Change to 2 degrees Celsius – the way ahead for 2020 and beyond".

The communication and the accompanying impact assessment indicated that the objective described in the title is technically and economically feasible, and suggested that the EU will adopt the necessary measures and take internationally a leading position to ensure that the rise in the average temperatures worldwide will be not more than 2 °C above pre–industrial levels. As the production and use of energy are the main sources of greenhouse gas emissions, to achieve this goal, the council proposed an integrated approach to climate and energy policy.

On January, 23rd 2008, the European Commission adopted a package of proposals that will enforce the commitments made by the European Council in the fight against climate change and the promotion of renewable energy. The measures will dramatically increase the use of renewable energy sources in every country and set legally enforceable targets for governments. Thanks to a thorough reform of the emissions trading scheme, which will impose a cap on emissions at a community level, all major CO_2 emitters will be encouraged to develop clean production technologies. The legislative package entered into force in June 2009 and will be valid from January 2013 until 2020.

The Directive provides, at European level:

1. the reduction of greenhouse gas emissions by 20%;

2. the raising to 20% of the amount of energy produced from renewable sources origin;

3. the achievement of the 20% of energy savings.

The climate–energy package also included measures on the emissions from cars and limits on the emission trading scheme. The goal was obviously to fight climate change and promote the use of renewable energy sources through binding targets for member countries.

The first objective for the EU was surely to find a way to engage in the period "post–Kyoto", without waiting for global agreements: the European measures would tow the international community in view of the COP (Conference of the Parties to the United Nations Framework Convention on climate change) in Copenhagen in December 2009, where it was assumed to be able to reach an agreement to fight climate change also on the European experience wake. As we know an agreement has not been reached and just at the COP 21, in Paris in 2015, 195 countries worldwide have adopted the first universal and legally binding global climate agreement. The agreement sets out a comprehensive action plan, which aims to put the world on the right way to avoid dangerous climate changes by limiting global warming well below 2 °C.

Governments have agreed to:

- keep the average global temperature increase well below 2 °C above pre–industrial levels as a long–term goal;
- aim to limit the increase to 1.5 °C, since this would reduce significantly the risks and impacts of climate change;
- countries aim to reach global peaking of greenhouse gas emissions as soon as possible, recognizing that peaking will take longer for developing countries;
- then proceed to rapid reductions in accordance with the most advanced scientific solutions available.

Before and during the Paris conference, countries have submitted national plans of action for the comprehensive climate (INDC), these are not enough to keep the global warming below 2 °C, but the agreement track the way to achieve this goal.

The EU has been at the forefront of international efforts to reach a global climate agreement: following the limited participation in the Kyoto Protocol and the lack of an agreement in Copenhagen in 2009, the European Union has worked to build a broad coalition of developed and developing countries in favor of the ambitious objectives that determined the positive outcome of the Paris conference.

Chapter 2

2.1 Renewable energy sources

Renewable energy sources are defined, in the field of energy engineering, as all of the resources which are naturally replenished on a human timescale for their intrinsic feature. These sources are therefore alternative forms of energy to conventional fossil fuels (which are part of non–renewable energy sources) and many of them are even classified as sources of clean energy (Johansson et al., 1993). Renewable resources, both matter and energy, are natural resources that, for intrinsic features or effect of human cultivation are renewed in few time and are, therefore, available for human survival almost indefinitely. The use of these resources have many advantages, the largest is undoubtedly the absence of polluting emissions during their use, for this reason they are called “clean sources”, accompanied by their inexhaustibility. The exploitation of these sources does not affect their availability in the future and they are precious resources to create energy while minimizing environmental impact. This will protect the nature in respect of the next generations and limit the costs of production and distribution of energy.

The main sources of renewable energy are as follows (Demirbas, 2005):

- solar radiation;
- wind;
- tides and marine currents in general;
- waterfalls;
- biomass.

2.2 Bioenergy production from biomass

Biomass is the organic matter derived from living, or recently living organisms. The term biomass means, in the energetic field, the biodegradable fraction of products, waste and residues from biological origin of agriculture, forestry and related industries including fisheries and aquaculture, as well as the biodegradable fraction of industrial waste urban (McKendry, 2002). Biomasses are primarily used for the production of valuable compounds or animal feed in order to avoid disposal as hazardous wastes, since they are characterized by a significant organic load.

At present the technologies available for the re–use of this waste are limited, however, there are companies that are working, with remarkable foresight, to develop activities aimed to obtaining high–value molecules. Thus, it can result in interesting opportunities for income support for the agro–industrial world and for the agriculture. Such byproducts are mostly used for the purpose of energy production and conveyed in the production of biogas and/or soil amendments. The combustion of the biomass release in the environment the amount of carbon sequestered by the plants during their growth, and an amount of sulfur and nitrogen oxides considerably lower than that released by an equal amount of energy produced by fossil fuels (UNFCC, 2003, IPCC, 2006).

The goal of the new technologies in the field of biomass is to recover the solar energy stored naturally in organic compounds through the photosynthesis. Draw energy from biomass helps to remove the waste products from agro–forestry activities and enhance them with the production of syngas, natural gas and electricity. They are also compatible with environmentally sustainable economic growth because they do not contribute to the greenhouse effect. Increasing the energy use from biomass would produce significant environmental benefits, employments and energy policy.

The bioelectrochemical systems (BESs) are part of a new technology of biomass exploitation along with biodigesters and incinerators (Gude, 2016). The latter are

mainly used for the disposal of solid waste through a high temperature combustion process that generates as final products a gaseous effluent, ashes and dusts. The heat developed during the combustion of waste is recovered and used to produce steam, then for the production of electrical energy. In Italy there are currently 44 "waste–to–energy" plants (WTE) (ISPRA, 2015). However, the biochemical conversion and energy recovery of the biomasses is more profitable from waste biomass sources containing high water levels (>40%), such as wastewaters (Ward et al., 2008). The energy could be harvested from wastewater through several processes: methane production from anaerobic digestions, biohydrogen production by fermentation, electricity or biogas productions in bioelectrochemical systems. The anaerobic digestion has been used for over a century and represents a traditional bioconversion process (Appels et al., 2011, Bouallagui et al., 2005, Pavan et al., 2000, Zhang et al., 2005). Four steps, hydrolysis, acidification, acetogenesis, and methanogenesis, take place in an anaerobic digester to convert the complex organic matter in the wastewater into the main end products of methane and carbon dioxide. In the first step, the hydrolysis, the organic matter is converted into smaller molecules soluble in water. Following hydrolysis, during the acidification step, simple molecules such as volatile fatty acids are produced from the hydrolyzed products. These products of the acidification are converted into acetic acids in the third step, with hydrogen and carbon dioxide as coproducts and finally are consumed by the methanogens bacteria during the methanogenic step into methane and carbon dioxide (Stafford et al., 1980). This multi–step, microbial methanogenic process requires complicated system designs and strict process control to achieve an optimum performance for high methane production (Buffiere et al., 2008, Schnurer et al., 1999). Various types of waste biomass are suitable for anaerobic digestion, from solid wastes, such as agricultural waste and sewage sludge (Appels et al., 2011), to wastewaters including dairy, food processing, palm oil mill, and acid whey wastewater (Li and Yu, 2011).

Hydrogen has been considered as a more desirable energy carrier than methane due to its higher energy content (Lee et al., 2010). Biological hydrogen production represents a renewable, sustainable and cost–effective option, compared with other chemical hydrogen production processes (Brentner et al., 2010). There are two different biohydrogen production mechanisms from waste biomass: photofermentation, and dark fermentation (Das and Veziroglu, 2008). In dark fermentation, microorganisms anaerobically break down complex substrates into volatile fatty acids and alcohols, releasing hydrogen and carbon dioxide (Brentner et al., 2010). Methanogenic hydrogen consumers must be eliminated from the system in order to produce hydrogen gas in bulk (Chen et al., 2002, Chong et al., 2009). In photofermentation, the photoheterotrophs utilize the organic acids produced from hydrolysis and acidification under anaerobic conditions to produce hydrogen and carbon dioxide (Brentner et al., 2010). The waste biomass materials that can be potential sources for the biohydrogen generation are similar to those used for methanogenic anaerobic digestion, such as food waste, dairy waste, palm oil mill effluent, and molasses (Chong et al., 2009, Ren et al., 2011). Although the biohydrogen production process has been advanced significantly over the past two decades by identifying efficient microorganisms, developing new bioreactors, and optimizing system operations, this biotechnology has not yet to be utilized on a scale large enough to replace the more traditional uses of the biomasses.

At present there is no established market for the re–use of wastewaters, thus, bioelectrochemical systems (BESs) are emerging bioconversion technologies for producing energy directly from liquid wastes (Logan and Rabaey, 2012). BESs use microorganisms to oxidize biodegradable substrates, such as waste biomass, and convert the chemical energy stored in these fuels to direct electrical current or energy storage chemicals like hydrogen and methane (Logan, 2008). The strength of BESs is that the bioenergy conversion can take place at lower substrate concentrations and under a wide range of temperatures, compared to the anaerobic

digestion that requires more concentrated waste streams (> 3 kg m^{-3} organic matter) and high temperatures (> 30 °C) to be economically feasible (Pham et al., 2006). BESs could definitely avoid the consumption of energy for wastewater treatment and replace the current energy–consuming aerobic biological wastewater treatment processes, such as the activated sludge, by providing a new source of electrical power (Logan and Rabaey, 2012).

Chapter 3

3.1 Microbial fuel cell

Microbial fuel cell (MFC) is an outstanding example of a rapidly developing biotechnology, generally known as bioelectrochemical systems (BESs), that combine biological and electrochemical processes to generate electricity. MFCs are one types of electrochemical cells. The electrochemical reactions of the cells occur at the surface of the two electrodes, an anode and a cathode, which are joined by an external wire to complete an electrical circuit, usually, an electrochemical cell consists of two chambers, separated in order to maintain the electroneutrality of the two compartments (**Fig. 3.1**).

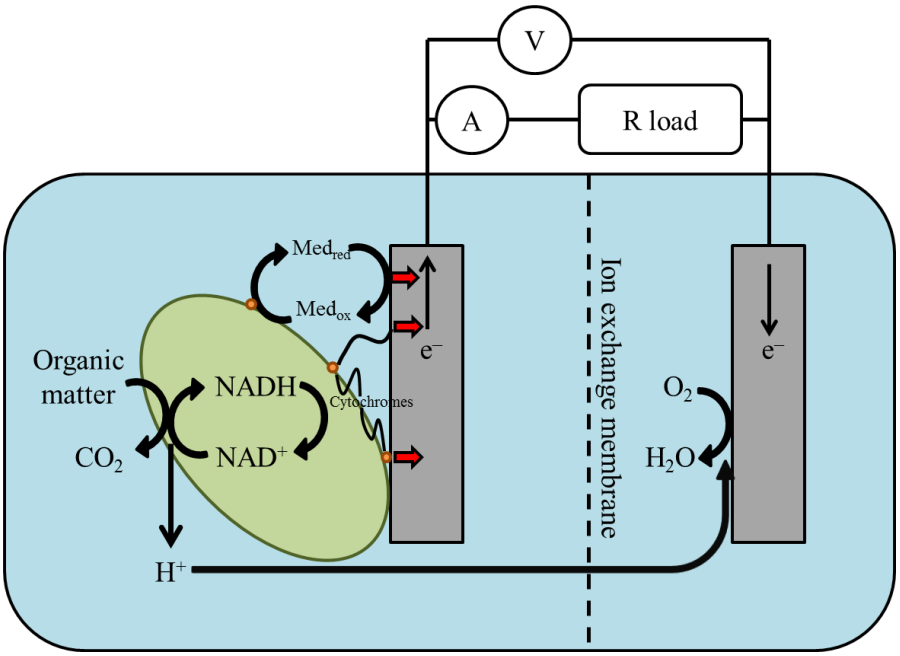

Fig. 3.1. Schematic illustration of a microbial fuel cell (not to scale). Anodic and cathodic compartments are separated by an ion exchange membrane.

MFCs are designed to produce electricity by using wastewater as a fuel and, in the process, can remove the organic matter from the wastewater (Logan, 2008). In

an MFC, the microorganisms oxidize the organic matter in solution, producing electrons that travel through a series of cytochromes or mediators of the cell and create energy for the microorganisms in the form of ATP. Then, the electrons are released to a substance able to accepts these electrons by reducing himself, the terminal electron acceptor (TEA).

The fundamental task of the microorganism in the anode compartment is to transform an electrochemically inactive substrate into an accessible form for the electrochemical oxidation and thus for the conversion into electric energy. For this transformation they make use of the microbial metabolism. The electrons generated by the metabolism of microorganisms, reach the anode surface of the fuel cell and are then conveyed to the cathode through the circuit, where they reduce the oxidant.

3.2 Microbial fuel cells architecture

So many different materials and configuration could be used in MFCs and each one somehow affects the performance of the device in terms of power output, amount of energy in the organic matter transformed in electricity (Coulombic efficiency), stability or longevity. Many researchers have sought to evaluate the immediate and practical application of the MFCs by developing designs that will not only produce high power and Coulombic efficiencies, but which are also economical to mass produce based on the materials being affordable and the manufacturing process being practical to implement on a large scale (Logan, 2008). The perfect design, that join lower costs and higher performance has not been found yet but economical and scalable system could be developed using graphite fiber brush anodes and air cathodes in tubular MFCs (Logan et al., 2015). However, these reactors have never had large implementation in a real, large scale MFC yet. The first test of MFC in a large plant was conducted at Foster's brewery in Yatala, Queensland (Australia), by the Advanced Water Management Center at

the University of Queensland, conducted under the direction of Jurg Keller and Korneel Rabaey (**Fig. 3.2**) (www.microbialfuelcell.org).

Fig. 3.2. Tubular microbial fuel cells tested for power production using wastewater produced at Foster's brewery in Yatala, Australia (www.microbialfuelcell.org).

The tubular bioreactor was designated using carbon fiber brush anodes, with flow up through the tubes and out over the outside of the reactor that was covered with graphite fiber brush cathodes. This design was similar to one tested in the laboratory with a ferricyanide catholyte (Rabaey et al., 2015). The plant consisted of 12 modules, each 3 m high, with a total volume of approximately 1 m^3. New innovations will no doubt continue to modify our view on the "perfect" MFC system, with improvements certain to be made in the coming years.

The performance of the MFCs are affected by several architectural parameters:

- electrodes, both anodes and cathodes;
- biocatalyst, i.e. the microorganisms in the anode compartment;

- anodic electron transfer;
- cathodic electron acceptor.

3.3 Electrodes in microbial fuel cells

3.3.1 Anodes

Even if remarkable improvements in power density due to newer catalysts and architectures have been made, the large–scale application of MFCs has yet to be implemented due to low yields of power generation and very high costs of materials. The electrode accounts for the most part of the MFC cost and represents a key component in deciding the performance of the MFCs (Logan et al., 2015). Recently, interest in the electrode material and its configuration has steadily increased in studies for MFCs. The most studied electrodes in the past decade was the bio–electrodes (both anode and biocathode) and chemical–electrodes (more specifically, air–cathode and aqueous air–cathode), according to whether or not the bacteria are used as catalysts.

The materials of all the types of the electrodes in MFC have some general characters: the base materials must generally be a good conductor, with high mechanical strength, good chemical and biochemical stability and preferably low cost. Carbonaceous materials and non–corrosive metals, which can basically meet the general requirements above, are currently the most–widely used base materials (Wei et al., 2011). The different purpose of the cathode and the anodes require some specific characteristic for each electrode. Anodes, as bioelectrodes should work not only as electronic conductor but also need to carry a high numbers of microorganisms through high surface roughness, good biocompatibility, and efficient electron transfer between bacteria and electrode surface. In order to improve bacterial adhesion and electron transfer, electrode surface modification has become a new topic of interest in the research field of MFCs.

The electrodes, especially as they are currently used in the cultivation of microorganisms, are not all the same. The surface chemistry of graphitic, glassy, or other carbon materials can be widely different, roughness can influence available surface area (McCreery, 2008), and 3–D structures (flat vs. fibrous) can affect diffusion. For example, the electrodes used for microbial fuel cell research can be carbonaceous materials such as brushes (Cheng et al., 2007, Logan et al., 2007), cloths (Nevin et al., 2008), carbon–coated titanium (Biffinger et al., 2008) or metals electrodes like gold (Richter et al., 2008) or stainless steel (Dumas et al., 2008). Another set of variables that affect measurements of microbial activity lie in the device used to house the electrode. As negative charges move into the electrode and travels via a wire to the cathode as electrons, positive charges must at the same time migrate the same distance, but through the biofilm and the electrolyte (Torres et al., 2008a; Torres et al., 2008b), here, porosity and three–dimensional effects can alter the environment and lead to incorrect interpretations of the bacterial capability. Simply changing the configuration of electrodes, (such as the ratio of electrode/surface area), dramatically altered how a pure culture would perform, as observed by Liang et. al (Liang et al., 2007), who inoculated reactors containing identical electrodes, but arranged in three different configurations that impacted charge equilibration between electrodes as internal resistance. The rate these electrodes could collect current from bacteria varied more than 20–fold, yet the bacterial inoculum and conditions were otherwise identical. The importance of the effect of the internal resistance could be evaluated by a simple comparison of the maximum power output by various laboratories, there are cited examples of "power output" by bacteria in fuel cells that vary over 100-fold (as high as 5 W m^{-2} of electrode to as low as 0.03 W m^{-2}) (Liang et al. 2007; Dewan et al. 2008; Zuo et al. 2008a; Yi et al. 2009). These difference can not be ascribed as differences in the bacterial electron transport rates but likely reflects differences in internal resistance or electrode configuration of the devices. In addition, as researchers have focused

their attention on controlling the electrode environment more precisely, specific abilities related to extracellular electron transfer have become more apparent.

Thus, the "electrode" is not a fixed or defined environment, but an electron acceptor that can vary widely in surface charge, porosity, and electron acceptor potential, which is incubated like any other electron acceptor in a medium controlled for salinity, microaerobic vs. strictly anaerobic conditions, mixing, and other factors. The diversity of possible electrode–based experiments, largely conducted in fuel–cell like devices, has led to isolation of a wider variety of organisms known to convey electrons beyond their outer surface, compared to experiments with Fe^{3+} as the electron acceptor (Bond, 2010).

3.3.2 Cathodes

The design of the cathodes is the greatest challenge for making MFCs a useful and scalable technology. The chemical reaction that occurs at the cathode is difficult to engineer as the electrons, protons and oxygen must all meet at a catalyst in a tri–phase reaction (solid catalyst, proton in water and oxygen in air). For this reason, the performance of most of the MFCs is limited by the cathode, and this problem is projected to remain for some time (Logan, 2009).

$$\tfrac{1}{2}\, O_2 + 2\, H^+ + 2\, e^- \rightarrow H_2O \qquad E_0'_{(O_2/\, H_2O)} = +\, 0.82\ V$$

The electrode material for air–cathodes with a catalyst is composed of a base material, a catalyst, a binder, and a waterproof coating. Material characteristics and functions are specific for each part. The base material generally only serves as supporting material and current collector. High conductivity and mechanical strength are critical for it. But there is no special requirement for bacterial adhesion. A catalyst is important for air–cathodes, but not absolutely necessary. If present, the catalyst is immobilized on the substrate surface with a binder, and a

hydrophobic coating is regularly added onto the cathode to avoid water loss. To reduce the cost of air–cathodes, several highly specific materials, such as activated carbon, that do not require a catalyst, have been developed and reported (Deng et al., 2010, Zhang et al., 2009). For aqueous air–cathode, only base material, catalyst and binder are needed.

Air–cathodes and aqueous air–cathodes with dissolved oxygen are two of the most commonly used configurations for cathodes in lab scale MFCs. The air–cathode usually consists of a diffusion layer which is exposed to air such as PTFE or PVDF, a conductive supporting material, and a catalyst/binder layer exposed to water (**Fig. 3.3**). Aqueous air–cathodes are made of conductive supporting materials, such as carbon paper, carbon cloth, and platinum mesh, coated with a catalyst/binder layer (Logan et al., 2005, Scott et al., 2008, Yu et al., 2008).

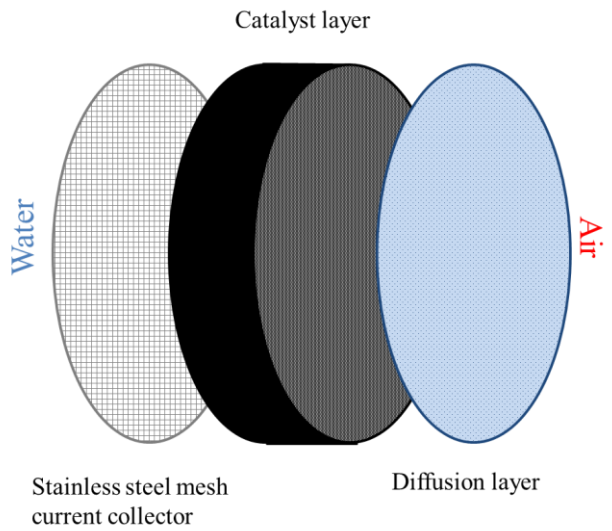

Fig. 3.3. Schematic illustration of an air–cathode. The stainless steel mesh permits the contact between the solution and the catalyst.

The performance of the aqueous air–cathodes is currently lower than the air–cathodes due to the low concentration of oxygen in water respect to air ($4.6 \cdot 10^{-6}$ (25 °C) in water compared to 0.21 mole fraction basis in air), moreover, air–

cathodes are believed to be a more practical design for MFC cathodes, and have attracted much more attention than other cathodes because they require no aeration and generate higher power densities. However, the air–cathodes are harder to make due to the involvement of several stages in the cathodes production such as the insertion of the catalyst, the addition of the binder and finally the application of the diffusion layer. Fail in one of these steps could drastically affects the performance of the cathode and the stability of the system: a not well–applied diffusion layer could reduce the Coulombic efficiency of the MFCs due to oxygen flux to the anode. In addition, there can be substantial water loss through the air–facing side and in some reactors that can result in the appearance of a gas headspace which could be composed of carbon dioxide, methane, nitrogen and oxygen depending on operational conditions. Obviously, the occurrence of an air phase in the anode chamber should be avoided as the oxygen in the air may affects power generation due to the increasing anode potential in the anodic chamber (Logan, 2008). At the same time, applying too much material as diffusion layer could result in insufficient oxygen transfer to the catalyst in the cathode (Cheng et el., 2006).

MFCs were originally constructed using cathodes containing precious metal catalysts such as platinum, due to its high catalytic activity (Cetinkaya et al., 2015, Rozendal et al., 2008). However, these cathodes are expensive and they are rapidly deactivated due to poisoning or loss of Pt from the cathode (Li et al., 2016, Zhang et al., 2014). The discovery that activated carbon (AC) had an oxygen reduction catalytic activity similar to Pt in MFCs, and much greater longevity, enabled the development of relatively inexpensive MFC cathodes that could have relatively stable performance over several months (Pant et al., 2010, Zhang et al., 2014, Zhang et al., 2013).

In order to further improve the MFC cathode performance, different procedures have been used to modify the AC to increase the kinetics of the oxygen reduction reaction, and consequently increase power. The most successful approaches to

increase the catalytic activity have been based on adding high concentrations of nitrogen into the catalyst (Feng et al., 2011, Shi et al., 2012). Even greater performance has been obtained using less nitrogen in a metal–organic framework (MOF), by carbonizing inexpensive metals and organic ligands containing nitrogen at high temperatures on AC (Bezerra et al., 2008, Yang and Logan, 2016). For example, power densities increased from 1.6 ± 0.1 W m^{-2} to 2.0 ± 0.1 W m^{-2} by adding N on the AC catalyst and to 2.6 ± 0.05 W m^{-2} using an iron–nitrogen–carbon MOF catalyst (Yang and Logan, 2016). Most of the studies using nitrogen–amended or MOF modified cathodes have been conducted with acetate in phosphate buffer solutions, rather than with actual wastewaters (Pan et al., 2016). In one study, it was shown that power was doubled (from 0.4 ± 0.03 to 0.8 ± 0.03 W m^{-2}) using domestic wastewater (Yang and Logan, 2016). However, as recently showed by Rossi et al., (2017) these increases in performance were not retained over time also in a very short period of only eight weeks.

When oxygen is not used at the cathode, no catalyst is needed and therefore plain carbon cathodes can be used. Several different aqueous catholytes have been tested, the most common is ferrycianide or hydrogen peroxide.

$$Fe(CN)_6^{3-} + e^- \rightarrow Fe(CN)_6^{4-} \qquad E_0'_{(Fe(CN)_6^{3-}/\ Fe(CN)_6^{4-})} = +\ 0.56\ V_{(0.1\ M\ HCl)}$$

$$H_2O_2 + 2\ H^+ + 2\ e^- \rightarrow 2\ H_2O \qquad E_0'_{(H_2O_2/H_2O)} = +\ 1.76\ V$$

The main disadvantage of these catholytes is that they must be chemically regenerated or replaced but, on the other hand, permit a more accurate control of the electrochemical half reaction in the cathodic compartment.

3.4 Anodic electron generation

The anodic performance is inextricably dependent on (i) the nature and the rate of the anaerobic metabolism, and (ii) the nature and the rate of the electron transfer from the microbial cells to the anode (Schröder, 2007).

Depending on the involvement of exogenous substances in the oxidation, two major pathways of metabolism can be distinguished: respiration and fermentation. In the former the electrons generated by the oxidation of the organic matter are transferred through a redox cascade mechanism, to be finally supplied to an external terminal electron acceptor. As higher the potential of the electron acceptor, as higher the energy gain for the microorganism. Aerobic respiration is the pathway that guarantees the highest energy gain but it is associated with an environment where oxygen is available; in the case of glucose respiration:

$$C_6H_{12}O_6 + 6O_2 \rightarrow 6H_2O + 6CO_2 \qquad \Delta G_o' = -2895 \text{ kJ mol}^{-1}$$

In anoxic conditions anaerobic microorganisms use other endogenous substances, organic or inorganic, as terminal electron acceptors. Examples of such substances may be nitrates, sulphates, CO_2, and metal ions (Bond, 2010). Because of the redox potentials less positive of these oxidants than oxygen, the energy gain for the cells that use these endogenous substances is significantly lower than would be obtainable by aerobic respiration. In the absence of exogenous oxidative substances, many microorganisms undertake the way of fermentation, a kind of disproportionation, in which part of the organic substrate works as electron acceptors and is reduced while at the same time the other part is oxidized:

$$C_6H_{12}O_6 \rightarrow C_3H_7COOH + 2CO_2 + 2H_2;$$

$$\Delta G_o' = -225 \text{ kJ mol}^{-1};$$

$C_6H_{12}O_6 + 2H_2O \rightarrow 2CH_3COOH + 2CO_2 + 4H_2$;

$\Delta G_o' = -206$ kJ mol^{-1};

The above reactions show how the fermentation of glucose to acetate or butyrate are pathways with a low energy gain, in which less than 10% of the energy content of the glucose is directly converted into energy immediately available to the microorganisms. The low energy extracted implied a poor recovery of the electrons contained in the substrate and the nature and the rate of the anaerobic metabolism is so important in MFCs because the lower the energy extracted from the substrate and the lower the energy transferred to the anode of the MFC.

A fundamental role in the MFCs performance is given by the electron transfer from the microbial cells to the anode. There are different requirements for an effective electron transfer between the microorganism and the surface of the electrodes. Since the latter are physical entities unable to penetrate the bacterial cell membrane, the most important requirement is that the electrons can be transferred from the inside of the cell membrane to the outer surface through a physical transfer of reduced mediator or an electronic hopping catalyzed by membrane enzymes (Kumar et al., 2017).

Regardless of the mechanism by which the electrons are transferred is always required the presence of redox active species able to electronically connect the cells to the electrode. By the nature of the electron transfer mechanism is possible to classify the different MFCs through:

- DET: direct electron transfer;
- MET: mediated electron transfer.

The DET takes place via direct physical contact between the cell membrane of the microorganism and the anode of the MFC, the direct transfer of electrons depends on the presence of enzymes, cytochromes or proteins on the membrane of the cells capable of transferring electrons directly from the microbial metabolism to

an external electron acceptor like the electrode. The first discovered bacterium able to do that (exoelectrogen) was *D. acetoxidans*, a microorganism performing complete oxidation of an organic substrate with electron transfer directly to the electrode (Bond et al., 2002). This microorganism is part of the Geobacteraceae and several subsequent studies involved this family in order to better understand the behavior of this mechanism. *Geobacter metallireducens* (Bond et al., 2002) and the predominantly freshwater *G. sulfurreducens* was found able to oxidize organic compounds and simultaneously reduce a solid electrode (Bond and Lovley, 2003). The Geobacteraceae predominance on the DET microbial fuel cells has been observed on anodes harvesting electricity from a diversity of marine and freshwater sediments (Holmes et al., 2004a), and on anodes harvesting electricity from organic waste matter, such as swine waste (Gregory et al., 2005). It has been observed that Geobacteraceae colonize only the anode connected to a cathode, where they account for over half of the total microorganisms, while they generally constitute less than 5% of the community on control electrodes not connected to a cathode. The spread of the Geobacteraceae microorganisms on the anode of the MFCs should be searched in the intrinsic physiological characteristic of these microorganisms to oxidize organic compounds with electron transfer to insoluble electron acceptors such as Fe^{3+} oxides (Lovley, et al., 2004), humic substances (Lovley et al., 1996), and Mn^{4+} oxides (Lovley and Phillips, 1988). Geobacteraceae are often the predominant Fe^{3+} reducing microorganisms in sedimentary environments in which the amount of oxygen is negligible and the organic matter oxidation is coupled to Fe^{3+} oxide reduction (Lovley, et al., 2004). Several studies were conducted on the identification of the electron transfer mechanism of these bacteria and just few years ago Nevin and Lovley discovered that Geobacteraceae do not produce electron shuttles, but need to be in direct contact with Fe^{3+} oxides in order to reduce them (Lovley, et al., 2004, Nevin and Lovley, 2000). The ability of Geobacter species to oxidize their typical electron donors with an electrode serving

as the electron acceptor, and to conserve energy to support growth from this metabolism, represents a novel form of microbial respiration.

The organic compounds are always oxidized to carbon dioxide, with nearly full recovery of the electrons derived from the organic–matter oxidation as electricity. Species of Geobacteraceae shown to be capable of this form of respiration include *Geobacter sulfurreducens*, *Geobacter metallireducens*, *Geobacter psychrophilus*, *Desulfuromonas acetoxidans* and *Geopsychrobacter electrodiphilus*. Many of the studies on electron transfer to electrodes in Geobacteraceae have focused on *G. sulfurreducens* because the genome sequence and a genetic system are available (Methé et al., 2003, Coppi et al., 2001), making it the species of choice for physiological studies. Once power production was established with *G. sulfurreducens*, the medium in the anode chamber could be replaced without affecting the performance, demonstrating that only the cells attached to the anode were responsible for the power production and that a soluble electron shuttle was not involved in electron transfer to the electrode, because the electron shuttle would have been removed when the medium was exchanged (Bond and Lovley, 2003).

Several exoelectrogens outside the Geobacteraceae have been described. *Rhodoferax ferrireducens*, was isolated from subsurface sediments as an Fe^{3+} reducer (Finneran et al., 2003) and was found able to oxidizes sugars, such as glucose, fructose, sucrose, lactose and xylose, to carbon dioxide with over 80% recovery of the electrons derived from sugar oxidation as electricity (Chaudhuri and Lovley, 2003). The ability of this organism to oxidize complex organic molecules is of special interest because of the limitation of the *Geobacter spp* to degrade only simple compounds like acetate and consequently a microorganism with a metabolism like that of *Rhodoferax spp* might be an ideal candidate for a pure culture system for converting sugars to electricity. As was observed with *G. sulfurreducens*, power production by *R. ferrireducens* could be attributed to the cells attached to the electrode surface and power production was sustained for long

periods of time. When the electrical connection in the *R. ferrireducens* fuel cell was disconnected for 36 hours, leaving *R. ferrireducens* with no means of energy generation, power production resumed as soon as the connection was restored. The capacity for storage under idle conditions without deteriorating performance is a desirable characteristic for a microbial fuel cell and further demonstrated the long–term survival abilities of *R. ferrireducens*.

Another exoelectrogen discovered from molecular analysis of the anode surfaces of sediment microbial fuel cells is *Desulfobulbus propionicus*. Electrodes harvesting electricity from sediments with high concentrations of sulphide (S^{2-}) were colonized by microorganisms in the family Desulfobulbaceae (Holmes et al., 2004a). Studies with *D. propionicus*, a pure culture representative of this family, revealed that microorganisms oxidized S^0 to sulphate (SO_4^{2-}) with an electrode serving as the sole electron acceptor (Holmes et al., 2004b). This might be an important reaction at the anode surface with high concentrations of sulphide, because the sulphide produced might abiotically react with electrodes generating S^0. This abiotic reaction only harvests two of the eight electrons potentially available from sulphide oxidation. Oxidation of S^0 to sulphate extracts six more electrons and regenerates sulphate as an electron acceptor for further microbial reduction.

Shewanella spp were discovered as exoelectrogens microorganisms and unusually high accumulation of a c–type cytochrome in *S. putrefaciens MR-1* outer membrane in the course of anaerobic growth was demonstrated as early as 1992 (Myers and Myers, 1992). It seems likely that there is wide diversity of exoelectrogens yet to be discovered.

One of the most formidable barriers to microorganisms transferring electrons onto Fe^{3+} or electrodes is the non–conducting lipid–membrane system that serves as an insulator, separating the cytoplasm, where electrons are extracted from organic matter during central metabolism, from the outside of the cell where the

final electron transfer must take place. A number of proteins in the cytoplasmic membrane, periplasm and outer membrane that are involved in dissimilatory mineral reduction have been identified by mutagenesis and biochemical studies (Logan, 2008). Researches on *G. sulfurreducens* suggested that a series of c–type cytochromes associated with the inner membrane, the periplasm, and the outer membrane might interact to transfer electrons to the outer membrane surface (Lovley et al., 2004). However, growth on Fe^{3+} oxides has required the evolution of appendices able to transfer the electrons via cytochromes far from the immediate vicinity of the cells. Thus, the microorganisms have developed particular nanowires: conductive pili carrying electrons from a cell to a surface few micrometers far from the microorganism (Reguera et al., 2005, Gorby et al., 2006). Initial studies showed that *G. sulfurreducens* formed little more than a monolayer on the surface of electrodes, suggesting that close contact between the cells and the anode was required. However, one of the most significant observation about the stability of an MFC biofilm is that the anode does not appear to foul over time, accordingly, the bacteria on the surface must remain viable or at least permit to the viable cells many layers of microorganisms far from the electrode to use the electrode as the final electron acceptor (Logan and Regan 2006). Current can be produced also in the absence of pili providing the cell retains the ability to produce the outer membrane electro–active cytochrome, called OmcS (Holmes et al., 2006). OmcS, which is also essential for Fe^{3+} oxide reduction, is displayed on the outer surface of the cell (Holmes et al., 2006) and trough this cytochrome can be maintained the electrical contact with the relatively flat surface of electrodes, alleviating the need for the conductive pili that seem to be required for effective contact with heterogeneously dispersed Fe^{3+} oxides (**Fig. 3.4**).

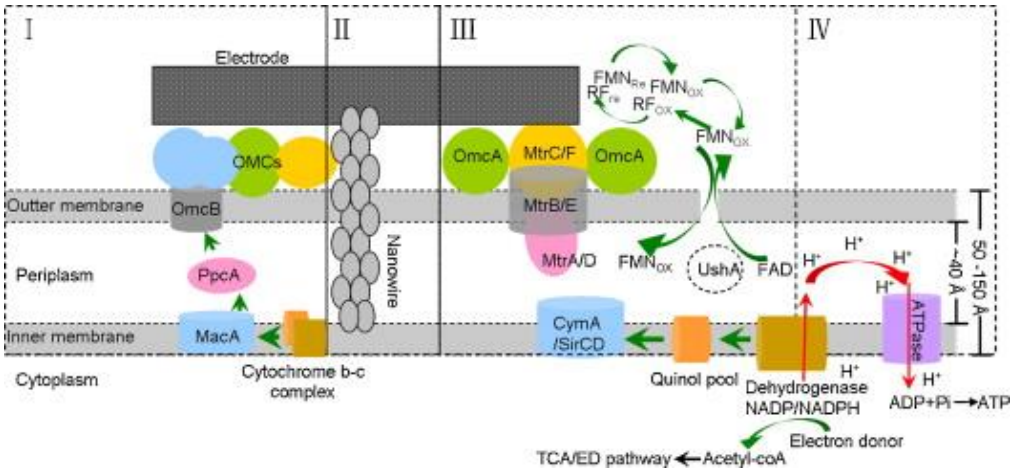

Fig. 3.4. The mechanism for extracellular electron transfer by *Geobacter* and *Shewanella*. In the panel (I) the OMC–based direct electron transfer of *Geobacter*; (II) bacterial nanowire; (III) electron transfer network of *Shewanella* including flavins and c–type cytochromes; (IV) electrode respiration–coupled proton motive force and energy (ATP) generation. (from Yang et al., 2012. Reprinted with permission of Elsevier).

Further understanding of the electron transfer mechanisms to electrodes is likely to accelerate the available techniques for monitoring gene expression during growth on electrodes. The firm attachment of *Geobacter* and *Rhodoferax* species to electrodes contrasts with the current model for the behavior of dissimilatory metal–reducing microorganisms in sedimentary environments, in which permanent attachment to the Fe^{3+} oxide surface is unlikely to be beneficial because Fe^{3+} reducers must have the mobility to search for new sources of Fe^{3+} once the Fe^{3+} oxide in one location is depleted. By contrast, electrodes represent a more enduring electron sink and therefore more permanent attachment to electrode surfaces might be advantageous. How *Geobacter* or other organisms make this distinction in the quality of the electron acceptors is unknown (Lovley, 2006).

Before metal-reducing bacteria were discovered, microbial–electrode research largely focused on fermentative growth of organisms (Kim et al. 2000, Choi et al. 2001), which could divert a small percentage of their metabolism to reduction of

soluble redox–active mediators, which could then be oxidized by electrodes. Different kinds of MET are available to the MFCs depending on the origin of the mediators:

1. MET via primary metabolites.
2. MET via secondary metabolites;
3. MET via artificial redox mediators;

1. The MET via primary metabolites is closely associated to the oxidative degradation of the substrate: the total amount of reducing equivalents produced corresponds to the amount of oxidized metabolites generated by the interaction with the anode (**Fig. 3.5**). To be used as a reducing agent for the anodic oxidation, the metabolite must meet certain requirements: its redox potential should be as negative as possible and accessible to the electrode. In principle, anaerobic respiration and fermentation can lead to the formation of reduced metabolites suitable for use in the MET via primary metabolites in the MFCs.

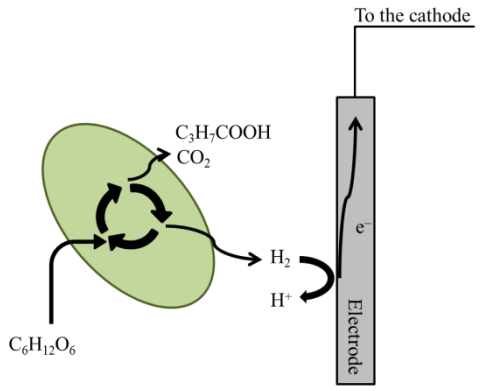

Fig. 3.5. Schematic illustration of MET via primary metabolites. The products of the metabolism are putative.

2. MET via secondary metabolites. Often the microorganisms grow in conditions in which electrons acceptors such as soluble solids are not available in

the immediate vicinity. The microorganism may, in these cases, synthesize independently low molecular weight mediators that would allow him to continue the metabolic cycle (**Fig. 3.6**). The production of these electronic shuttles involves additional biological losses and is consequently energetically expensive.

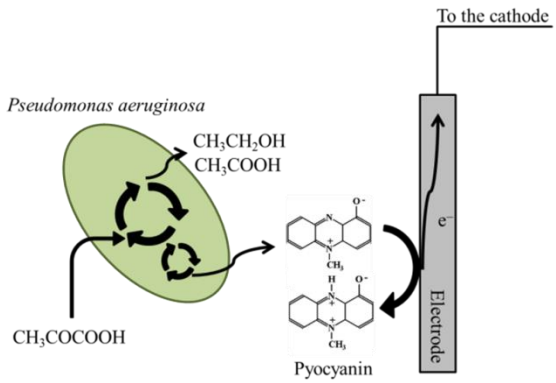

Fig. 3.6. Schematic illustration of MET via secondary metabolites. Just two of the several products derived from the metabolism of the pyruvate from *Pseudomonas aeruginosa* are shown. (Eschbach et al., 2004).

3. In 1930 B. Cohen declared that some bacterial cultures, grew in anaerobic conditions, interfaced as MFCs catalyst, although showing a large negative potential, resulted in low current production (Cohen, 1930). The poor performance of these MFCs were attributed to the lack of electrochemically active species in the anodic compartment. As a solution to this problem has been proposed the introduction of organic or inorganic substances such as benzoquinone or potassium ferricyanide, capable of facilitating the electron transfer from the microorganisms to the electrode surface (**Fig. 3.7**).

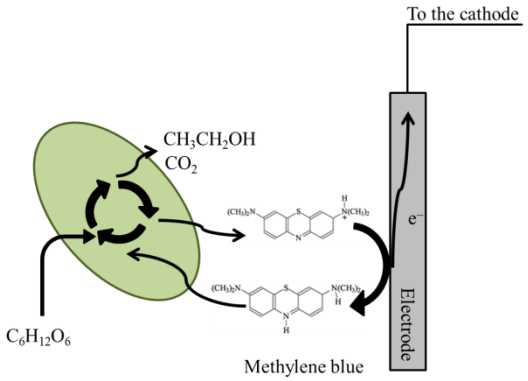

Fig. 3.7. Schematic illustration of MET via artificial redox mediator. The products of the metabolism are putative.

All the above processes make use of mediators: reversible electron acceptors, which can exchange electrons in the layers of the aerobic biofilm and with an inorganic solid electrode, from which are re–oxidized and become available to more redox processes. A single molecule can then serve for thousands of redox cycles. Consequently, the use of small quantities of these compounds allows the microorganisms to transfer their electrons at a very fast rate.

3.5 Materials for stabilizing and immobilizing biocatalysts

As described above, the crux of effectively utilizing biomolecules in microbial fuel cells is the effective orientation and interaction between a microorganism and a conductive transducer surface. The exoelectrogenic bacteria described above showed the capability of interact with an external, solid, conductive electrode, however, despite the fact that more and more exoelectrogens are expected to be found, they are still few in number and thus may not find wide range of applications. Considering that it is non–exoelectrogens that are mostly used in agricultural and industrial area, it is important to evaluate the application of MFCs using these non–exoelectrogens. Difficulties, however, arise from the fact that molecules involved in the electron–transfer reactions are not exposed on the outer

membrane but bound in the cytoplasmic membrane. Therefore, direct electron-transfer to the anode is not favored.

Nevertheless, several attempts have been made to construct mediator-less MFCs using electrochemically inactive Gram–negative and Gram–positive microbes. Zhang et al. (2006) showed that *Escherichia coli* (*E. coli*), after electrochemical activation process acquired ability to directly transfer electrons to the anode. This ability was enhanced by using a graphite/PTFE composite anode while suspending *E. coli* cells in an anodic chamber (Zhang et al., 2007). Endogenous redox compounds were thought to be responsible for the electron–transfer. Later, they identified several metabolites as possible electron carriers (Zhang et al., 2008). Liu et al. (2010), in the meantime, tested *Corynebacterium sp.*, a Gram–positive bacterium as a biocatalyst. Although electricity could be produced, the maximum power density (Pmax) of 7.3 mW m^{-2} was much lower than that of *E. coli* probably due to the thick cell wall structure. Secreted soluble redox compounds were also believed to be involved in the electron–transfer.

Several attempts were made to immobilize the microorganisms on the electrode surface, in order to maintain an high cells density near the electrode and to favor the interactions between electrode and cells, moreover, the immobilization of the biocatalyst has increased reaction rates and longevity of biocatalyst (Fidaleo et al., 2006, Flickinger et al., 2007, Gosse et al., 2007, Lyngberg et al., 1998, 2000, 2001, 2005). Yuan et al., (2011) immobilized *Proteus vulgaris* on carbon paper electrodes in a mediator–less setup and achieved a maximum power density of 269 mW m^{-2} while Wagner et al. (2012), immobilized bacteria on a flat electrode by applying latex layer to hold bacteria on surfaces.

3.6 Yeast catalyzed fuel cell

The yeasts have been utilized for centuries in numerous biotechnological processes of the food industry, which generated huge amounts of wastewaters rich of organic matter. Thus, the yeasts, used in the respective production, could be used as biocatalysts in MFCs for purification of such wastewaters, instead of additional inoculation of the wastewater with other microbial species (Hubenova and Mitov, 2015). Literature reports MFCs catalyzed by eukaryotic microorganisms (Potter, 1911), even though the efficiency of direct electron transfer by the prokaryotic cells made the scientists concentrate their efforts on the characterization of the electron transfer mechanism only of bacteria (Cohen, 1931, Logan, 2009). Yeasts could be ideal biocatalysts for MFCs; most are non-pathogens, many have high growth rates, some display very wide substrate ranges and they are robust and easily handled. Because of the higher physiological complexity, as well as of the absence of nanowires, eukaryotic cells need a mediator for the electrochemical connection of cells to the anode in MFC (Gunawardena et al., 2008, Schaetzle et al., 2008). Although the regular addition of exogenous mediators is a deeply criticized practice, mainly due to the poisoning of the medium (Schröder, 2007), in recent years, the development of microbial fuel cells catalyzed by eukaryotic microorganism, like yeasts, has attracted great attention (Mao and Verwoerd, 2013). Nowadays the performance of the yeast fuel cells are doubtless not comparable with those of the prokaryotic based MFC (Hubenova and Mitov, 2015), even if a large improvement could be possible if the electron transfer mechanism between cells and electrode is better explained (Mao and Verwoerd, 2013).

As previously mentioned, the major limitation in the application of yeasts as catalysts in flow–through fuel cells is related to their eukaryotic nature and thus the catabolic pathway is located within the cytoplasm (glycolytic pathways) and in the matrix or the inner membrane of the mitochondria (TCA and catabolic electron

transport, respectively), which result in the majority of catabolic electrons not being directly accessible from the exterior of the cell.

However, the yeast cells, as the other common exoelectrogens, have trans Plasma Membrane Electron Transport systems (tPMET) also referred to as Plasma Membrane Oxido-Reductase systems (PMOR). These systems lie across the membrane and are involved in the transport of electrons from reduced cytoplasmic molecules such as NADH and NADPH to an external electron acceptor. The exported electrons are, for example, used to prepare external nutrients for uptake as in the reduction of Fe^{3+} to Fe^{2+} (Lesuisse and Labbe, 1992). Some electrons are thus available at the surface of the cell membrane for either direct or mediated transfer to the electrode. However, the number of electrons exiting the cell by this route is smaller than the total number of electrons available from the catabolism of aerobically grown cells.

Although some evidence supports direct electron transfer from yeasts in MFCs (Wartmann et al., 2002),the yeast cell wall is very dense and the exterior of the cell membrane is far from the outside of the cell wall. Thus, direct contact between the cell membrane and an electrode seems difficult to be accomplished.

3.7 Future perspective in yeast fuel cells

The components of the yeast cell membranes, contributing to the electron transfer mechanism, were insufficiently investigated. The evolutionary conservativeness of respiratory chain complexes allows only partial comparison between the EET mechanism in prokaryotes and eukaryotes, because the bacterial ETCs are located on the cellular membranes, while their equivalents in the eukaryotes are situated on the mitochondrial membranes. The only yeast species with proven respiratory chain complexes expressed on the yeast surface is *S. cerevisiae* (Schröder et al., 2003). The presence of a cell wall and the non–homogeneous structure of the cell plasma membrane (Cabib et al., 2001)

additionally impede the yeast ions and electrons transport. The extracellular transfer is dependent on the surface electrical charge of the cell determined by the polymers of the cell wall (the chitin possesses charged amino groups; the proteins have several charged chemical groups). The difficulty in identification of membrane and cell wall components concerns the changes of the surface electrical charge depending on pH and the ion composition of the medium (Volkov, 2015). The yeast membrane potential is another parameter governing the ion and electron transfer. The membrane potential, however, could be changed by proton pumps within seconds. Microelectrode technique measurements performed with *S. cerevisiae* have determined membrane potentials ranging between − 70 and − 45 mV (Borst-Pauwels, 1981).

Dissertation objectives and outline

Chapter 4

Microbial fuel cell (MFC) technology represents a newest approach for generating electricity from biomass using microorganisms. In an MFC, the microorganisms on the anode oxidize the organic matter in solution and release electrons to the anode. The electrons are conveyed through an external circuit to the cathode, where oxygen reduction reaction takes place (Logan et al., 2006, Logan, 2008, Lovley, 2006). The development of processes that can use microorganisms to produce electricity represents an outstanding method for bioenergy production as the cells are self–replicating and thus the catalysts for organic matter oxidation are self–sustaining. Potentially, any biodegradable organic matter could be used in an MFC, including volatile acids, carbohydrates, proteins and alcohols (Logan, 2008).

The yeasts have been utilized for centuries in numerous biotechnological processes of the food industry, generating huge amounts of wastewaters rich in organic matter. MFCs are a valid alternative for purification of such wastewater. From this point of view, the yeasts, used in the respective production, could be exploited as biocatalysts, instead of additional inoculation of the wastewater with other microbial species. The easy cultivation, wide substrate range, fast growth and tolerance to a wide range of environmental conditions are advantageous for the development of yeast–catalyzed fuel cells. The more sophisticated organization, richer genome and compartmentalization of the eukaryotic cells, however, complicate the analyses and the mechanisms of the extracellular electron transfer performed by yeasts still remain unclear (Hubenova and Mitov, 2015). Understanding the electron transfer mechanism is fundamental for the improvements of the MFCs performance since a better explication of how the electrons are transferred to the anodes, might be useful in selecting the best

materials and conditions in the anodic chamber to properly interact with the electron transfer mechanism of the microorganism (Mao and Verwoerd, 2013).

The main objective of this research was to discover and explicate the electron transfer mechanism of an MFC using *Saccharomyces cerevisiae* as anodic biocatalyst, evaluating the influence of the addition of redox mediator to the anodic solution and the variation of the operative conditions such as the concentration of the electron acceptor. Initially, it was investigated the ability of the selected mediator to oxidize the most important intracellular electronophore, NADH, and transfer the electrons accumulated to an external electrode. It was deeply characterized the mechanism of oxidation of the NADH, mediated by the methylene blue (MB). Preliminary studies assessed the influence of the carbon source concentration and of the electron acceptor concentration in the cathode chamber on the overall electrochemical process. The presence of MB could shift the yeast catabolism to predominant aerobic respiration and enhance the biofuel cell electrical outputs (Babanova et al., 2011), for this reason, it was investigated the effect of the latter on the microbial metabolism by screening the end–products of the fermentation in the presence and the absence of MB. Then, the electrochemical response of the MFC in the presence of different concentration of MB was evaluated.

Oxygen at the cathode represents an ideal terminal electron acceptor because of its high redox potential, availability, and sustainability. However, the oxygen reduction reaction (ORR) is kinetically sluggish, resulting in a large proportion of potential loss and the electrochemical response could show a large variability (Fan et al., 2008). For these reasons the terminal electron acceptor was substituted with hydrogen peroxide. The effect of various concentrations of the electron acceptor was evaluated and the importance of methylene blue as mediator was investigated. The evaluation of the anode colonization was presented in the last part of the chapter.

A new method for immobilize and cultivate the yeast cells on the electrode was developed in Chapter 9 and the abilities of *S. cerevisiae* to directly transfer electrons and produce electrical energy through iron–reducing cytochromes were evaluated in a pure–culture MFC system.

Materials and Methods

Chapter 5

5.1 Microbial fuel cells construction and operation

MFCs were double–chambered, glass reactors, with anodic and cathodic compartment connected by a salt bridge. The volume of each chamber was 0.10 L (working volume 0.05 L) and the internal diameter was 4.5 cm. Anode and cathode were graphite rod purchased from Sigma Aldrich (6 mm diameter and 6.3 cm length, 4.0 cm immersed in solution, total area 7.8 cm^2) connected with copper wire to the electrochemical system. The electrodes were cleaned before each experiment by sonication for 5 min in HNO_3 7% and another 5 min in distilled water.

The salt bridge was a solution of KCl 10 g L^{-1} in phosphate buffer (PB) 0.1M (Na_2HPO_4, 12.98 g L^{-1}; $NaH_2PO_4 \cdot H_2O$, 1.17 g L^{-1}; pH 7.8), stirred and heated until it reached 85°C, then Agar Agar was added until it got to 2.5 g L^{-1}. The solution was then poured into a silicon tube 29 cm long, with an 8 cm internal diameter.

The anodic chamber was purged with gaseous nitrogen (14 L h^{-1}) during all the experiment. Anodic and cathodic solutions were stirred continuously at the same rotational speed for all the experiments and the temperature of each chamber was 27.5 ± 2.5 °C. Sampling was avoided in the MFCs in order to limit the volume alteration.

MFCs operated under different conditions in the cathode compartment using oxygen or hydrogen peroxide as electron acceptor. An aerated solution of HCl 0.2 M or hydrogen peroxide at various concentration (0.00 M; 0.18 M; 0.88 M; 4.41 M) in phosphate buffer 25 mM pH 6.0 was used as cathodic solution.

The current–voltage, i–V, characteristics were measured from –0.1 V to round up OCV at the scan rate of 10 mV s^{-1} by an electrochemical measurement system

(Keithley series 2400, Keithley Instrument, OH) each 30 min. Power (*P*) was calculated as $P = iU$, where i is the current generated at the correspondent voltage U.

All chemicals and reagents used for the experiments were analytical grades and supplied by Sigma–Aldrich. The pHmeter, Crison micropH2001 with Hamilton glass electrode was employed for measuring pH of the working solution.

Different anolytes and catholytes were used during the various experiments:

- *Enzymatic fuel cell*

  OCV and P produced were recorded using an aerated solution of HCl 0.2 M in the cathodic chamber as electron acceptor. The anolyte was purged with nitrogen gas for 15 min. and then the electrode was inserted into the chamber. The medium (0.05 L) contained NADH 0.4 mM (β–nicotinamide adenine dinucleotide reduced disodium salt hydrate, ≥ 94%, anhydrous basis, SigmaAldrich) in PB 0.1 M (pH 7.8) and methylene blue (MB) 0.08 mM. The concentration of the enzyme (Diaphorase from Clostridium kluyveri, 27,3 U mg^{-1}, lyophilized powder, Worthington), when present, was 0.4 U mL^{-1}.

- *Effect of each component on the MFC performance*

  OCV and P produced were recorded using an aerated solution of HCl 0.2 M in the cathodic chamber as electron acceptor. The anolyte (0.05 L) was purged with nitrogen gas for 2 h and then the electrode was inserted into the solution. The medium contained glucose 5 g L^{-1}; MB 5.00 mM or a combination of those two in PB 0.1 M (pH 7.8).

  The MFCs with yeast used *Saccharomyces cerevisiae* cells (baker's yeast, CLECA S.p.a. Mantova Italy) as a biocatalyst. Anodic solution was 5 g L^{-1} sample of the dried yeast and glucose 27.8 mM in phosphate

buffer 0.1 M pH 7.8 in the presence of methylene blue in a concentration of 0 mM and 5 mM.

- *Effect of glucose concentration on MFC performance*

  OCV and P produced were recorded using an aerated solution of HCl 0.2 M in the cathodic chamber as electron acceptor. The anolyte (0.05 L) was purged with nitrogen gas for 2 h and then the electrode was inserted into the solution. The medium contained glucose 0 g L^{-1}; 5 g L^{-1} or 10 g L^{-1} and MB 5.00 mM in PB 0.1 M (pH 7.8). The MFCs with yeast used *Saccharomyces cerevisiae* cells 5 g L^{-1} (baker's yeast, CLECA S.p.a. Mantova Italy) as a biocatalyst. The measures were carried out immediately, 22 h and 46 h after the inoculum.

- *Effect of methylene blue concentration on MFCs performance*

  OCV and P produced were recorded using an aerated solution of HCl 0.2 M in the cathodic chamber as electron acceptor. The anolyte (0.05 L) was purged with nitrogen gas for 2 h and then the electrode was inserted into the solution. The medium contained 5 g L^{-1} of glucose in PB 0.1 M (pH 7.8) and various concentrations of MB (MB 0.00 mM; 0.05 mM; 0.50 mM; 1.00 mM; 5.00 mM). The MFCs with yeast used *Saccharomyces cerevisiae cells* 5 g L^{-1} (baker's yeast, CLECA S.p.a. Mantova Italy) as a biocatalyst. The measures were carried out 22 h and 46 h after the inoculum.

- *Hydrogen peroxide as terminal electron acceptor in cathodic chamber*

  OCV and P produced were recorded using several concentration of H_2O_2 (0.00 M; 0.18 M; 0.88 M; 4.41 M) in the cathodic chamber as electron acceptor. The anolyte (0.05 L) was purged with nitrogen gas for 2 h and

then the electrode was inserted into the solution. The medium contained 5 g L^{-1} of glucose in PB 0.1 M (pH 7.8) and various concentrations of MB (MB 0.00 mM; 0.05 mM; 0.50 mM; 5.00 mM). The MFCs with yeast used *Saccharomyces cerevisiae* cells 5 g L^{-1} (baker's yeast, CLECA S.p.a. Mantova Italy) as a biocatalyst. The measures were carried out 22 h and 46 h after the inoculum.

After different times of starvation the methylene blue was completely reduced and the anodic solution resulted completely discolored. The cell circuit was then closed and i–V curves were recorded. The electrode was inserted immediately after the inoculum or after the completely discoloration of the methylene blue solution. As far as the experiments carried out in the absence of methylene blue, the cell performances were recorded after having waited the same period of time.

- *Yeast immobilization on a functionalized anode*

  OCV and P produced were recorded using H_2O_2 (4.41 M) in the cathodic chamber as electron acceptor. The anolyte (0.05 L) was purged with nitrogen gas for 2 h and then the functionalized electrode was inserted into the solution. The medium contained 5 g L^{-1} of glucose in PB 0.1 M (pH 7.8) and MB in concentration of 0.00 mM or 0.50 mM.

- *Voltage and power production in a S. cerevisiae catalyzed fuel cell by Ferric reductase enzymatic complex*

  OCV and P produced were recorded using H_2O_2 (4.41 M) in the cathodic chamber as electron acceptor. The anolyte (0.05 L) was purged with nitrogen gas for 15 min and then OCV was recorded for 30 h Polarization curves were recorded after 30 h at different scan rate (0.1

mV s^{-1}; 1.0 mV s^{-1}). The medium contained 5 g L^{-1} of glucose in PB 0.1 M (pH 7.8) and MB in concentration of 0.00 mM or 0.05 mM.

5.2 Electrochemical analysis

A graphite rod (6 mm diameter and 6.3 cm length, 4.0 cm immersed in solution, total area 7.8 cm^2) working electrode, a platinum wire counter electrode, and an Ag–AgCl reference electrode were used in an electrochemical cell with a working volume of 50 mL. Cyclic voltammetry was performed by using a potentiostat (model 7050; AMEL) connected to a Sony personal computer data acquisition system. Prior to use, the working electrode was cleaned by sonication for 5 min in HNO_3 5% and another 5 min in distilled water, and the electrochemical cell was thoroughly washed. Oxygen was purged from the solution by bubbling it with oxygen–free N_2 for 10 min before electrochemical measurements were obtained. The scanning rate used was 25 mV s^{-1} over a variable range from −0.4 to 1.2 V. PB 0.1 M (pH 7.8) was used as the electrolyte.

5.3 Spectrophotometric studies

- *Correlation between glucose concentration and methylene blue reduction*

  The solution used for the spectrophotometric studies contained yeast cells 0.25 g L^{-1}, MB 9 µM, and glucose in variable concentrations (0.00 g L^{-1}, 0.10 g L^{-1}, 0.25 g L^{-1}, 1.00 g L^{-1}, 5.00 g L^{-1} and 10.00 g L^{-1}). The medium was prepared and stored in a glove box (MBraun MB 150 G 2, M. Braun InertgasSystem GmbH, Garching bei München) with an oxygen concentration lower than 1 ppm. After 4 h, 21 h, 28 h and 76 h the absorbance at 664 nm (MB + turbidity) and 750 nm (turbidity) was measured and the difference between those two was normalized and plotted.

- *Effects of the presence and absence of external carbon source in methylene blue reduction*

  The cells (0.25 g L^{-1} dry weight) were harvested by centrifugation and washed twice with 0.1 M PB pH 7.8, then, methylene blue was added until got to 9 µM. The solution was stored at 30°C with different glucose concentrations in sealed quartz cuvette (Hellma). After 19, 20, 43, 44, 67, 68, 91 h the absorbance was measured either at 750 nm and 664 nm. After 19, 43 and 67 h the solution was aerated.

- *Iron III reduction by Saccharomyces cerevisiae*

  A modified ASTM (ASTM E 394) procedure was used. Initially, 2 mL of sodium acetate (2 M) and 100 µL $ZnSO_4$ (0.01 M) (Koopman et al., 1985) were degassed into a 20 mL flask through pulsed ultrasound for 3 min, then 2 mL of 10 mM 1,10–phenanthroline (Sigma Aldrich) were added and the solution was degassed for one more minute before adding 1 mL of sample. The flask was filled to the final volume with distilled water and the iron concentration was measured at 510 nm. The reactors used for the determination of the amount of iron reduced by the cells were vials with an internal volume of 15 mL (working volume 12 mL), continuously purged with 1 L h^{-1} oxygen–free nitrogen. The medium contained FeEDTA 1.0 mM, glucose 5 g L^{-1}, *S. cerevisiae* cells 5 g L^{-1} and variable concentration of MB of 0.00 mM or 0.05 mM.

5.4 Chromatographic studies

Effects of methylene blue on Saccharomyces cerevisiae metabolism

Chromatographic studies were performed at the same operative conditions of the electrochemical cell. Crude samples of the fermentation broth were filtered using 0.20 µm Sartorius Stedim Minisart® syringe tip filter after different times of

starvation. Filtered aliquots of 10 μL were injected in an HPLC operating at a flow rate of 0.6 mL min^{-1} (mobile phase 0.05 M HCl) and the HPLC column was heated to 60 °C. All analyses were run on an Agilent 1260 Infinity Quaternary LC equipped with UV DAD (G4212B) and RID (G1362A) detector. Rezex ROA–Organic acid, dimensions: 300 x 7.8 mm (Phenomenex Inc., Torrance, California) was used as column.

5.5 Yeast immobilization on a functionalized anode

- *Functionalized electrode development*

All the equipments were sterilized in autoclave for 15 min at 121°C. A 0.5 g sample of the dried yeast (*Saccharomyces cerevisiae* baker's yeast, CLECA S.p.a. Mantova, Italy) was dissolved in 4.0 mL of PB solution 0.1 M (pH 6.0), then was added 5.0 g of glucose. The paste formed was immediately transferred in a 15 mL vial and the electrode was covered for four–fifths of the height by a dip–coating techniques (immersion speed 1.5 cm s^{-1}). The glucose–yeast paste was dried 2 h at room temperature before use.

- *Immobilization of the yeast cells on the functionalized electrode*

The functionalized electrode was covered by cellulose acetate membrane by a dip–coating technique through immersion in a solution of 5 % w/v (Mr ≈ 61000, 40% acetyl groups, Fluka) cellulose acetate in acetone–THF (60:40). The immersion speed of the dip–coater was 1.5 cm s^{-1} and the electrode was dried at room temperature for 18 h. After dryness the electrode was transferred in a sterile YPD solution (10 g L^{-1} yeast extract, 20 g L^{-1} peptone, 2% glucose) to allowed the growth of the cells for at least 76 h. The cells growth was determined by turbidity measurement and the glucose concentration by a modified colorimetric method by Bailey et al. (1992).

Results and Discussion

Chapter 6

6.1 Enzymatic fuel cell

The NADH/air fuel cell was developed to mimic the respiration process of the microorganisms. In the cells the metabolites are oxidized and the electrons are temporary stored in the NADH. The energy gained by the oxidation of the NADH is then used for the production of ATP into the mitochondria. If this energy is conveyed trough an electrode it is possible to directly produce electricity from the molecules metabolized by the cells.

In this experiment, the oxidation of the nicotinamide cofactor, spontaneous or catalyzed by the NADH dehydrogenase, was accompanied by the reduction of an electrons acceptor such as methylene blue (MB). The mediator is necessary since the NADH can't directly interact with the electrode. The electrons acceptor works as a shuttle and transfer the electrons directly to the anode, then the electrons are conveyed through an external circuit to the cathode, where oxygen reduction reaction takes place (**Fig. 6.1**). Obviously, the anode chamber needs an anoxic atmosphere.

The following reactions are involved in the process:

$NAD^+ + 2\ H^+ + 2\ e^- \rightarrow NADH + H^+$ $\qquad E_0'_{(NAD^+/NADH)} = -0.32$ V

$MB^+ + H^+ + 2\ e^- \rightarrow MBH$ $\qquad E_0'_{(MB/MBH)} = +0.01$ V

(I) $\mathbf{NADH + H^+ + MB^+ \rightarrow NAD^+ + MBH + H^+}$

$\mathbf{\Delta E_0'_{(I)} = +0.33\ V}$

$MB^+ + H^+ + 2\ e^- \rightarrow MBH$ $\qquad E_0'_{(MB/MBH)} = +0.01$ V

$½O_2 + 2\ H^+ + 2\ e^- \rightarrow H_2O$ $\qquad E_0'_{(O_2/\ H_2O)} = +\ 0.82\ V$

(II) $\qquad$ **$MBH + ½\ O_2 + H^+ \rightarrow MB^+ + H_2O$**

$\Delta E_0'_{(II)} = +0.81\ V$

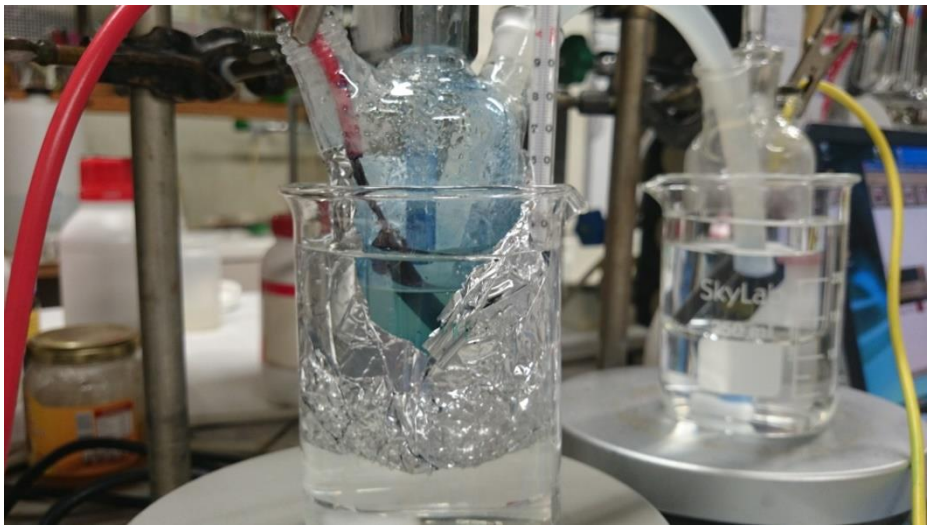

Fig. 6.1. Biofuel cell with the two chambers, on the right side the cathodic compartment and on the left side the anodic chamber connected by a salt bridge.

The previous equations connect the voltage output of the cell directly with the concentration of NADH, MB and oxygen in the chambers. The NADH dehydrogenase works as a catalyst in the anodic chamber and enhance the reaction between NADH and MB. The presence of the catalyst from 0 min caused an increase in the reduced methylene blue concentration, as demonstrated by the color of the solution that immediately turns from blue to colorless. In the absence of the enzyme the solution slowly turns from blue to pale blue.

The voltage and the power output of the cell were directly correlated to the concentration of MB in the reduced form in the anodic chamber (**Fig. 6.2**).

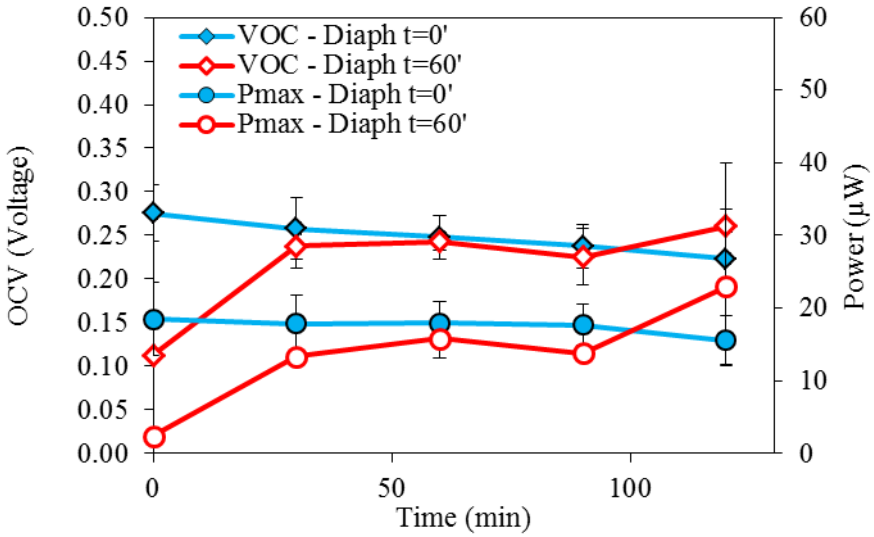

Fig. 6.2. VOC and maximum power generated over time by the biofuel cell in presence of NADH dehydrogenase added (closed symbols) before or (open symbols) 60 minutes after the first analysis.

The MB was able to transfer the electrons of the NADH directly to the electrode. The VOC registered at 0 min with low concentration of reduced methylene blue (0.11 ± 0.01 V) was 60% lower compared to the VOC with the highest reduced MB concentration (0.28 ± 0.03 V) and the maximum power produced (18 ± 5 µW) was 90% lower in the absence of the NADH dehydrogenase (2.4 ± 0.5 µW). The VOC and the power generated in presence of the enzyme from 0 mins generally followed the same decreasing trend over time, caused by the consumption of the reagents both in the anode and the cathode chambers.

The effect of the delayed addition of the NADH dehydrogenase was shown only at 0 min since 30 min before the addition of the catalyst the OCV and the power generated were comparable with the values registered in the presence of the catalyst. The discoloration of the solution, both in the presence or the absence of the NADH dehydrogenase, was not accompanied by the recoloring after closing the circuit and let that the electrons flow from the anode to the cathode. Therefore, the

efficiency of the overall reaction was limited by the poor kinetics of the oxidation of the reduced methylene blue at the anode or the slow oxygen reduction reaction.

Cyclic voltammograms of a 0.5 mM MB solution with and without NADH 5.00 mM were shown in **Fig.6.3**. The MB oxidation (upper) and reduction (lower) peaks were higher when NADH was added. NADH allowed more electrons to pass unidirectionally from NADH to the electrode via MB. These experiments established that transfer of electrons between oxidized and reduced forms of MB and NADH was reversible.

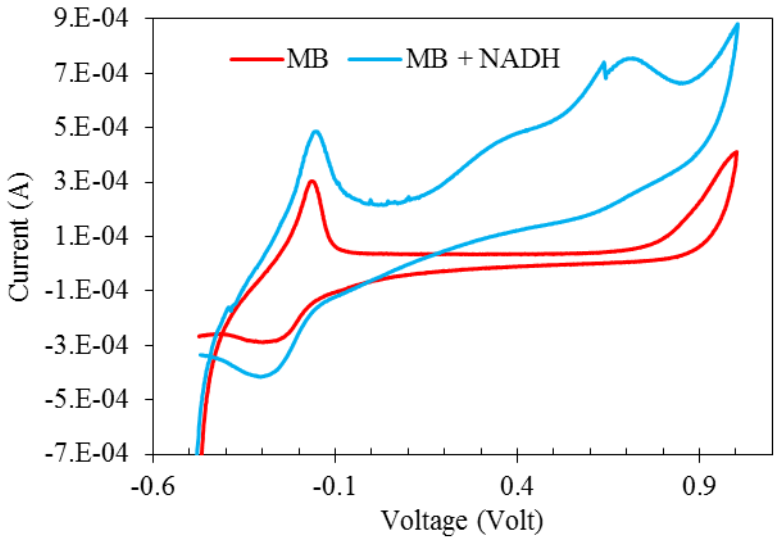

Fig. 6.3. Cyclic voltammogram obtained with a graphite electrode following introduction of the electrode into a 0.5 mM MB solution (red line) and 0.5 mM MB and 5.0 mM NADH.

Chapter 7

7.1 Correlation between glucose concentration and methylene blue reduction

As previously mentioned, the NADH into the living eukaryotic cells is mainly stored and then oxidized during the respiration process into the mitochondria. The presence of barriers to the diffusion of the methylene blue, like the external membrane and the mitochondrial membrane, could limit the overall process of mediated electron transfer. Therefore, in our view, was fundamental to evaluate the capability of the cells to reduce the MB, the effect of the substrate concentration on this reaction and consequently on the reduced MB concentration.

In biochemistry, methylene blue is a well–known redox indicator; in fact, the solution of the dye results blue, with a maximum adsorption at 664 nm, in oxidizing conditions while it is colorless when it is exposed to reducing agents (Mowry and Ogren, 1999) (**Fig. 7.1**).

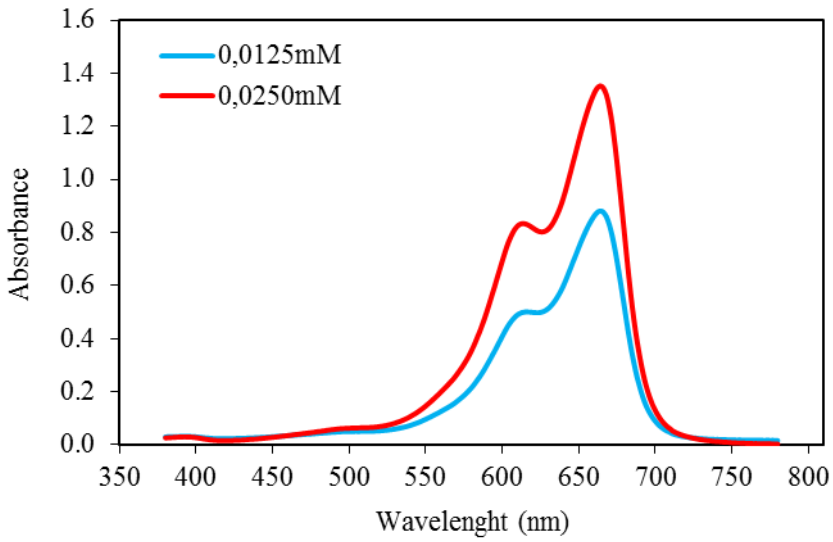

Fig. 7.1. Absorption spectrum of methylene blue in aqueous solution in two concentration.

The reduction of the methylene blue by the yeast cells was followed by recording the decolorization of the blue solution in the absence of oxygen as shown in **Fig. 7.2**.

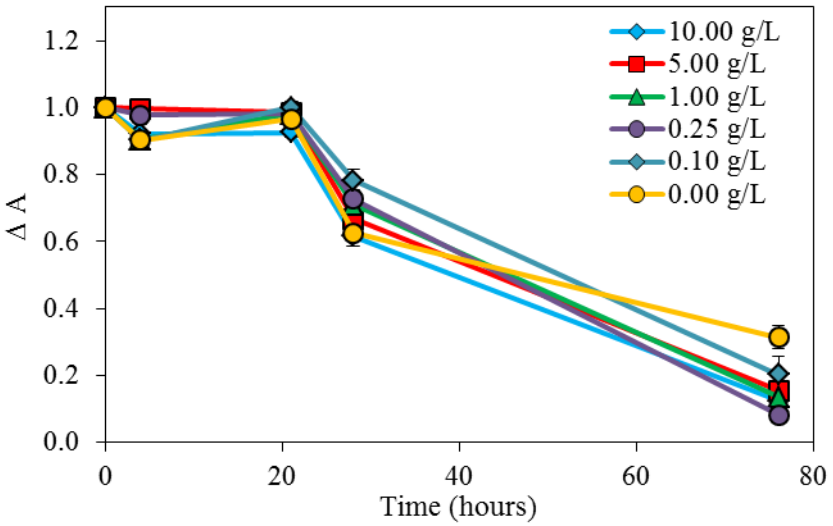

Fig. 7.2. Comparison of the absorbance variation at 664 nm over time in the presence of different concentration of glucose in solution.

Varying the concentration of glucose in solution did not affects the kinetic of the reduction of methylene blue in solution (**Fig. 7.2**). The initial lag phase of 20 h was probably due to some oxygen infiltrations into the cuvettes and to the not optimal growing conditions of the cells (just glucose, not minerals, vitamins and nitrogen).

7.2 Effects of the presence and absence of external carbon source in methylene blue reduction

In the absence of external carbon source the cells were able to reduce the MB in solution with similar rate of the experiments carried out in the presence of glucose. Rossi et al. (2016) demonstrated that this phenomenon was due to the presence of nutrients accumulated during the industrial production of the cells.

Suspension of yeast cells in phosphate buffer at pH 7.8 showed a fast reduction of methylene blue even in the absence of glucose as electron source. After 19h, the yeasts cell suspension was aerated causing the instantaneous oxidation of methylene blue. The cuvettes were then sealed again observing, consequently, a new reduction of the methylene blue. This redox cycle was repeated almost every 20h and the results in terms of normalized absorbance values of the solution were reported in **Fig. 7.3**. Alternation of methylene blue reduction and oxidation reactions into the yeast cell suspension in the absence of glucose suggested the presence of an unknown reduced compound in the solution which could be probably attributed to an accumulated residual carbon source from the yeast production or the presence of glycogen inside the cells (François and Parrou, 2001). After four cycles the reduction step of methylene blue in the absence of glucose did not takes place anymore as a consequence of the exhaustion of the accumulated carbon source into the yeast cells. Furthermore, after each redox cycle a progressive decrease in the concentration of the oxidized form of the methylene blue was observed. These results was probably due to a biochemical transformation of the methylene blue during the redox cycles as well as to its accumulation into the cells as demonstrated by Rossi et al., 2016 and May et al., 2004. This experiment shows that an electron acceptor like oxygen can immediately oxidize the reduced methylene blue in solution and it is possible to continuously repeat the redox cycle of methylene blue until there is enough carbon source in solution.

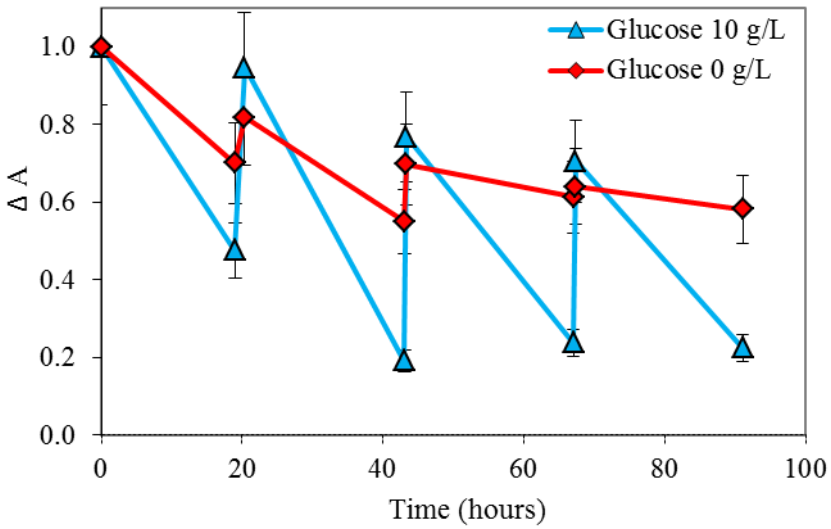

Fig. 7.3. Normalized values of absorbance at 664 nm carried out at different incubation times in the presence (blue line) or in the absence (red line) of glucose. After 19, 43 and 67 hours the solution was aerated.

7.3 Effects of methylene blue on Saccharomyces cerevisiae metabolism

The effects of the mediator on the *Saccharomyces cerevisiae* metabolism were tested by HPLC analysis on fermentation reactors with yeast incubated both in the presence and in the absence of the methylene blue, using glucose (27.8 mM) as electron donor (**Fig. 7.4A**). Chromatographic analysis at different times of incubation demonstrated that the glucose was completely depleted after 42 h both in the presence and in the absence of methylene blue (**Fig. 7.4B**). Furthermore, preliminary chromatographic analysis of the end–products showed different molecules produced by the yeast metabolism in the presence or absence of methylene blue (**Table 7.11**). This result suggested that methylene blue affected the yeast metabolism by activating new metabolic pathways to be deeply investigated in the next future.

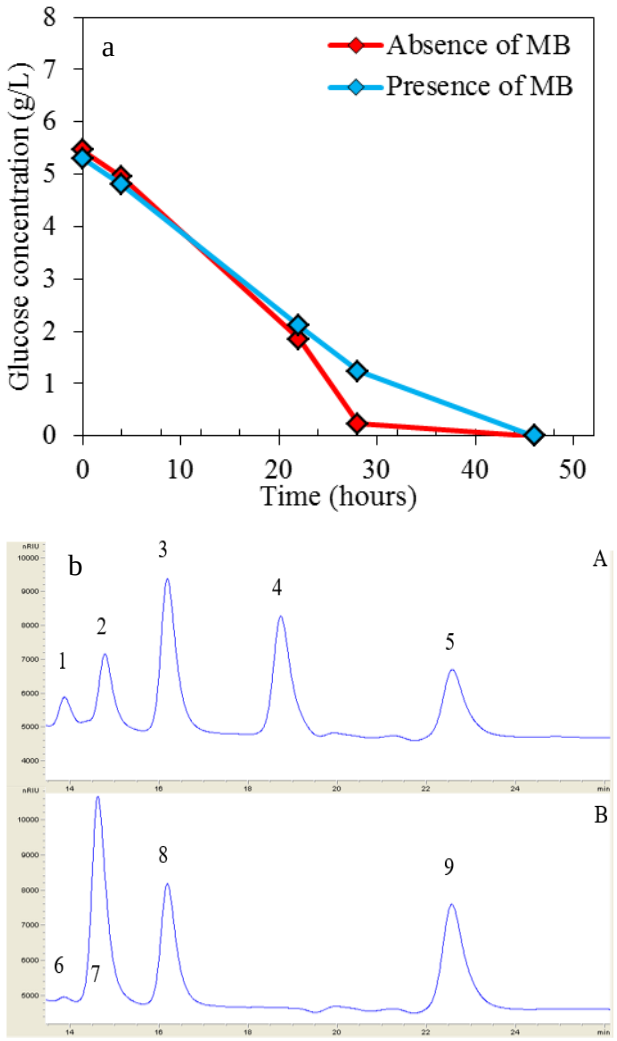

Fig. 7.4. Glucose consumption (a) and end–products of fermentation (b) in the absence (A) and in the presence (B) of methylene blue (MB).

Table. 7.1. HPLC analysis data of crude samples of fermentation broth in the presence or the absence of methylene blue after 42 hours of incubation.

Peak number	Presence/Absence of MB	Compound	Retention time (min.)	Concentration (mM)
1	Absence	Lactic acid	13.8	1.17
2	Absence	Glycerol	14.7	2.00
3	Absence	Acetic acid	16.1	11.40
4	Absence	Unknown	18.7	/
5	Absence	Ethanol	22.5	1.00

6	Presence	Lactic acid	13.8	0.14
7	Presence	Formic acid	14.6	2.27
8	Presence	Acetic acid	16.1	8.70
9	Presence	Ethanol	22.5	1.54

7.4 Effect of each component on the MFC performance

In this work, the power production is not as interesting as the microorganisms that grow onto the anode and most important as the identification of the electron transfer mechanism in the anodic compartment. Despite the high internal resistance, the simplest lab–scale design with two chambers and a salt bridge as electrolyte permitted to evaluate the effects of some different operative conditions such as the organic load and the concentration of the electron donor (Logan, 2008).

Yeast worked as biocatalyst in the MFC using glucose in the anode chamber as the only carbon source, the electrons derived from the oxidation of glucose were accepted by oxygen in the cathodic chamber. Open circuit voltage (OCV) and power produced (P) resulted closed to zero in the presence of only glucose while, in the presence of only methylene blue, increasing values of OCV (0.24 V) and power (14 μW) after 400 minutes were observed (**Fig. 7.5**). The contemporary presence of glucose and methylene blue led to a further increase of OCV and of the power generated at 0.27 Volt and 22 μW. These trends could be explained by a progressive accumulation of the reduced methylene blue in solution due to both the reductive condition in the anode chamber and the presence of reducing sugars such as glucose.

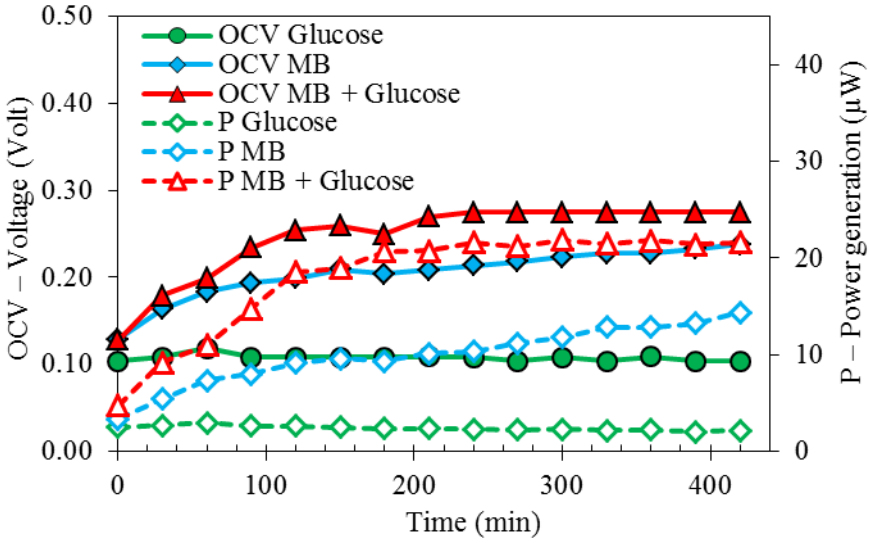

Fig. 7.5. Comparison of open circuit voltage (OCV) and power (P) produced, carried out in the presence of each single component (glucose, methylene blue (MB) 5.00 mM) or in different combinations.

In the presence of the yeasts, the reduction of methylene blue increased largely as demonstrated by the discoloration of the solution in the anode chamber. OCV reached the maximum values of 0.46 V after 30 min, 0.15 V in the absence of the mediator, and the maximum power generated was 65 µW after 60 min while the power registered without MB was 5 µW. The performance of the cell followed opposite trends in the presence or in the absence of methylene blue, the power produced with the mediator decreased over time to a final 48 µW and an OCV of 0.40 V. Without MB, the end products of the fermentation reduced the electrode and more the incubation time, more the performance of the MFC that grew to 51 µW and 0.42 V. The yeast had a great potential in reducing methylene blue, showing an important role in enhancement of the bioelectricity generation of the MFC (**Fig. 7.6)**.

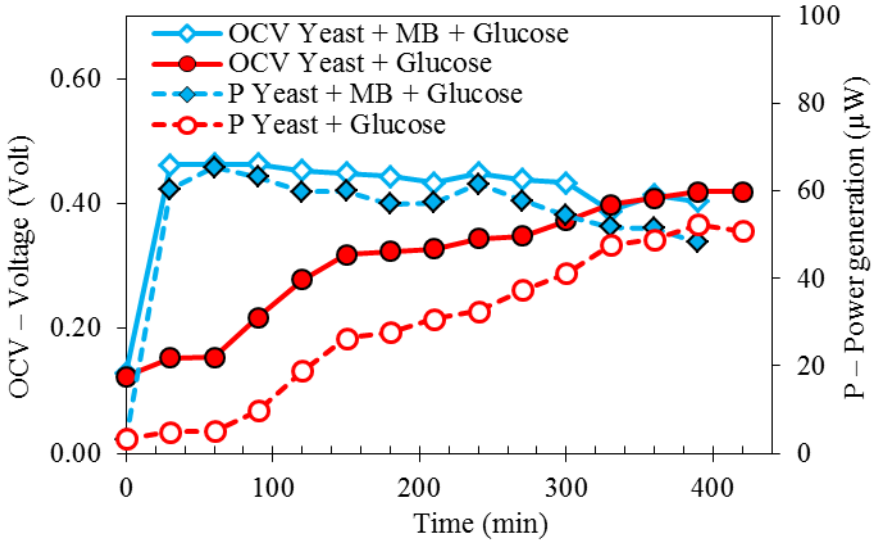

Fig. 7.6. Comparison of Open Circuit Voltage (OCV) and power (P) carried out by the MFCs in the presence or absence of MB as electron mediator.

Electron mediators, such as methylene blue, were demonstrated necessary to improve the power output of the MFC (Najafpour et al., 2010), even though methylene blue showed a positive answer to the current generation also in the absence of the yeasts. The solution in the anode chamber did not turn blue when the circuit of the electrochemical cell was closed as shown in **Fig. 7.2** and **Fig. 7.3**. Thus, the slow step of the reaction was related to a limited diffusion of the reduced methylene blue to the electrode in the anode compartment and/or to a weak electrons transfer from the electrode to the oxygen in the cathode compartment. Furthermore, the negative slope of the power density of the MFC in the presence of yeast, methylene blue and glucose was related to the depletion of oxygen in the cathode chamber and the slow rate of oxygen diffusions in solution.

7.5 Effect of glucose concentration on MFC performance

The concentration of glucose did not affects the concentration of reduced MB produced by the *S. cerevisiae* (**Fig. 7.2**), however, the effect of the substrate concentration should be tested on the MFC output. For this reason, were tested

three different MFCs using different concentrations of glucose in solution, the effect is shown in terms of OCV and power produced (**Fig. 7.7**).

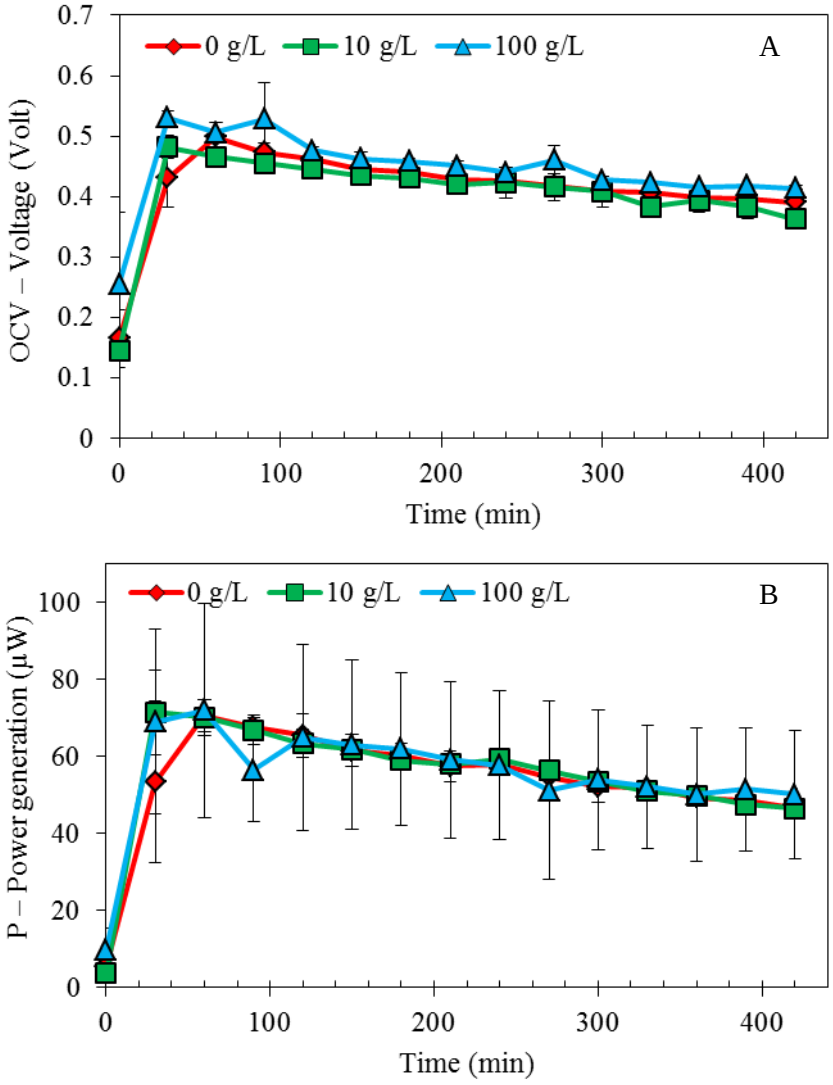

Fig. 7.7. Comparison of (A) OCV and (B) power produced over time in presence of different concentration of glucose in solution.

The OCVs output were similar for all of the reactors and followed the same trend with and initial low performance registered at 0 min and then increased to the maximum value of the series to 0.53 ± 0.01 V (100 g/L), 0.48 ± 0.02 V (10 g/L)

and 0.43 ± 0.05 V (0 g/L). The decrease over time of the OCV was comparable for all of the reactors and caused by the depletion of the reagents both in the anode and the cathode chambers. The last point at 420 min showed the highest performance by the 100 g/L MFCs (0.41V), followed by the 0.39 ± 0.02 V of the MFCs without glucose in solution. The OCV at 420 min of the MFCs with 5 g/L of glucose in solution was 0.36 V.

The power generated by the MFCs were similar for all of the experiments showing large variability for the MFCs with 100 g/L of glucose. The power production at 0 min were under 10 µW for all of the reactors, followed by an increase at 30 min where the MFCs with 10 g/L showed the largest power produced over time (72 ± 11 µW). The MFCs without substrate in solution and with 100 g/L of glucose showed the highest power production after 60 mins, in the series, the MFCs with 100 g/L produced 72 ± 28 µW and 71 ± 4 µW was produced without additional glucose in solution. The same decreasing trend observed for the OCV was followed also by the power generation, the power registered at 420 mins was 47 ± 1 µW (0 g/L), 46 µW (10 g/L) and 50 ± 17 µW (100 g/L). The higher variability of the power registered with the highest concentration of glucose (100 g/L) was related to a large variability in the current produced by the cell, related to small changes in the area of the electrode submerged in the anodic chamber (SCC ranged from 471 µA to 823 µA).

The decreasing of the OCV and of the power generated was related to the depletion of the reagents of the redox reaction, both in the anode and the cathode chambers, where glucose, if present, was consumed by the yeast cells while oxygen in the cathode chambers reacts with the electrons on the cathode producing water as a product. The small differences in the OCV and the power produced over time was due to the increased conductivity of the solution by the addition of salts and the parameters of the cell were not affected by the presence of substrate in the first 7 hours of reaction.

Increasing the time of the experiment did not alter the results (**Fig. 7.8A** and **Fig. 7.8B**), after 22 hours the voltage registered by the MFCs with different glucose concentration were comparable between them (0.55 V, 0 g/L; 0.52 V, 10 g/L; 0.49 V, 100 g/L), even though the potential was higher than previously registered (**Fig. 7.7**). After 7 hours of measurements the OCV decreased to 0.44 V (0 g/L), 0.40 V (10 g/L) and 0.38 V (100 g/L). The final point was registered after 46 hours from the first measurement and the OCV increased again proportionally to the substrate concentration, the measured open circuit potential was 0.46 V (0 g/L), 0.50 (10 g/L) and 0.52 (100 g/L). The power produced by the MFCs followed the same general trend of the OCV with the first point inversely proportional to the glucose concentration (96 µW, 0 g/L; 81 µW, 10 g/L; 65 µW, 100 g/L) and a progressive decrease after 7 hours of measurements (69 µW, 0 g/L; 49 µW, 10 g/L; 42 µW, 100 g/L). The last power density registered after 46 h showed an inversion and the performance were proportional to the glucose concentration (63 µW, 0 g/L; 75 µW, 10 g/L; 87 µW, 100 g/L).

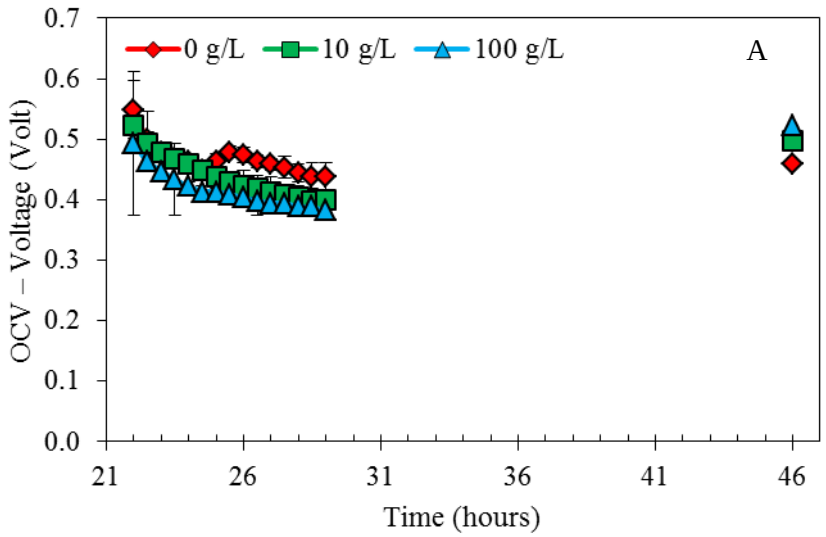

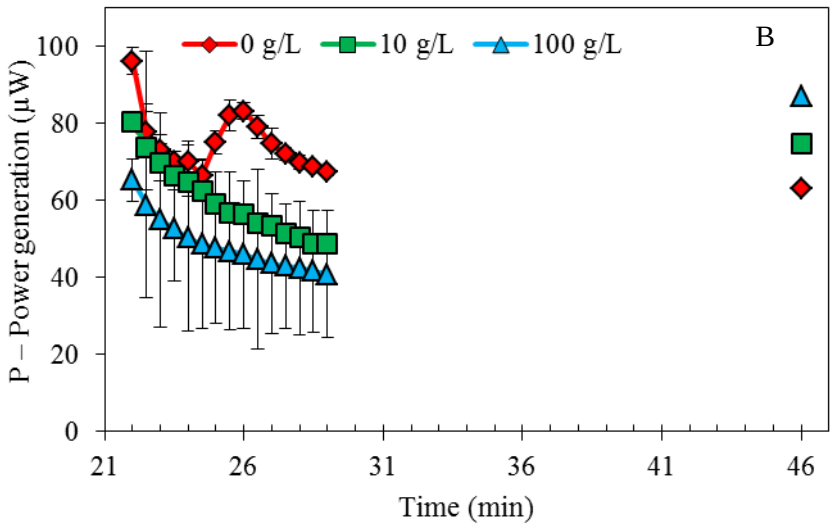

Fig. 7.8. Comparison of (A) OCV and (B) power produced over time in presence of different concentration of glucose in solution after 22 h of incubation.

The smaller increase in the OCV and the power produced after 46 hours could be related to the depletion of the nutrients in the anode chamber, however, from these experiments it was not possible to associate a correlation between the glucose concentration and the MFC output.

The color of the solution in the anode chamber was monitored during the long term experiment and a slightly decrease of the intensity of the blue color over time was observed (**Fig. 7.9**).

Fig. 7.9. Pictures of the anodic solution (from left to right) after 22 h, 25 h, 27 h, 29 h.

The decrease in the color intensity was related to the reduction of the MB and since closing the electrical circuit did not cause the re–oxidation of the MB, the limiting step of the reaction should be investigate into the discharge of the electron mediator (MB) on the anode or the oxygen reduction reaction.

7.6 Effect of methylene blue concentration on MFCs performance

The concentration of the methylene blue affected the last stage of the electrochemical process in the anode compartment and the mediator is also involved in the diffusion in and out of the cell to be reduced by the NADH and oxidized by the electrode. In order to investigate the effects related to the presence of methylene blue as well as the concentration of the latter in the anode compartment five different experiments were carried out using different concentrations of MB in solution (**Fig. 7.10A** and **7.10B**). To study the MFCs performance at their best operational condition the OCV and the power density were registered after 22 h and 46 h.

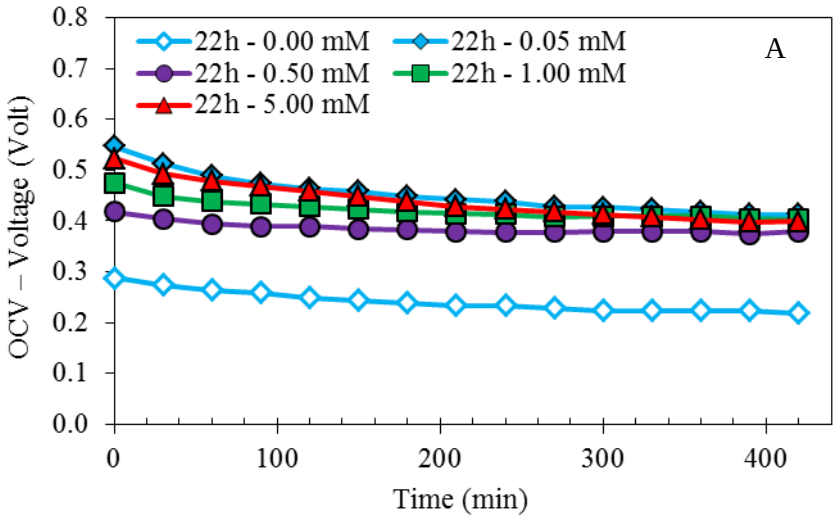

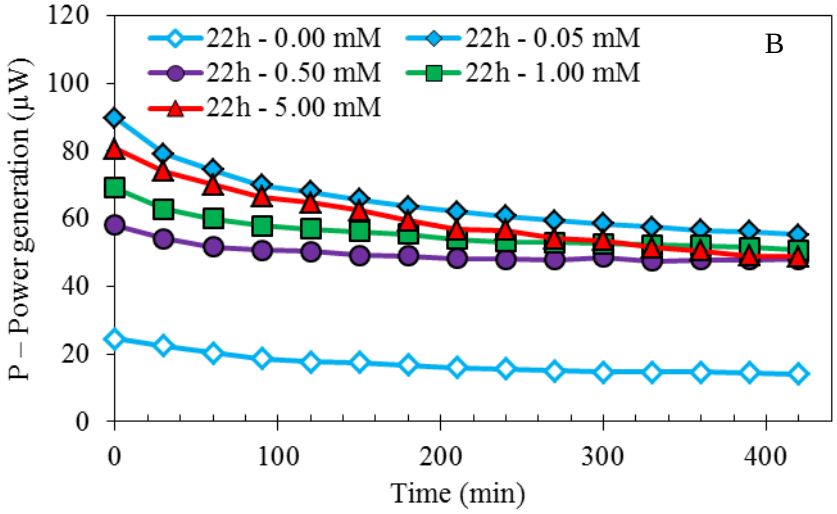

Fig. 7.10. Comparison of (A) OCV and (B) power produced over time after 22 h of incubation in presence of different concentration of methylene blue in solution.

The highest OCV was obtained by the lowest concentration of MB (0.55 V, MB 0.05 mM), followed by the MFC with the highest concentration (0.52 V, MB 5.00 mM), before the 1.00 mM (0.47 V) and 0.50 mM (0.42 V). In the absence of the mediator the performance of the MFC were just the 56% (0.29 V) of the MFC with 0.05 mM of MB. These results confirmed that the exogenous mediators such as methylene blue are a necessity since *Saccharomyces cerevisiae* is not known to produce such mediators indigenously (Gunawardena et al., 2008). All of the MFCs showed decreasing performance over time and the OCV reached after 7 hours of measurent was comparable for all of the experiments with the mediator (0.40 ± 0.01 V). The experment carried out in the absence of MB showed a decrease to 0.22 V.

The power generated in the presence of 0.05 mM of MB was the highest with 90 µW and then 5.00 mM (81 µW), 1.00 mM (69 µW) and 0.50 mM (58 µW). In the absence of the mediator the power produced was 25 µW. At the end of the experiment the power produced by the MFCs in the presence of any mediator concentration was close and comparable (49 µW, 5.00 mM; 51 µW, 1.00 mM; 48

µW, 0.50 mM; 55 µW, 0.05 mM), due to the establishment of a steady state, limited by the diffusion of the oxygen in the cathodic solution, indipendent from the concentration of MB. The power generated at the end of the experiment was higher compared to the setup without the mediator (14 µW).

Waiting 46 hours after executing new experiments lowered the performance of the MFCs as previously observed (**Fig. 7.11A** and **7.11B**). The maximum OCV (0.50 V) was observed by the MFC with the highest concentration of MB (5.00 mM) while all the others MFCs in the presence of MB showed similar performance (0.42 V). The performance were most stable over time with a low decrease in the OCV after 7 hours (0.43 V, 5.00 mM; 0.40 V, 1.00 mM; 0.38 V, 0.50 mM; 0.41 V, 0.05 mM). The MFC in the absence of MB showed stable and lower performance in respect to 22 h, with the OCV that decreased from 0.25 V to 0.18 V. The power produced by the MFC with the highest concentration of mediator of 5.00 mM was the highest (75 µW) and decreased to 60 µW after 420 minutes. In the absence of MB the initial power generated was 16 µW and decreased to 8 µW after 420 min. All the other MFCs showed stable power generation around 50 ± 6 µW for all of the experiment.

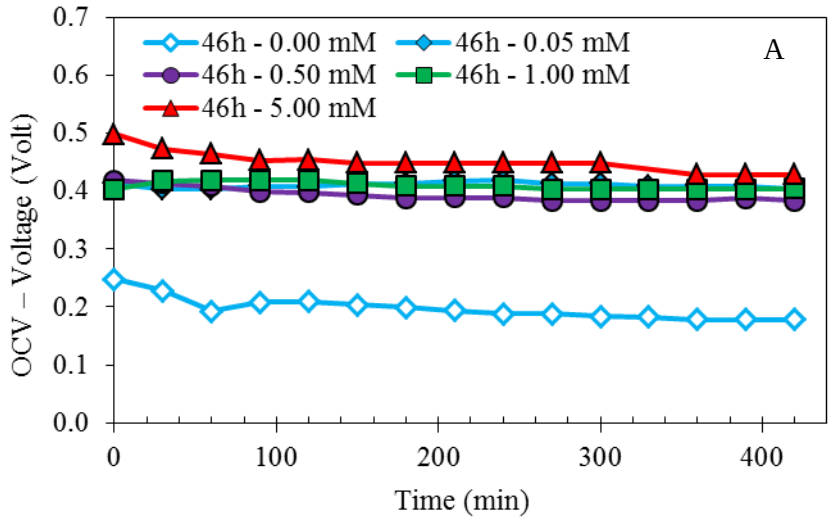

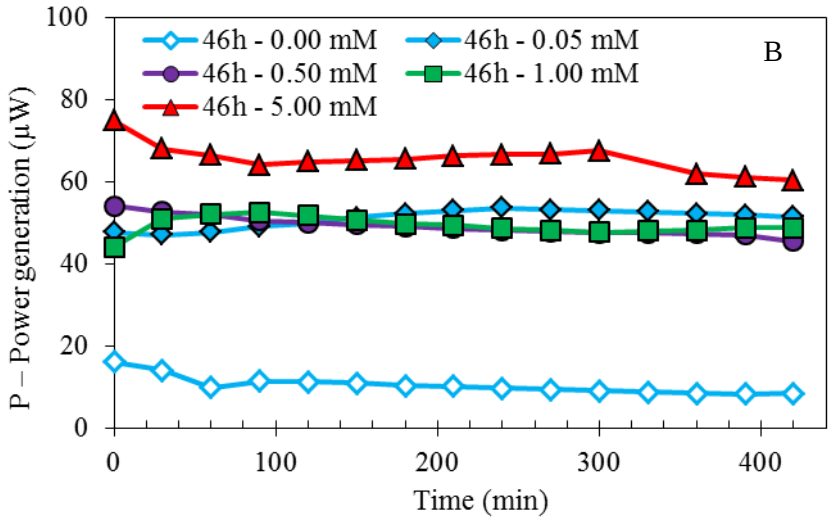

Fig. 7.11. Comparison of (A) OCV and (B) power produced over time after 46 h of incubation in presence of different concentration of methylene blue in solution.

Plotting the OCV and the maximum power registerd after 22 and 46 hours against the MB concentration (**Fig. 7.12A** and **7.12B**) showed a strong influence of the mediator concentration on the performance of the cell. OCV and power produced were lower after 46 hours due to the depletion of oxygen in the cathodic compartment and of nutrients in the anodic compartment. Both OCV and power generated followed an hyperbolic model but the high variability of the oxygen concentration in the cathode compartment caused oscillations in the response of the MFC.

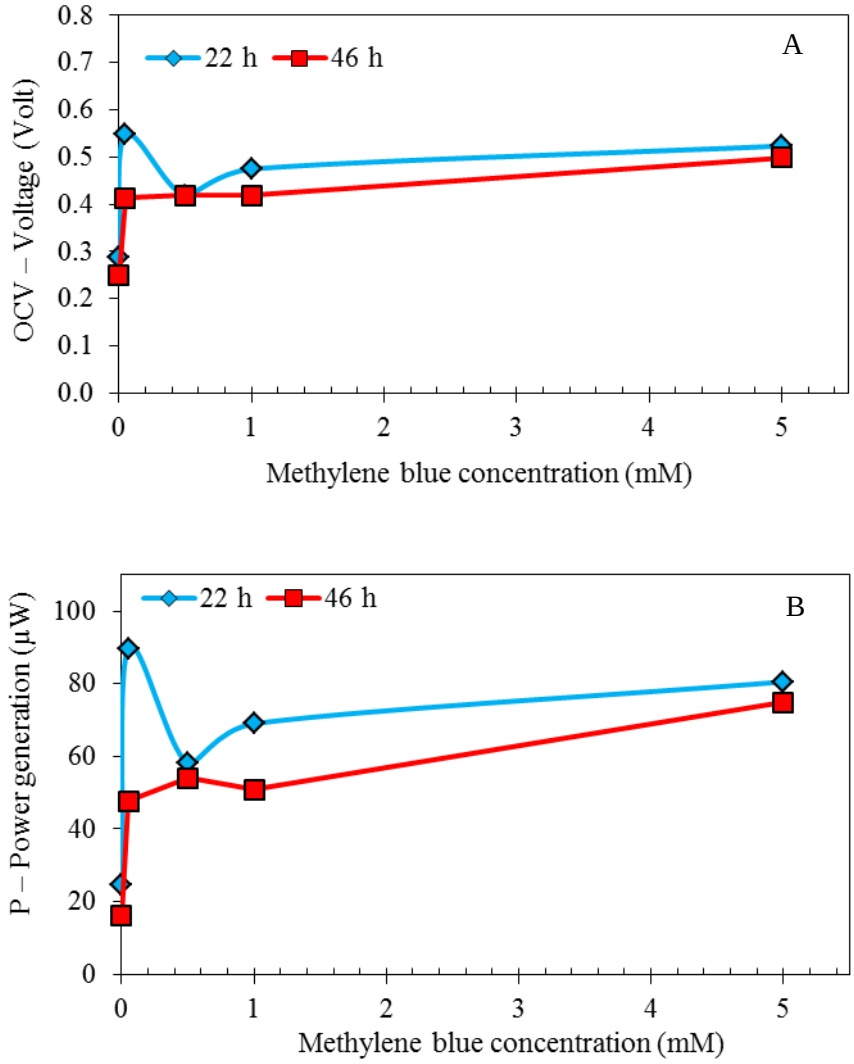

Fig. 7.12. Comparison of (A) OCV and (B) power produced after 22 h and 46 h of incubation in presence of different concentration of methylene blue in solution.

For these reasons, the output of the cell was evaluated using a more stable electron acceptor in the cathodic compartment.

Chapter 8

8.1 Hydrogen peroxide as terminal electron acceptor in cathodic chamber

In the previous experiments, the presence of oxygen in the cathodic chamber represented a limiting factor in the control of the electron acceptor concentration. On this basis, oxygen was replaced by hydrogen peroxide and the open circuit voltage and the power generated under different operative conditions of the MFCs were recorded. The overall reactions using hydrogen peroxide as electron acceptor changed as follow:

$MB^+ + H^+ + 2\ e^- \rightarrow MBH$ $\qquad E_0'_{(BM+/BMH)} = + 0.01$ V

$H_2O_2 + 2\ H^+ + 2\ e^- \rightarrow 2\ H_2O$ $\qquad E_0'_{(H_2O_2/H_2O)} = + 1.76$ V

(I) $\qquad$ **$MBH + ½\ O_2 + H^+ \rightarrow MB^+ + H_2O$**

$\Delta E_0'_{(II)} = +1.75$ V

An increase in the theoretical OCV of the MFCs was observed, however, the aim of this thesis was to better understand the electron transfer mechanism in the anode compartment, rather than improving the power production of the cell, and the stabilization of the OCV and the power produced over time given by the presence of highly concentrated electron acceptor was fundamental in the study of the electron transfer mechanism (Logan, 2008).

The operative conditions of the microbial fuel cells were chosen in order to have a similar behavior to that observed using oxygen as electron acceptor even if OCV and power in the presence of methylene blue 5.00 mM and glucose 5 g L^{-1} resulted higher in the presence of oxygen at the cathode (**Fig. 8.1**).

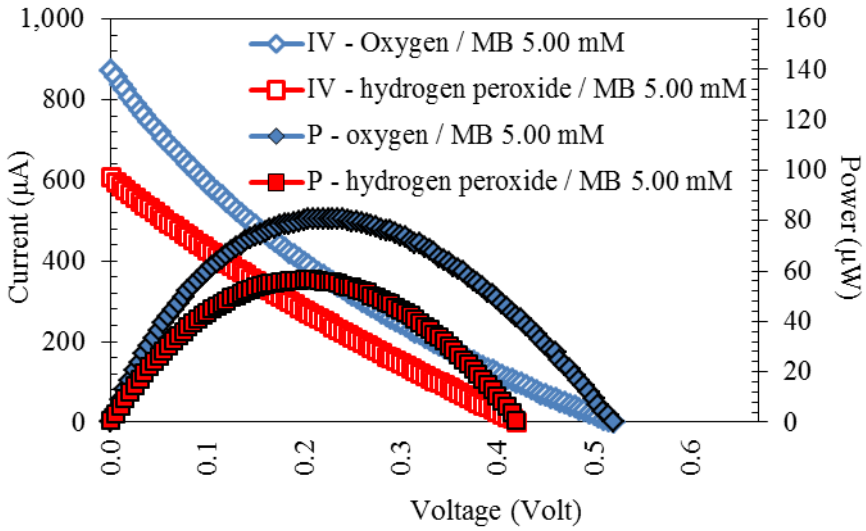

Fig. 8.1. MFC i–V polarization curve (IV) and power generated (P) using oxygen as electron acceptor in presence or absence of methylene blue (5.0 mM); and with hydrogen peroxide (4.41 $molL^{-1}$)as electron acceptor in the presence of methylene blue (5.0 mM).

Due to presence of the resistance, the power and voltage registered were considered as operational electricity. Using methylene blue as electron mediator in the anaerobic compartment of an yeast catalyzed MFC resulted in maximum power of 81 µW, the OCV was 0.52 V and the short circuit current (SCC) 870 µA. Replacing the terminal electron acceptor with hydrogen peroxide resulted in OCV of 0.42 V and the maximum power registered was 57 µW while the SCC dropped to 419 µA. Even though the reduced performance of the MFC using hydrogen peroxide as electron acceptor in the cathodic compartment, oxygen was replaced with hydrogen peroxide due to the more stability in terms of OCV, power and current generated over time (Rossi and Setti, 2016). The influence of the mediator concentration and electron acceptor concentration on battery output was investigated. Several concentrations of hydrogen peroxide (0 M; 0.2 M; 0.9 M and 4.4 M in PB 25 mM pH 6) were evaluated at fixed methylene blue concentration

(5.0 mM). The results of the i–V curves after 22 hours of incubation, are shown in **Fig. 8.2A** and **Fig. 8.2B** in terms of OCV and power produced.

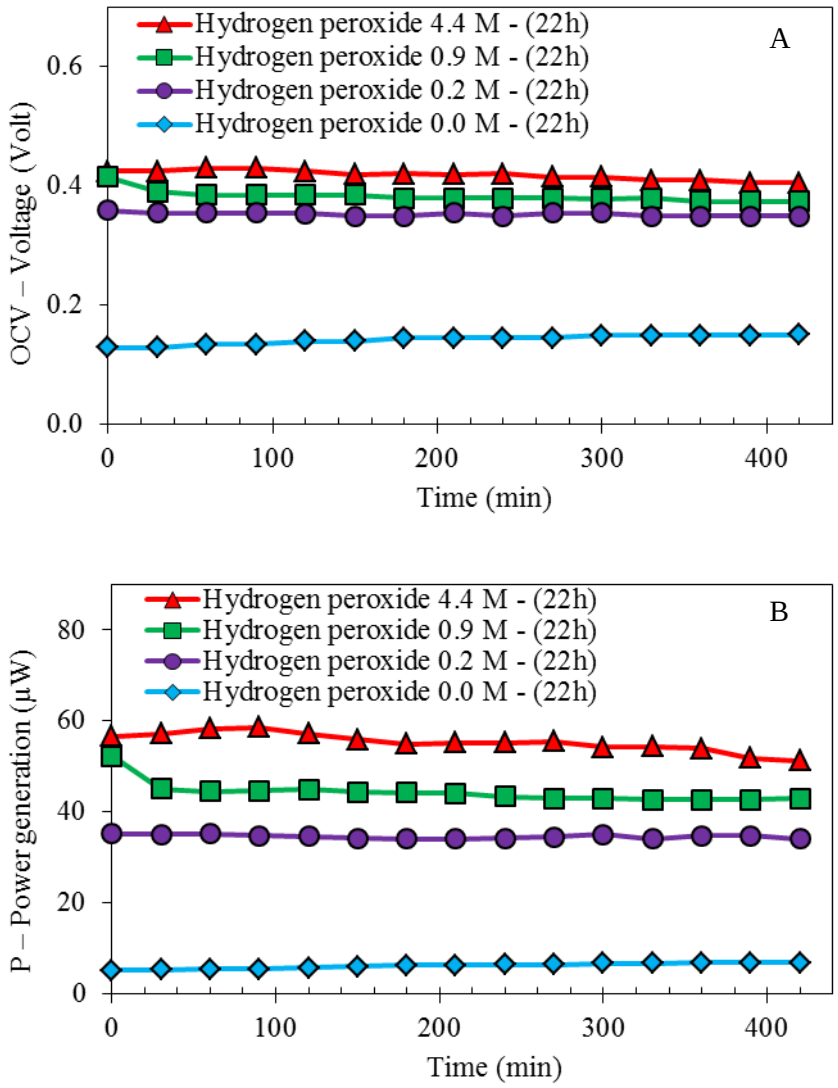

Fig. 8.2. Comparison of (A) OCV and (B) power produced over time after 22 h of incubation in presence of different concentration of hydrogen peroxide in solution.

The concentration of the hydrogen peroxide in the cathode compartment greatly affected the performance of the MFCs. As previously mentioned, the power output

and the OCV of the cells was more stable with a maximum slope of $–6 \cdot 10^{–5}$ observed for the OCV with hydrogen peroxide at a concentration of 4.4 M and $–1 \cdot 10^{–2}$ observed for the power produced by the MFCs with the same configuration but using oxygen as the electron acceptor. The initial OCV (0.42 V) and the power generated (57 µW) were lower than previously observed using oxygen as electron acceptor (0.52 V; 81 µW MB 5.00 mM – 22h). The MFC with the highest concentration of hydrogen peroxide (4.4 M) performed better (0.42 V; 57 µW) in terms of OCV and power produced, followed by the 0.9 M (0.42 V; 52 µW) and the 0.2 M (0.36 V; 35 µW). The MFC without the hydrogen peroxide produced the lowest OCV (0.13 V) and power (5 µW), the output in the absence of hydrogen peroxide was due to the reduction of water and hydrogen ions in the cathodic chamber since the oxygen was stripped by purging pure nitrogen into the solution for 22h prior to the analysis. After 46 hours the circuit was closed again to observe any changes in the performance of the MFCs related to the higher concentration of reduced methylene blue in the anode chamber (**Fig. 8.3A** and **Fig. 8.3B**).

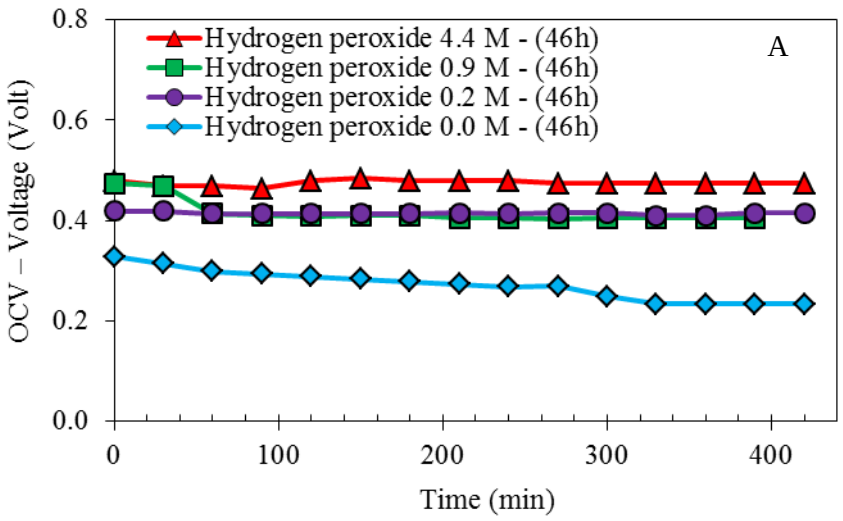

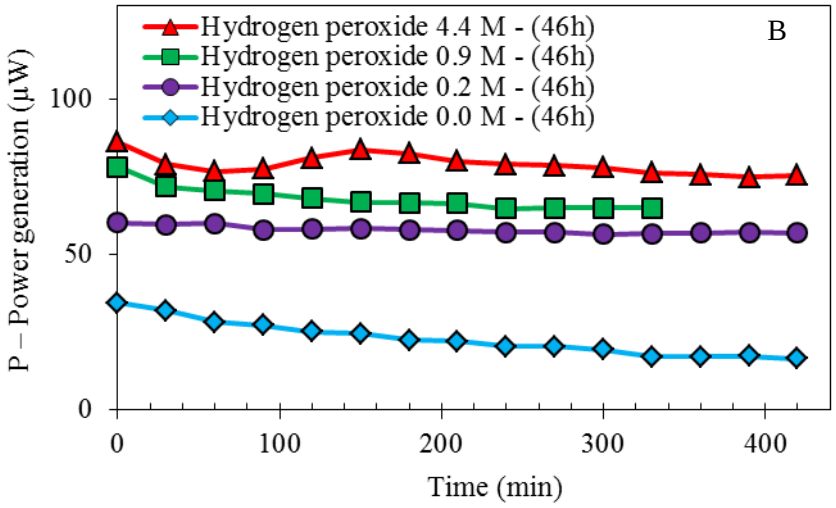

Fig. 8.3. Comparison of (A) OCV and (B) power produced over time after 46 h of incubation in presence of different concentration of hydrogen peroxide in solution.

The MFCs performance were higher after 46 h of incubation, producing more power and showing higher OCVs due to the increased concentration of the reduced methylene blue in the anodic chamber. The OCV shifted from 0.42 V to 0.48 V while the power produced increased of the 51% from 57 µW to 86 µW in the presence of 4.4 M hydrogen peroxide. The MFC with 0.9 M hydrogen peroxide showed very stable OCV (0.41 V) and power (54 µW) similar to that observed after 22 h while a final OCV of 0.42 V (17% increase) and power generated of 60 µW (70 % increase) was registered with hydrogen peroxide 0.2 M. The OCV and power increased also in the absence of hydrogen peroxide to 0.33 V and 34 µW.

The OCV and the power registered after 22 h and 46 h followed an hyperbolic model, as shown by the panel in each figure, in respect to the hydrogen peroxide concentration evidencing a saturation of the cell response at the hydrogen peroxide concentration close to 0.9M. In order to determine if the saturation was due to the anode or cathode chamber, the concentration of the electroactive species in the anode compartment was increased increasing the lag phase until the complete discoloration of the aqueous solution, waiting for the methylene blue in reduced

form. The results of polarization curves showed higher values of OCV and SCC when the lag phase was 46 h. Our findings demonstrated that the electrochemical reaction was limited by the anode chamber (**Fig. 8.4A** and **Fig. 8.4B**).

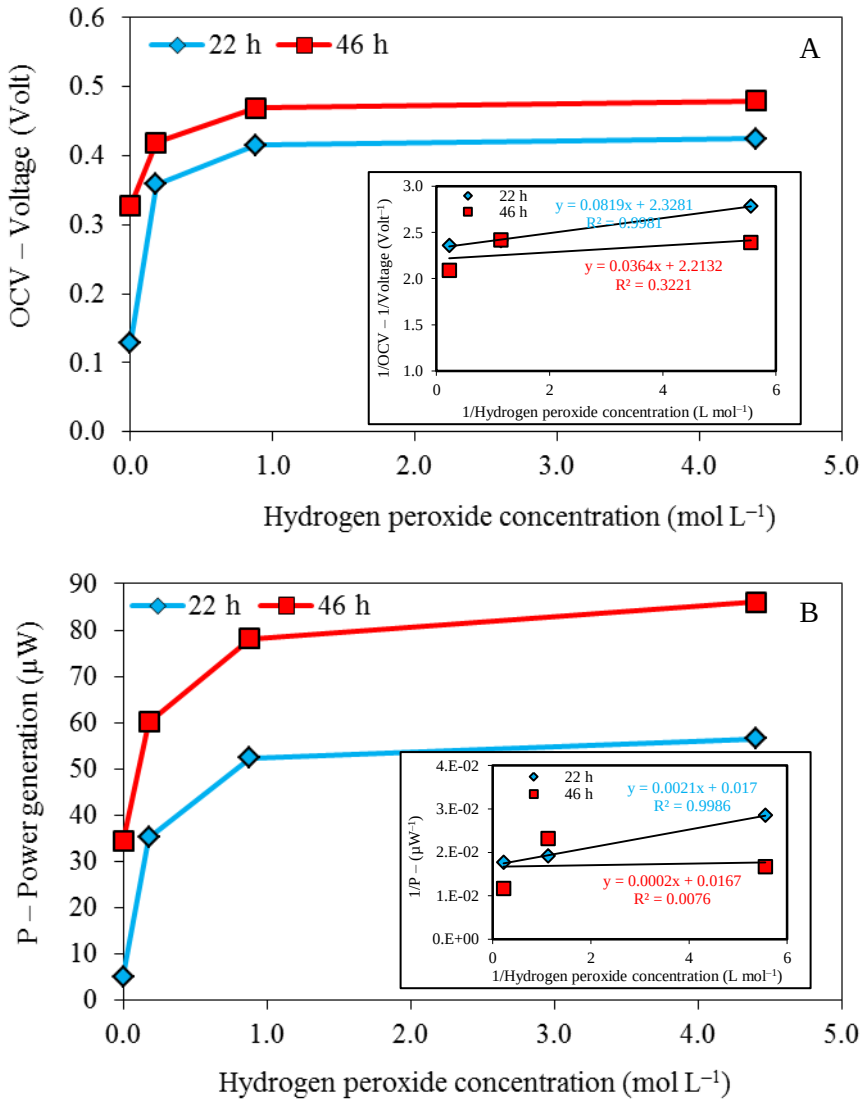

Fig. 8.4. Comparison of (A) OCV and (B) power produced after 22 h and 46 h of incubation in presence of different concentration of hydrogen peroxide in solution.

However, these findings were not confirmed by the values of OCV and power generated at different concentration of mediator using hydrogen peroxide as electron acceptor in the cathodic chamber. The experiments were carried out at different concentrations of MB (0.01 mM, 0.05 mM, 0.50 mM and 5.00 mM) and the OCV and the maximum power produced from the polarization curves are reported in **Fig. 8.5A** and **Fig. 8.5B**. The electrochemical experiments were carried out after a variable lag phase led to the complete reduction of the methylene blue, this reaction could be followed by the discoloration of the aqueous solution, which is blue when the mediator is oxidized and colorless when reduced.

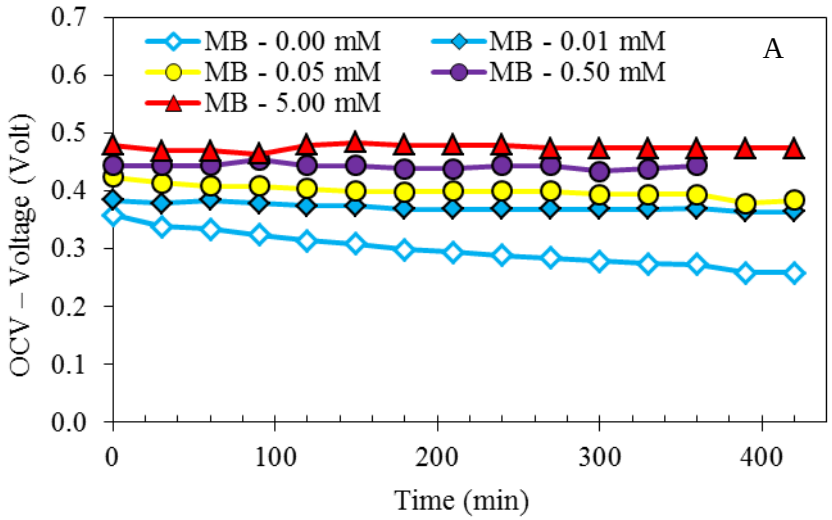

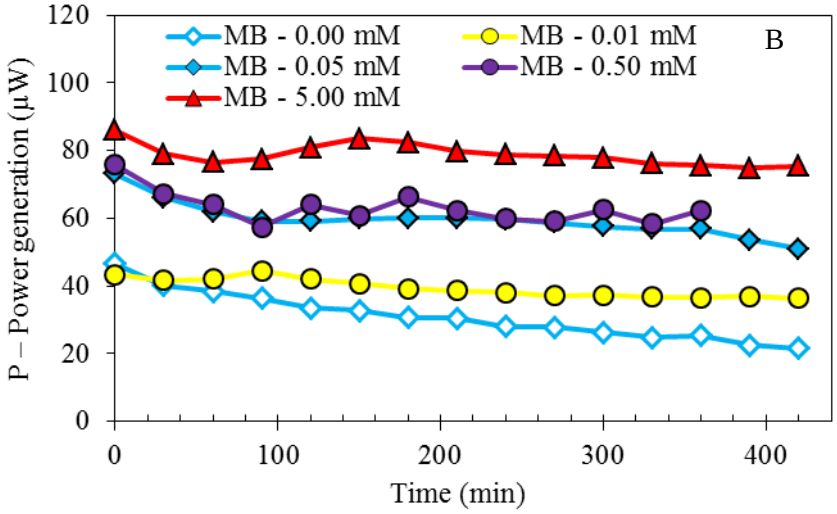

Fig. 8.5. Comparison of (A) OCV and (B) power produced over time after 46 h of incubation in presence of different concentration of methylene blue in solution.

The initial OCV registered by the MFC increased by increasing the mediator concentration. The reactor without MB produced 0.36 V and 0.38 V were registered in the presence of 0.01 mM of mediator, the other concentrations resulted in 0.42 V (0.05 mM), 0.44 V (0.50 mM) and 0.48 V (5.00 mM). The OCV decreased during the experiment and the largest drop (– 30%) was observed in the absence of the mediator to a final OCV of 0.26 V. The MFCs with MB in the anodic solution dropped of less than 10% and the final OCV were 0.36 V (0.01 mM), 0.38 V (0.05 mM), 0.44 V (0.50 mM) and 0.47 V (5.00 mM).

The power generated followed the same general trend of the OCV with a large gap in the initial power between the experiments without MB and with 0.01 mM and the three reactors with the higher MB concentration. The initial power produced was 47 µW in the absence of MB, 44 µW with 0.01 mM and shifted to 73 µW (0.05 mM), 76 µW (0.50 mM) and 86 µW (5.00 mM). The decrease over time of the power was higher in the absence of mediator and the performance registered at the end of the experiment was 22 µW while 7 hours of polarization curves

affected the final power generated by decreasing it to 36 µW (0.01 mM), 51 µW (0.05 mM), 62 µW (0.50 mM), 76 µW (5.00 mM).

The performance of the MFCs after the complete reduction of the methylene blue as observed in **Fig. 7.9** were correlated to the concentration of the mediator in solution, but not directly. The MFCs with the highest concentration of the mediator showed similar performance in respect to the MFCs with 0.50 mM and 0.05 mM of MB while has been observed a large gap between the MFCs with 0.01 mM and in the absence of MB. The initial point of each set of experiment was reported in **Fig. 8.6** and the proposed model followed by the values was validated in **Fig. 8.7**.

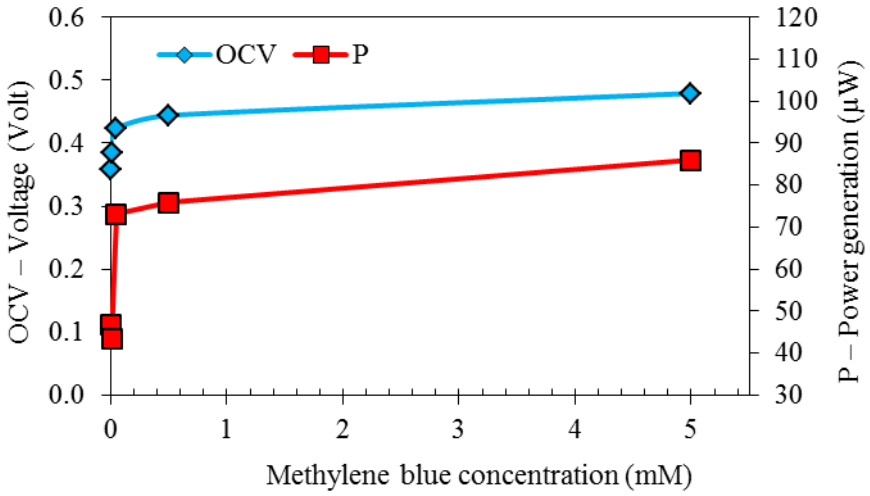

Fig. 8.6. OCV and power generated by the MFCs at different times of starvation in the presence of different concentration of methylene blue in the anodic solution.

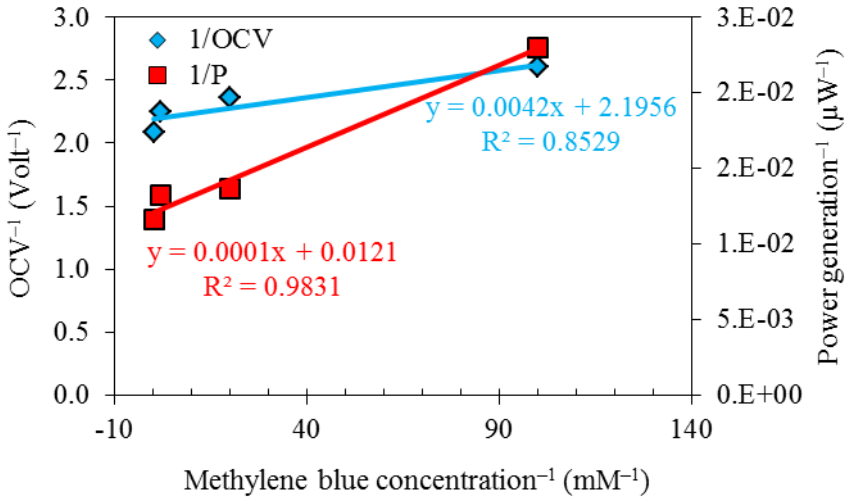

Fig. 8.7. Comparison of OCV^{-1} and power $produced^{-1}$ over time at different times of starvation in respect to the inverse of the methylene blue concentration at which the values were achieved.

The electrochemical experiments were started after the complete reduction of the methylene blue in anode chamber between 22 h and 46 h of lag phase. The OCV and the power produced followed an hyperbolic model showing a saturation of the cell response when the concentration of the mediator was higher than 0.01 mM and the electrochemical reaction would be independent to the mediator concentration into the bulk of the aqueous solution in the range 0.05 mM – 5.00 mM. These results were apparently in conflict with previous discoveries obtained by varying the concentration of the hydrogen peroxide.

These findings demonstrates that the MFCs performance was limited not by the reduction reaction of the hydrogen peroxide, when the concentration of the latter was higher than 0.9 M, nor by the oxidation of the mediator when the methylene blue concentration was at least 0.05 mM nor by the reduction of the mediator operated by the yeast cells since the discoloration of the solution. The limiting step must be searched in the capability of the biocatalyst to address the mediator in the

reduced form to the electrode surface rather than on the ability of the MB to interact with the anode.

The development of a diffusive regime in the anodic compartment was investigated by submerged the anode into the fermentation broth and register the polarization curves just after the complete reduction of the mediator, in order to outline if the anode reaction was limited by the diffusion of the reduced mediator on the electrode or by the adhesion of the cells on the anode. After different times of starvation the methylene blue was completely reduced and the anodic solution resulted discolored (**Fig. 7.9**), the electrode was then inserted in solution, the cell circuit was closed and the i–V curves were recorded (**Fig. 8.8A** and **Fig. 8.8B**).

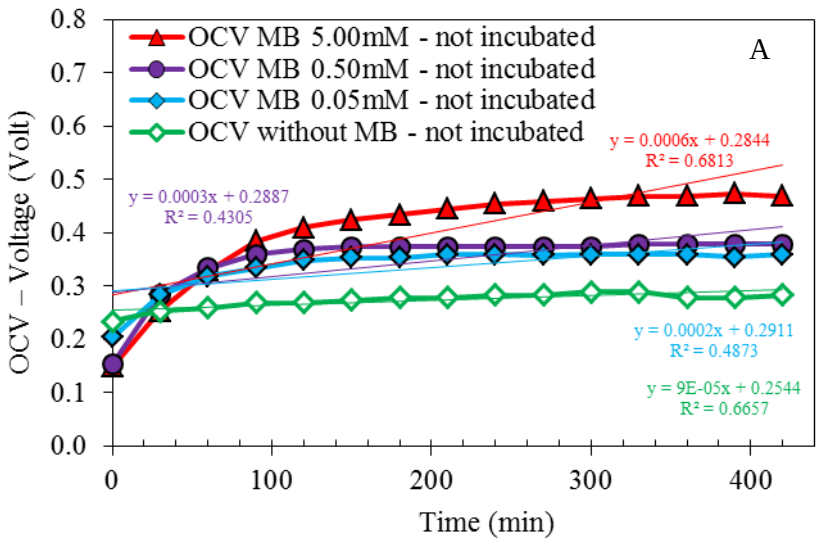

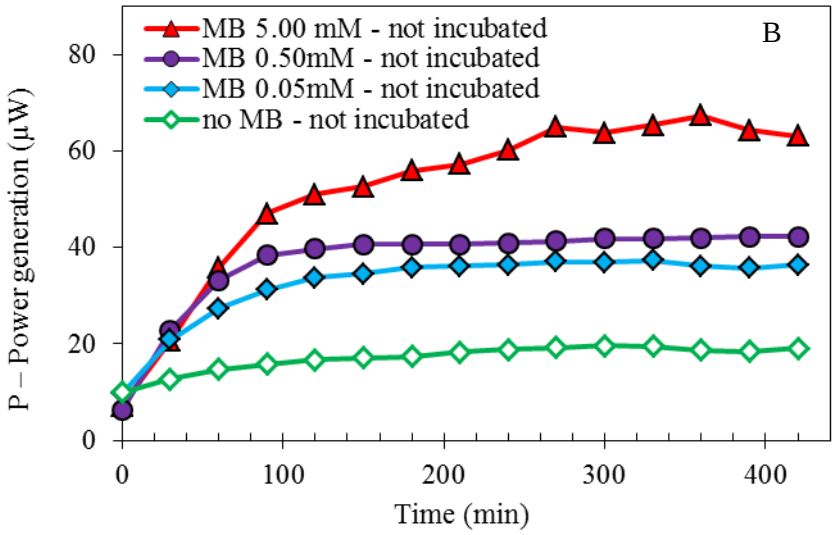

Fig. 8.8. Open circuit voltage (A) and power produced (B) carried out after the complete reduction of the methylene blue with the electrodes inserted only 30 min. before the first measurement (not incubated).

All the MFCs showed similar behavior in the first polarization curve, the initial OCV was independent by the time of starvation and by the concentration of the mediator in solution. The MFCs with 5.00 mM and 0.50 mM of MB started from an OCV of 0.15 V while the lower concentration of mediator (0.05 mM) resulted in 0.20 V. The experiment without MB in solution showed the highest initial OCV of 0.23 V. The MFC in the presence of 5.00 mM of MB showed the largest increase in the open circuit voltage to the final 0.47 V registered after 7 hours from the initial measurement (+ 318%), the MFC with MB in the concentration of 0.50 mM increased of 247% to the final 0.38 V while the MFC in the presence of the lower MB concentration (0.05 mM) shifted from 0.20 V to 0.36 V with a 180% increase. In the absence of the MB the final OCV was just 22% higher (0.28 V) than the initial (0.23 V). The OCVs reached at the end of the experiment were comparable with the OCVs registered by the incubated electrode after 7 hours of measurements (MB 5.00 mM: 0.47 V; MB 0.50 mM: 0.44 V; MB 0.05 mM: 0.38 V; no MB: 0.26 V). The slope of the plotted linear curve increased by increasing the concentration

of the methylene blue in solution, from $9.0 \cdot 10^{-5}$ (0.00 mM MB) to $2.0 \cdot 10^{-4}$ (0.05 mM MB), and then $3.0 \cdot 10^{-4}$ (0.50 mM MB) and $6.0 \cdot 10^{-4}$ (5.00 mM MB) (**Fig. 8.8A**).

The power generated by the MFCs in the presence of the different MB concentration started from a very close value of 8.2 ± 1.6 μW and then, as observed for the OCV, the increase in the power produced over time was related to the MB concentration in solution. The power produced at the end of the measurement in the presence of 5.00 mM of MB in solution was 63 μW, eight times higher than the initial one. The 0.50 mM MB MFC shifted to 42 μW, the 0.05 mM MB to 36 μW while without mediator the initial power was doubled in the final 19 μW. The final power produced was lower than that observed for the incubated experiment, due to a lower control on the surface area of the electrode caused by the necessity of insert the anode and close the compartment as quick as possible in order to limit the oxygen poisoning of the anode chamber.

When the electrode was submerged into the anode chamber after the complete reduction of methylene blue by yeasts (not incubated electrode), OCV and power generated progressively increased until reaching a final steady performance similar to that obtained while maintaining the electrode submerged into the solution during the reduction step (incubated electrode) (**Fig. 8.8A** and **Fig. 8.8B** and **Fig. 7.9**). These results suggested a diffusive regime dependent by the migration of the yeast instead of the methylene blue onto the electrode surface. The diffusive regime outlined that the electron transfer depended more on the adhesion of the cells on the surface of the electrode than by the diffusion of the reduced mediator on the electrode. Increasing the methylene blue concentration showed a nonlinear trend in respect to the values of OCV and PD. This behavior could be explained by a stable microenvironment on the surface of the anode, due to the saturation of the electrode by the cells. The electron transfer mechanism should therefore be dependent on the capability of the yeast to address on the electrode. When the electrode was not

incubated in the anodic chamber during the methylene blue reduction, the current density reached its maximum after 100 min with respect to immediate response obtained by the incubated electrode. Today, the activity of methylene blue is known to mediate the electron transfer between cells and electrode (Gunawardena et al., 2008); however, our findings demonstrated that the limiting factor is probably due to the cells adhesion on the electrode surface.

Chapter 9

9.1 Yeast immobilization on a functionalized anode

The performance of an MFC was strictly related to the adsorption of the yeast cells on the electrode surface and the most part of the power produced was related to the cells adhering on the anode. For this reason, it has been developed a novel immobilization technique in order to ensure the maximum concentration of cells onto the electrode surface and limit the consumption of the carbon source from the microbes not involved in the electrochemical reaction. The microorganisms have been attached to the electrode using an inoculum dispersed in a viscous glucose paste, ensuring bacteriostatic effect on the yeast cells as well as a prevention to an external microbial contamination. The electrode was firstly covered by a glucose paste containing the inoculum and then dried under a sterile fume hood. Then, the functionalized electrode was dip–coated into a cellulose acetate solution, dried again and stored into a growth medium. The cellulose acetate membrane hindered the diffusion of the cells from the electrode but permitted the diffusion of the nutrients ensuring the replication of the cells between the electrode and the membrane. The glucose paste protects the cells from the contact of the very toxic cellulose acetate solution (Acetone/THF 60/40), ensures the adhesion of the cells to the electrode and creates a space between the external membrane and the electrode suitable for the growth of the colonies (**Fig. 9.1**).

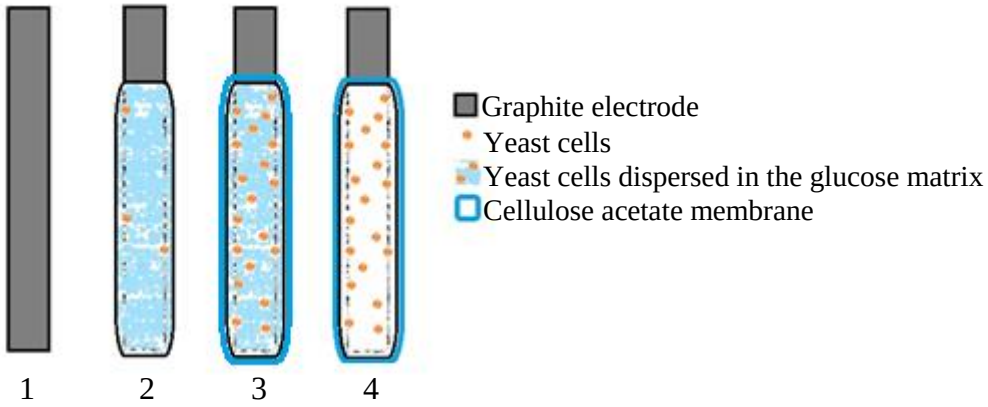

Fig. 9.1. Phases of the electrode preparation; (1) bare electrode, (2) glucose paste with the inoculum adherent on the electrode; (3) cells dispersed in the glucose matrix encapsulated into the cellulose acetate membrane before the cultivation (4) electrode at the end of the cultivation phase. The proportions are not exact and number of cells is arbitrary.

The growth of *Saccharomyces cerevisiae* was tested using a functionalized electrode suspended in yeast–extract, peptone, dextrose (YPD) solution, the electrode was just covered by the glucose paste containing the inoculum and not encapsulated into the cellulose acetate membrane to better examine the effect of the glucose paste on the cells. The growth curve of the free yeasts showed a logarithmic trend in the first 18 h reaching a stationary phase after 42 h (**Fig. 9.2**).

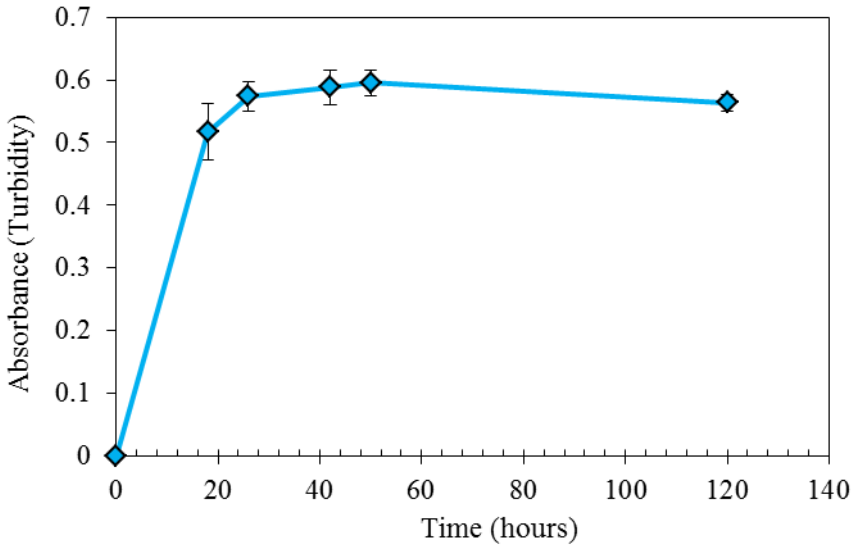

Fig. 9.2. Growth curve of yeast cells in YPD medium after deposition of the inoculum onto the electrode surface. The solution were diluted 1:10.

The increase in the turbidity of the solution demonstrated that the glucose paste did not limit the yeast growth. The capability of the cells, immobilized on the functionalized electrode by the cellulose membrane, to degrade the carbon source present outside the membrane was evaluated by the consumption of the glucose in phosphate buffer solution (**Fig. 9.3**).

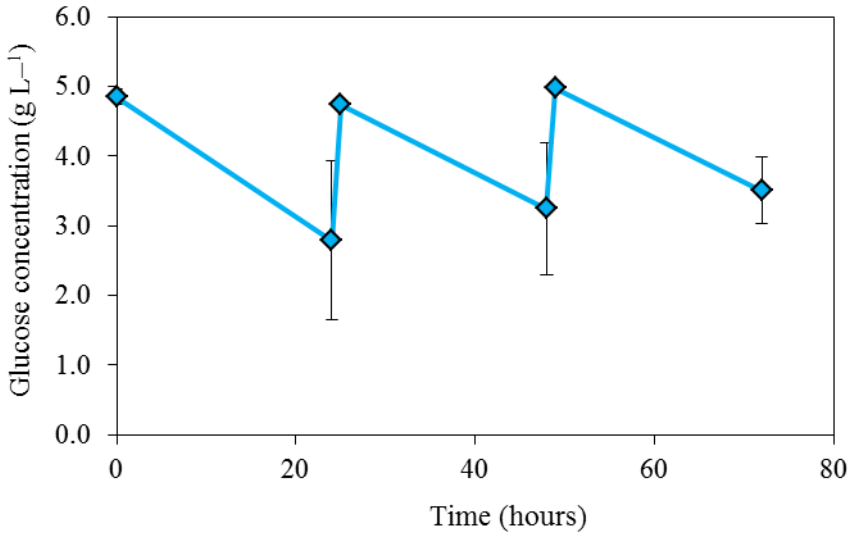

Fig. 9.3. Glucose consumption by the yeast cells encapsulated on the electrode surface by the cellulose membrane in a glucose solution changed each 24 hours.

The electrode was tested in three different glucose solutions, one after the other. The results in **Fig. 9.3** showed a stable glucose consumption for all of the immersions demonstrating that the cellulose acetate membrane was permeable to the glucose as well as the immobilization technique did not inhibit the yeast. Furthermore, the largest amount of the cells was immobilized on the electrode as it was showed by the scarce release of free yeast after the extraction of the electrode from the glucose solution. However, the reproducibility of the process could not be exactly addressed, as observable by the large error bars after 24, 48 and 72 hours of measurements. The variability of the system was caused by some differences in the amount of cells on the electrode, related to the free space between the membrane and the electrode, by the roughness of the electrode itself and by the consequently diversity of the membrane area.

The cultivation phase of the electrode was electrochemically followed by registering cyclic voltammetry after different times of starvation in the growth medium in order to evaluate the electrochemical variations caused by the colonization of the electrode surface (**Fig. 9.4**).

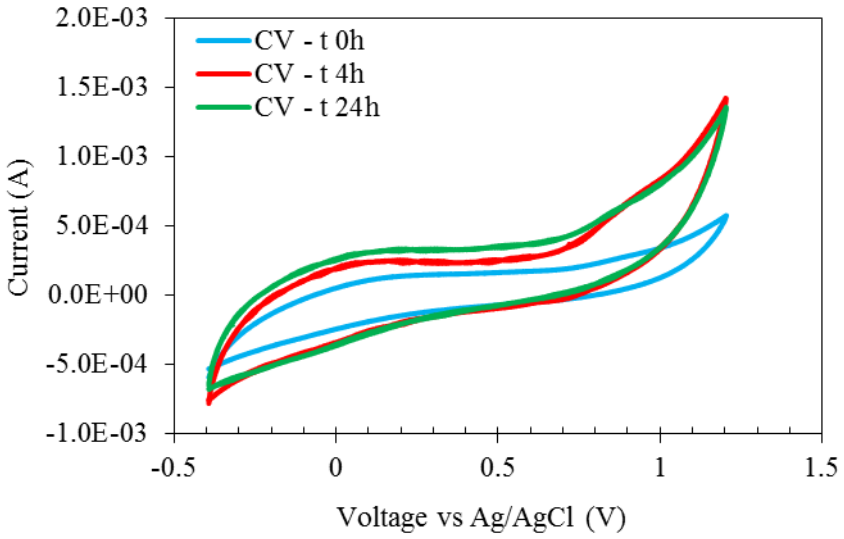

Fig. 9.4. Cyclic voltammetry of the functionalized electrode registered 0 h, 4 h and 24 h after the immersion in the growth medium.

The cultivation time affected the cyclic voltammetry by increasing the capacitive current due to the increased number of cells on the electrode surface. The differences between the CVs registered after 0 h and 4 h of cultivation were caused by the diffusion resistance due to the cellulose acetate membrane. The large peak at 0.95 V was related to electroactive species present in the growth medium but was comparable between the CV at 4 h and 24 h. No other peaks were observed.

A parallel experiment was conducted on the functionalized electrode cultivated in a growth medium amended with MB 0.5 mM (**Fig. 9.5**).

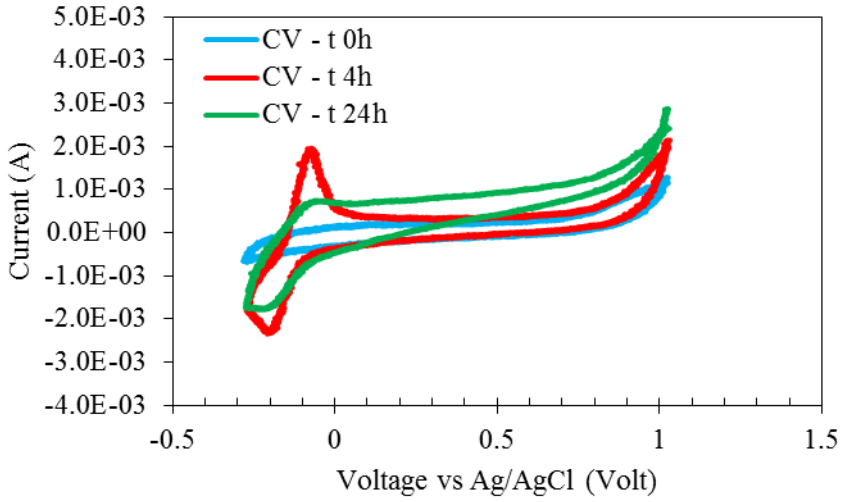

Fig. 9.5. Cyclic voltammetry of the functionalized electrode registered 0 h, 4 h and 24 h after the immersion in the growth medium amended with 0.5 mM of methylene blue.

The CV registered at 0 h did not shows the peaks of the methylene blue due to the diffusion resistance caused by the membrane to the passage of the mediator. After 4 h the diffusion of the methylene blue through the membrane and its interaction with the electrode caused the oxidation and reduction peaks (oxidation: 1.7 µA; reduction: 2.0 µA) (**Fig. 9.5)**. However, after 24 h, all of the MB in solution was reduced and the solution was discolored (**Fig. 7.9**), the CV registered after 24 h showed lower oxidation and reduction peaks (oxidation: 0.4 µA; reduction: 1.3 µA) by the MB. The reduction of the MB by the yeast cells caused the sequestration of the mediator.

The functionalized electrodes were tested also in the MFCs by polarization curves using hydrogen peroxide (4.41 mol L^{-1}) as electron acceptor in acidified aqueous solution (PB 25 mM pH 6) at the cathode chamber, with and without methylene blue as electron mediator in the anode chamber. The experiment was performed in both open and closed circuit configurations under different loads (**Fig. 9.6**).

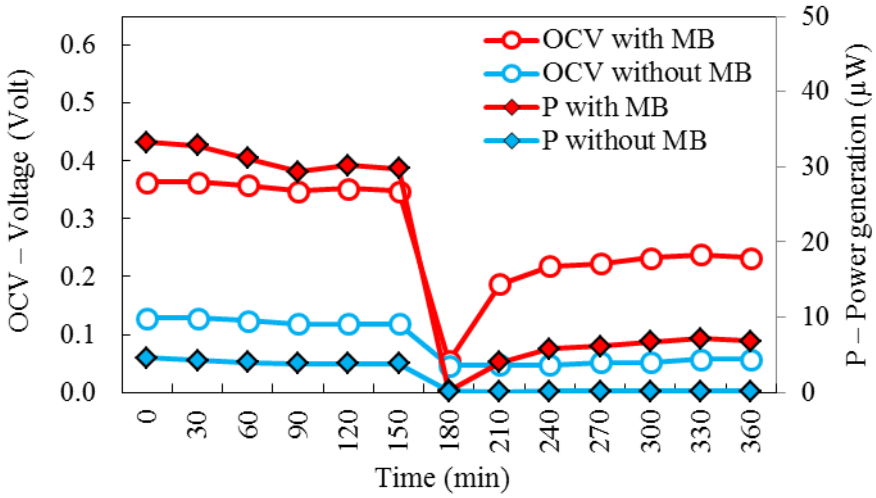

Fig. 9.6. Values of OCV and P recorded by a functionalized and immobilized electrode in the presence (red) or absence (blue) of the electron mediator methylene blue (MB). After 180 min. the electrode was extracted and substituted with a clean one.

Open circuit voltage and power produced determined in the presence of methylene blue in anaerobic conditions in the anodic compartment were respectively 0.36 V and 33 µW while, in the absence of mediator, OCV and P resulted in 0.13 V and 4.6 µW. These results confirmed that an exogenous mediator enhanced the electron transfer on the electrode surface (Rossi et al., 2015). After 180 min, the functionalized and immobilized electrode was removed and substituted with a cleaned graphite electrode. In the absence of the methylene blue the power and the OCV collapsed to 47 mV and the P to 0.13 µW. The performance were stable over the entire the experiment with a final value of OCV of 57 mV and P of 0.18 µW. In the presence of the mediator, after the initial decrease, OCV and P began to rise up to 0.23 V and 6.8 µW (**Fig. 9.6**). The different behavior was due to the presence of a residual community of yeast, detached from the electrode, that moved himself to the clean electrode surface (**Fig. 9.7**), with a behavior similar to that observed in **Fig. 8.8A** and **Fig. 8.8B**.

Fig. 9.7. Picture of the anodic chamber showing cells on the surface of the clean electrode at the end of the experiment.

At the end of the experiment in the presence of the mediator the concentration of the methylene blue in the anode chamber was determined spectrophotometrically and although the initial concentration of 0.5 mmol L^{-1}, the final resulted in 12.5 µmol L^{-1}, 2.5% of the initial concentration. Our findings demonstrated that the largest part of methylene blue was enclosed between membrane and electrode.

On this basis, a similar experiment was conducted replacing the functionalized and immobilized electrode (WE) with a clean graphite electrode covered with cellulose acetate membrane in the absence of the yeast cells (**Fig. 9.8**).

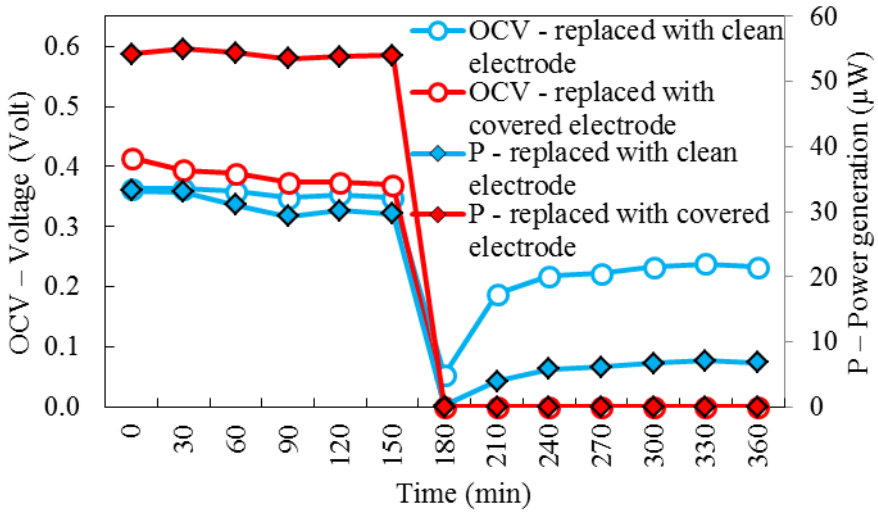

Fig. 9.8. Values of OCV and P recorded by a functionalized and immobilized working electrode (WE) in presence of the electron mediator methylene blue. After 180 min. the working electrode was extracted and substituted with a clean one (blue) or with a clean graphite electrode covered with cellulose acetate membrane without yeast cells (red).

The OCVs at 0 mins of the two MFCs were similar (0.41 V and 0.36 V) but the differences in the power produced over time in the first 180 min showed a large variability (54 µW and 33 µW) between the electrodes caused by some differences in the amount of cells on the electrode, related to the free space between the membrane and the electrode, by the roughness of the electrode and by the consequently diversity of the membrane area.

The substitution of the electrode after 180 min caused the drop in both OCV and power produced but replacing the anode with a new, not covered graphite electrode permitted to produce a small amount of voltage and power by the colonies of cell detached from the external side of the membrane. Replacing the functionalized anode with a new graphite electrode, covered with the cellulose membrane but not functionalized with the yeast cells hindered the interaction between the free cells and the new electrode but at the same time permitted the diffusion of the mediator to the electrode surface. Thus, only preventing the cells to reach the anode caused

the lack of the electron transfer after the electrode replacement. This means that the methylene blue expressed its electron transfer enhancing activity inside of the cells and not as a shuttle across the external membrane.

The MFCs output was directly correlated to the number of cells on the electrode surface, for this reason, it was studied the relation between the time of cultivation and the power produced and the voltage measured by the MFCs. The functionalized electrode was cultivated in the raw growth medium or amended with methylene blue. Every 24 h the electrode were extracted from the medium, tested in an MFC using hydrogen peroxide as electron acceptor in the cathode chamber and then a cyclic voltammetry was registered. The output of the MFCs was strongly affected by the incubation time of the electrode (**Fig. 9.9**)

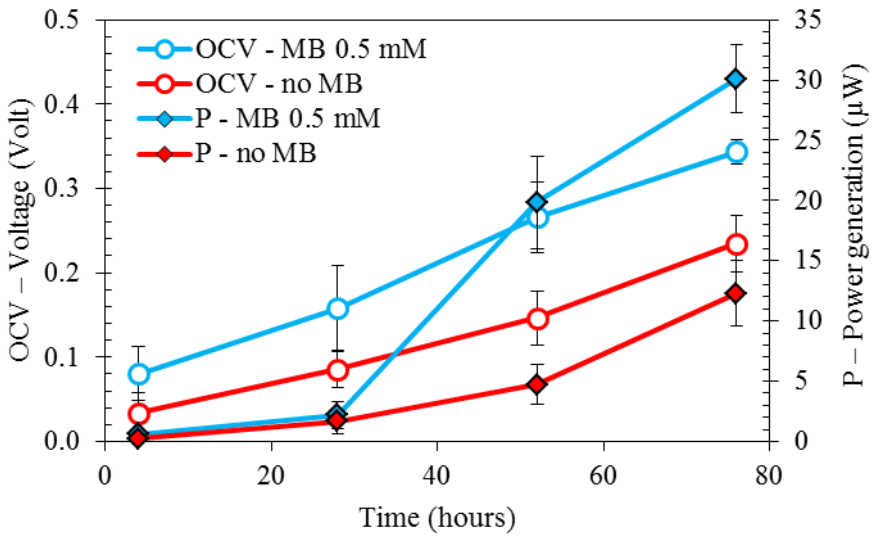

Fig. 9.9. OCV and P registered over time of an MFC using the functionalized electrode as the anode cultivated in the presence (blue) or absence (red) of MB.

The initial OCV produced by the MFCs was under 0.1 V for both the experiments and very close between the two electrodes but after 24 h the voltage produced by the anode cultivated in the medium amended with MB was 0.16 ± 0.05 V and grew again to 0.27 ± 0.04 V after 52 h to the final 0.34 ± 0.01 V,

reached after 76 h of incubation. In the absence of the mediator the increase in the OCV over time was smaller and only after 52 h the voltage at open circuit grew over 0.1 V to 0.15 ± 0.03 V and after 76 h was 0.24 ± 0.03 V.

The power produced by the two anodes was comparable in the first 28 h before the large increase observed in the anode cultivated with MB: the maximum power produced after 52 h was 20 ± 4 µW and 30 ± 3 µW after 72 h. The functionalized electrode cultivated in the absence of mediator showed a more linear trend producing 5 ± 2 µW at 52 h and 12 ± 3 µW after 76 h. The cells cultivated in the presence of methylene blue performed better in respect to the cells cultivated in the absence of the mediator, showing increasing performance while the cultivation time increased.

In order to evaluate the presence of oxidation/reduction peaks related to the growth of the cells, a cyclic voltammetry was registered every 24 h. The CVs were recorded in PB 0.1 M (pH 7.8) and glucose 5 g L^{-1} after the polarization tests (**Fig. 9.10A** and **Fig. 9.10B)**.

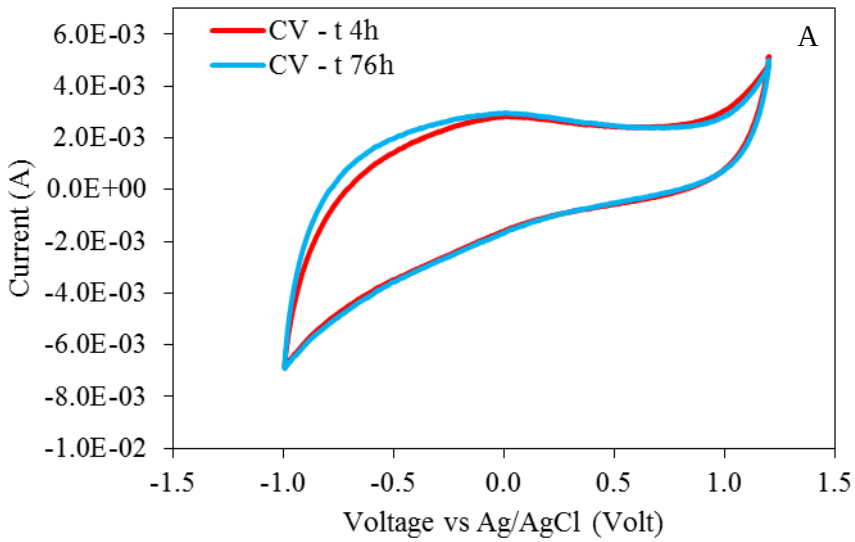

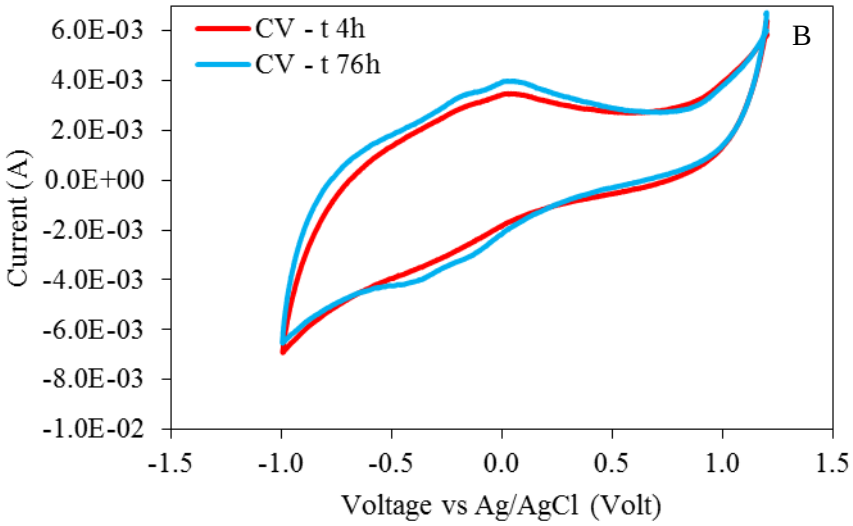

Fig. 9.10. Cyclic voltammetry of the functionalized electrode registered 4 h and 76 h after the immersion in the (A) growth medium or in growth medium amended with 0.5 mM of methylene blue.

Both the CVs showed an increase in the capacitive current in the range –1 / 0 V vs Ag/AgCl due to the growth of the cells on the anode surface. Unknown peaks around 0 V, shifted in respect to the peaks of the MB (**Fig. 3**), was observed particularly in the last CV. Further analysis are requested to identify the nature of this peak and evaluate if it is related to the development of a direct electron transfer through trans Plasma Membrane Electron Transfer (tPMET) between the cells and the electrode.

Chapter 10

10.1 Direct electron transfer by S. cerevisiae

The exoelectrogenic bacteria are the most employed microorganisms in MFCs, due to the high Coulombic efficiency, the versatility and the intrinsic ability to form electrochemically active communities (Logan, 2009). The exoelectrogenic bacteria on the anode can directly oxidize the organic matter in solution and release the electrons to the anode trough specific cytochromes on their outer membrane. These cytochromes derived from the evolution of metal–reductase enzymes, used by the microorganisms, in the absence of oxygen, to transfer the electrons accumulated trough the oxidation of carbon sources, to an external electron acceptor (Holmes et al., 2006, Gorby et al., 2006, Hubenova and Mitov, 2015). However, the metal–reductase was a common system in the nature domains (Schröder, 2007, Shena et al., 2017), due to the necessity of the microorganism to use the solid minerals in the environment not only as acceptor of electrons for dissimilatory metal reduction but also as nutrients, in the proper oxidation state, in assimilatory metal reduction (Eide, 1998). For these reasons, the large part of the microorganisms, including yeasts such as *Saccharomyces cerevisiae*, possess several metal–reductase enzymes, and use them to reduce external metals and transport them into the cell, thus, the reduction system is accompanied by a transport system (Eide, 1998). *Saccharomyces cerevisiae* has two different transport systems for elemental iron, a low–affinity system and a high–affinity system (Schröder et al., 2003). The low–affinity system, defined by the Fet4 gene, could transports different kind of metals, such as manganese and cadmium, into the cells across the external membrane. The high affinity system is mediated through an high affinity ferroxidase/permease complex (*Fet3/Ftr1*), based on two different steps: the first one is the reduction of the complexed ferric iron to the ferrous state by a plasma membrane–bound ferric reductase, and the second is the transport of

the not–complexed, relatively soluble, ferrous iron by two independent transport systems (Dancis et al., 1992, Georgatsou and Alexandraki, 1994).

The present work shows that the ferric reductase activity and the direct electron transfer to an external electrode in the anode compartment of an MFC by *S. cerevisiae* cells are closely parallel. To examine the ability to reduce iron III and the effect on this reaction of the presence of mediator such as methylene blue, S. cerevisiae was incubated with glucose as the only carbon source using iron(III)–EDTA as electron acceptor (Ramalho et al., 2005). To evaluate the contribution of the ferric–reductase complex in the iron–reduction reaction, the enzyme was inhibited with carbonyl cyanide m–chlorophenyl hydrazine (CCCP). *S. cerevisiae* was then employed as biocatalyst in the anode chamber of an MFC and we demonstrated the involvement of the ferric–reductase complex in the current produced in mediatorless MFC. Our results will be relevant for biotechnological applications of this activity and also for a broader understanding of the electron transfer mechanism activities associated with the yeast plasma membrane redox system.

10.2 Iron III reduction by Saccharomyces cerevisiae

The yeast *S. cerevisiae* reduced the iron(III), in solution as iron(III)–EDTA complex (**Fig. 10.1**). The concentration of the iron(III) reduced in the first 8 h increased from 0.2 ± 0.1 mg L^{-1} to 0.5 ± 0.3 mg L^{-1}, and grew again reaching 0.7 ± 0.3 mg L^{-1} after 30 h. The presence of methylene blue as electron mediator promotes the reaction by increasing the amount of iron reduced during the entire experiment, reaching 1.2 ± 0.5 mg L^{-1} after 8 h from the initial 0.3 ± 0.2 mg L^{-1} and achieved the maximum concentration of 1.3 ± 0.1 mg L^{-1} after 22 h, doubling the concentration obtained in the absence of MB. After 26 h and 30 h the concentration of iron decreased, probably due to the contamination of the reactors

by residual oxygen. The plateau observed after 8 h was due to the substrate depletion (Rossi and Setti, 2016).

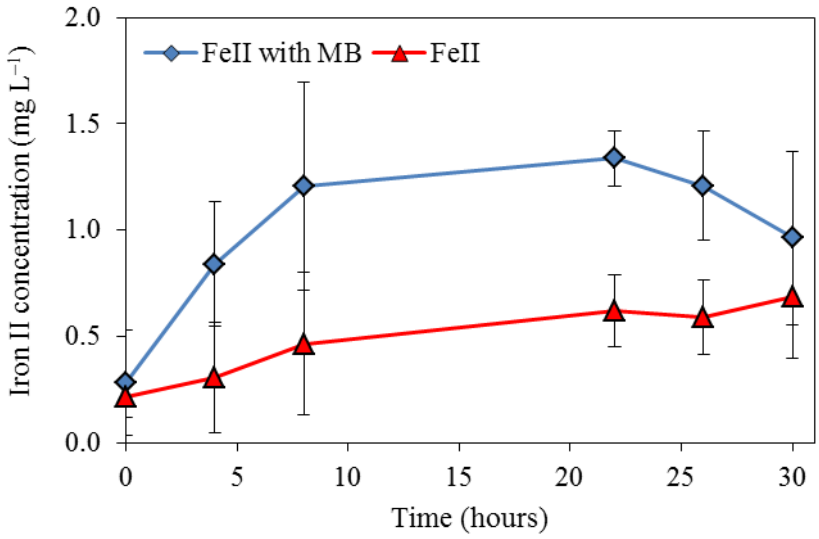

Fig. 10.1. Iron II concentration reduced by *S. cerevisiae* free cells with glucose as the only carbon source in raw PB (red), or PB amended with (blue) methylene blue in solution.

The presence in solution of carbonyl cyanide m–chlorophenyl hydrazine (CCCP), caused a large drop in the iron reduced by the cells (**Fig. 10.2**). CCCP is an uncoupler of the proton gradient that is normally established during the activity of electron carriers in the electron transport chain. The inhibitor did not modify the viability of the yeasts (Reid and Schatz, 1982). The activity of CCCP as an iron reductase inhibitor in yeast cells has been previously well documented (Schröder et al., 2003, Sasaki et al., 1998, Lesuisse and Labbe, 1994). In the absence of MB the iron concentration was 0.1 ± 0.2 mg L^{-1} at 0 h and reached 0.3 ± 0.1 mg L^{-1} after 30 h of incubation, less than a half of the iron reduced without inhibition. The inhibitor hampered the electron transfer also in the presence of methylene blue and the iron reduced increased from 0.2 ± 0.3 mg L^{-1} at 0 h to the maximum 0.5 ± 0.2

mg L^{-1}, registered at 22 h, 62% less of the concentration observed without inhibition. The final iron II concentration was 0.4 ± 0.1 mg L^{-1}, at the end of the experiment (30h).

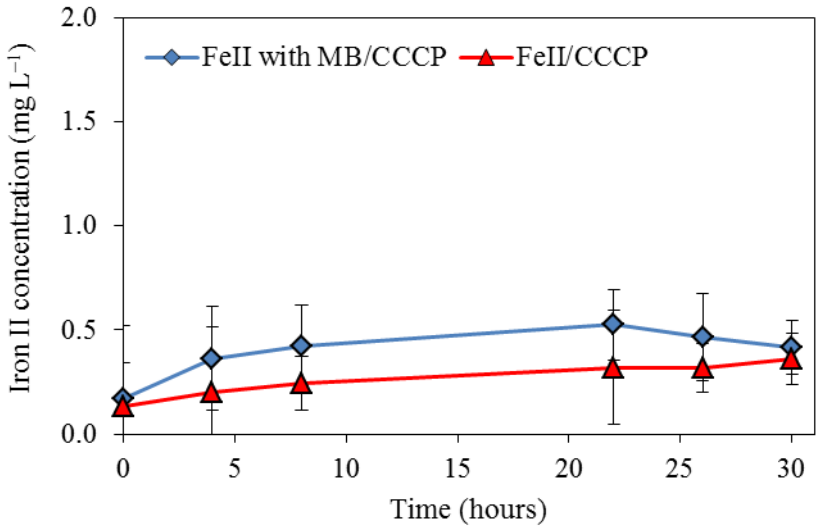

Fig. 10.2. Iron II concentration reduced by S. cerevisiae free cells with glucose as the only carbon source in raw PB (red), or PB amended with (blue) methylene blue in the presence of CCCP as inhibitor of the iron reductase.

10.3 Voltage and power production in a S. cerevisiae catalyzed fuel cell by Ferric reductase enzymatic complex

Parallel experiments were conducted using a graphite electrode instead of the iron complex as electron acceptor in the anode compartment of an MFC. The OCV was registered for the first 30 h (**Fig. 10.3A** and **Fig. 10.3B**) and then a polarization curve was recorded on each MFC, in the presence or absence of MB and CCCP (**Fig. 10.4**).

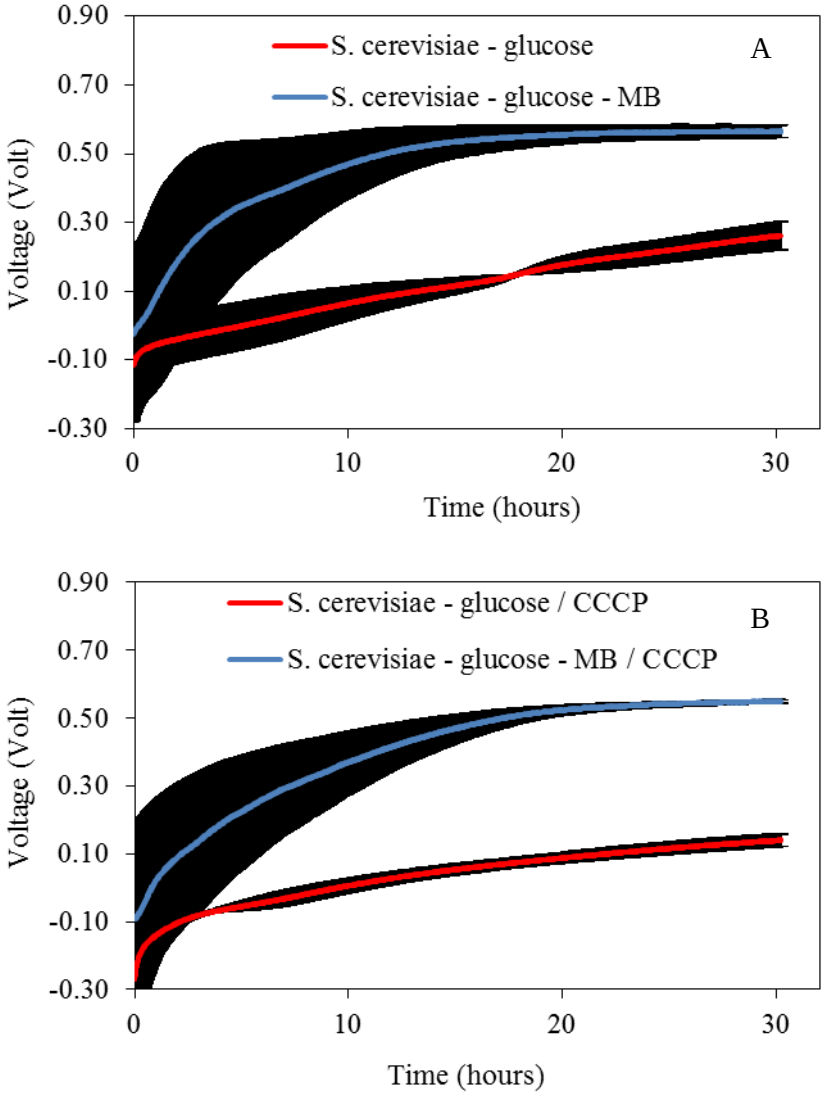

Fig. 10.3. OCV registered for 30 h in MFCs (A) in the presence or absence of methylene blue and (B) in presence or absence of MB with CCCP as inhibitor of the iron reductase.

The OCV of the MFCs in the presence or absence of MB started from similar voltage at 0 h (with MB: –0.02 ± 0.2 V; without MB: –0.1 ± 0.1 V) with a large variability particularly in the MFC with the mediator due to small differences in the initial content of oxygen of the anodic solution. After 15 h the OCV in the presence of MB reached a plateau over 0.5 V and maintained this value to the final OCV of

0.56 ± 0.02 V registered after 30 h. The OCV in the absence of MB showed less variability in the initial part of the experiment and continuously grew to the final 0.26 ± 0.04 V, registered after 30 h.

The presence in solution of the inhibitor affected the OCV of the MFCs. The initial OCV in the solution amended with MB was –0.09 ± 0.28 V and again grew to a steady OCV after 15 h and then reached 0.549 ± 0.005 V after 30 h. Without the mediator the initial OCV was –0.27 ± 0.04 V and the final was 0.14 ± 0.02 V, 50% less than the value obtained by the MFCs without the CCCP in solution.

After the OCV measurements, the MFC circuit was closed and a polarization curve was registered (**Fig. 36**). In order to evaluate the effect of the scan speed on the polarization curve and the contribute of the capacitance of the cells to the MFCs output (Logan, 2012), the experiment was conducted at two different scan speed (0.1 mV s^{-1} and 1.0 mV s^{-1}).

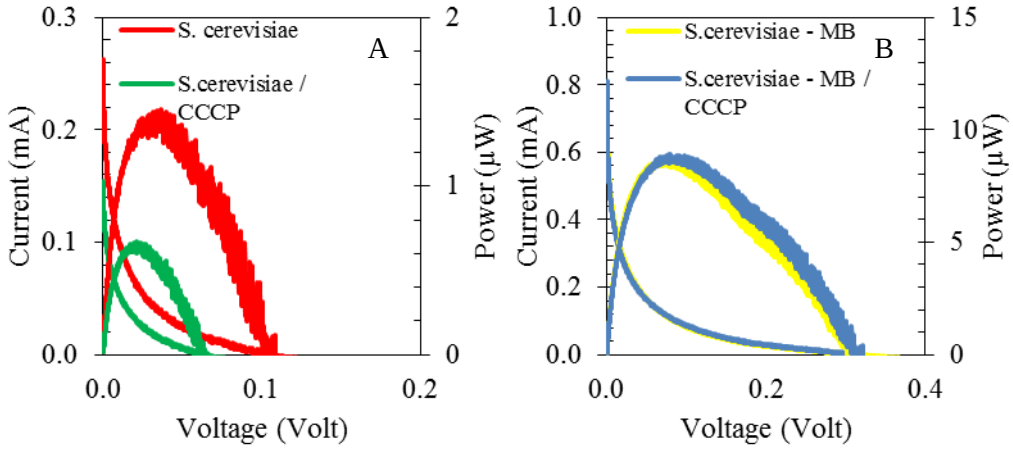

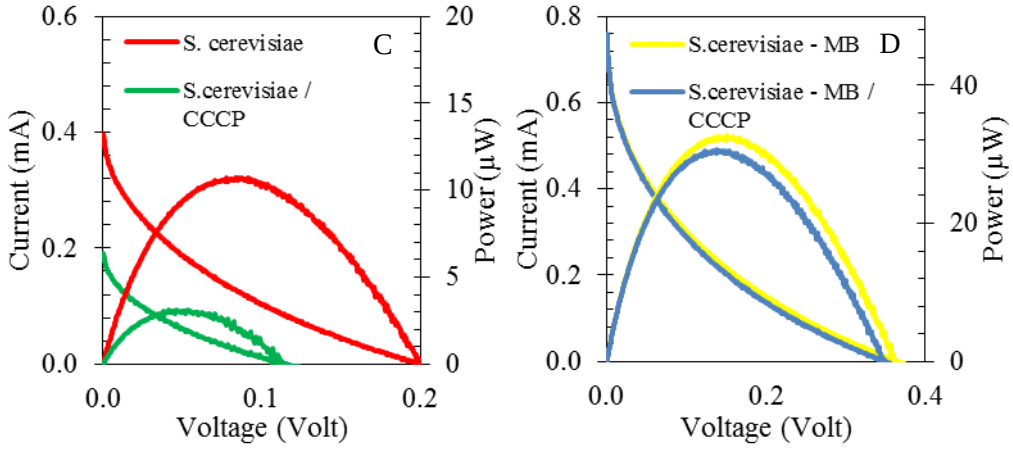

Fig. 10.4. Polarization and power density curves registered in presence and absence of methylene blue (MB) and CCCP at different scan speed (A, B 0.1 mVs^{-1}) (C, D 1.0 mVs^{-1}).

The polarization curves showed the effect of the CCCP on the voltage and power produced by an MFC. In the curves registered at a scan speed of 0.1 mV s^{-1} the maximum power density produced was 2.01 mW m^{-2} but adding the iron reductase inhibitor to the solution resulted in 0.96 mW m^{-2}, more than 50% less of the initial value. Moreover, all of the parameters of the MFCs were affected by the inhibitor, with the OCV that drop from 0.11 V to 0.06 V and short circuit current, that decreased from 0.38 A m^{-2} to 0.22 mA m^{-2}. Methylene blue drastically improved the performance of the MFC and the power density increased of more than 600% due to the addition of the mediator while the reduced iron was increased of just 200% in respect to the experiment without the MB in solution. The CCCP showed a negligible effect on the MFC with the anodic solution amended with MB: maximum power density generated (PD), OCV and short circuit current (SCC) were exactly the same (PD: 12.5 mW m^{-2}; OCV: 0.32 V; SCC: 1.1 mA m^{-2}).

The polarization curves registered at an higher scan speed (1.0 mV s^{-1}) showed higher performance (Logan, 2012) and without any mediator the maximum power density produced was 15.3 mW m^{-2}, fivefold the previous results using complex

medium in the anode compartment (Sayed et al., 2012). With CCCP in solution the power generated was 4.49 mW m^{-2}, a drop was observed also in the OCV, from 0.20 V to 0.12 V, and in the SCC, that decrease from 0.57 A m^{-2} to 0.27 A m^{-2}. The presence of the mediator in solution prevented similar effects in the MFCs with the inhibitor and the curves showed similar parameters: the maximum power density decrease due to the presence of the CCCP just from 46.7 mW m^{-2} to 43.8 mW m^{-2}. The OCV was comparable, 0.36 V without CCCP and 0.35 V with the inhibitor and the SCC was 1.1 A m^{-2} for both the experiments.

These results evidenced the exoelectrogenicity of the yeast *Saccharomyces cerevisiae*, in fact, the yeast cells was able to reduce an external solid electrode trough the iron reductase, a membrane enzyme commonly used for the reduction of iron based minerals. The presence in solution of the MB as electron mediator overcame the inhibiting effect of the CCCP, by using different channels for the reduction of the electrode.

Conclusions

Microbial fuel cells (MFCs) could potentially solve the problem of the disposal of organic rich wastewaters, by lowering the COD and contemporary producing electric energy. Different wastewaters require different MFC configurations, and the *S. cerevisiae* catalyzed MFC developed in this dissertation could be used in the many biotechnological processes of the food industry based on this microoganism.

The NADH stored into the cells was easily oxidized by an electron mediator such as the methylene blue and a conductive electrode accepted the electrons derived from this reaction. It was demonstrated that more the reduced methylene blue, more the electrical output of the cell, however, the efficiency of the overall reaction was limited by the poor kinetics of the oxidation of the reduced methylene blue at the anode and the slow oxygen reduction reaction.

The concentration of glucose did not affect the kinetic of the reduction of methylene blue and the yeast cells, using their reservoir of glycogen, were able to reduce the mediator also in the absence of an external carbon source. The glucose in the medium was consumed for the continuous reduction of methylene blue, also after several hours of incubation.

Methylene blue worked as an electron shuttle, entering into the cells, accepting the electrons and then discharging these electrons to an external electrode after the diffusion through the cellular membrane. The presence of an exogenous redox molecule into the cells affected the metabolic pathways causing different patterns of the end–products of fermentation by altering the $NADH/NAD^+$ ratio.

The performance of the MFC was initially tested using glucose, methylene blue and yeast cells, showing negligible effect of each component in the absence of the biocatalyst on the power output. The presence of methylene blue increased the power produced from 5 μW to 65 μW in the initial stage of the experiment while the performance of the MFC in the presence or in the absence of MB converged to 50 ± 1 μW and 0.41 ± 0.01 V. Glucose in three different concentration (0 g L^{-1}, 10

g L^{-1}, 100 g L^{-1}) did not largely affected the electrochemical output of the MFCs on a 22 h (96 µW, 0 g/L; 81 µW, 10 g/L; 65 µW, 100 g/L) or 46 h (63 µW, 0 g/L; 75 µW, 10 g/L; 87 µW, 100 g/L) incubation time. Increasing the methylene blue concentration from 0.0 mM to 5.0 mM increased the power produced from 25 µW to 81 µW after 22 h and from 18 µW to 75 µW after 46 h of operation but the high variability of the oxygen concentration in the cathode compartment caused oscillations in the response of the MFC.

Replacing oxygen as electron acceptor in the cathodic chamber with hydrogen peroxide stabilized the MFC output in terms of OCV, power and current generated over time. Increasing the concentration of hydrogen peroxide from 0.0 M to 4.4 M increased the power produced by the MFC of more than ten times from 5 µW to 57 µW after 22 h and from 34 µW to 86 µW after 46 h. The hyperbolic model obtained suggested that the electrochemical process was limited by the anodic reaction when the concentration of hydrogen peroxide was higher than 0.9 M. However, these findings were not confirmed by the OCV and power generated at different concentration of mediator using hydrogen peroxide as electron acceptor in the cathodic chamber. OCV and power produced followed an hyperbolic model in respect to the methylene blue concentration showing a saturation of the cell output when the concentration of the mediator was higher than 0.01 mM while the electrochemical reaction would be independent to the mediator concentration into the bulk of the aqueous solution in the range 0.05 mM – 5.00 mM. Our findings suggested that the MFCs performance was limited not by the reduction reaction of the hydrogen peroxide, when the concentration of the latter was higher than 0.9 M, nor by the oxidation of the mediator when the methylene blue concentration was at least 0.05 mM nor by the reduction of the latter operated by the yeast cells since the discoloration of the solution. The limiting step was identified in the capability of the biocatalyst to address the mediator in the reduced form to the electrode surface.

The development of a diffusive regime in the anodic compartment was confirmed by the results obtained by the incubated and not incubated electrode. All the MFCs with the not incubated electrode showed similar behavior in the first polarization curve, the initial power generated was independent by the time of starvation and by the concentration of the mediator in solution. The power generated by the MFCs in the presence of the different MB concentrations started from a very close value of 8.2 ± 1.6 μW and then, as observed for the OCV, the power produced increased over the incubation time, in strictly relation to the concentration of mediator in solution. The power produced at the end of the measurement in the presence of 5.00 mM of MB in solution was 63 μW, eight times higher than the initial one. The 0.50 mM MB MFC shifted to 42 μW, the 0.05 mM MB to 36 μW while without mediator the initial power was doubled in the final 19 μW. Our results evidenced a diffusive regime dependent by the migration of the yeast instead of the methylene blue onto the electrode surface. The diffusive regime outlined that the electron transfer depended more on the adhesion of the cells on the surface of the electrode than by the diffusion of the reduced mediator on the electrode.

We developed a novel immobilization technique in order to ensure the maximum concentration of cells onto the electrode surface and limit the consumption of the carbon source from the microbes not involved in the electron transfer. The cells immobilized between electrode and membrane grew forming colonies directly on the electrode surface but still maintaining their abilities to consume glucose in the medium.

The functionalized electrodes were tested in MFCs both in the presence or in the absence of methylene blue, showing greater performance with the mediator and through spectrophotometric analysis we discovered that the reduction of the MB by the yeast cells caused the sequestration of the mediator from the solution. Thus, methylene blue expressed its electron transfer enhancing activity inside of the cells

and not as a shuttle across the external membrane. The presence of unknown peaks in the cyclic voltammetry after 76 h of growth were referred to the presence of trans plasma membrane electron transport (tPMET) system.

The ferric reductase activity and the direct electron transfer to an external electrode in the anode compartment of an MFC by the *S. cerevisiae* cells are closely parallel. *S. cerevisiae* reduced iron(III)–EDTA through the iron reductase enzyme to a maximum of 0.7 ± 0.3 mg L^{-1} after 30 h. The presence in solution of an electron mediator such as methylene blue increased the maximum iron (II) concentration of 216% to 1.3 ± 0.1 mg L^{-1} after 22 h. Inhibiting the iron–reductase activity with an uncoupler such as CCCP dropped the iron (II) concentration in the presence of MB of 62% to 0.5 ± 0.2 mg L^{-1}, registered at 22 h, and of 42% in the absence of the mediator to 0.4 ± 0.1 mg L^{-1}, observed after 30 h of incubation. After 30 h the performance of the MFCs were stable and the polarization tests revealed the involvement of the ferric–reductase in the direct electron transfer of the *S. cerevisiae* catalyzed MFC. At the highest scan speed the inhibition of the enzymatic complex caused a decrease of 70% of the maximum power density (from 15.3 mW m^{-2} to 4.49 mW m^{-2}). Although the presence in solution of the mediator drastically improved the performance of the cell, the inhibition of the ferric–reductase caused a drop in the maximum power density of 7%, from 46.7 mW m^{-2} to 43.8 mW m^{-2}. These results showed the participation of an externally directed plasma membrane redox system in *S. cerevisiae* in the electron transfer mechanism of an MFC.

Dissemination activities

Publications

Rossi, R., Yang, W., Setti, L., Logan, B.E., 2017. Assessment of a metal–organic framework catalyst in air cathode microbial fuel cells over time with different buffers and solutions. Bioresource Technology, 233, 399–405.

Rossi, R., Setti, L., 2016. Effect of methylene blue on electron mediated microbial fuel cell by Saccharomyces cerevisiae. Environmental Engineering and Management Journal, 16, 2011–2018.

Rossi, R., Cavina, M., Setti, L., 2016. Characterization of electron transfer mechanism in mediated Microbial Fuel Cell by entrapped electron mediator in Saccharomyces cerevisiae. Chemical Engineering Transactions, 49, 559–565.

Rossi, R., Fedrigucci, A., Setti, L., 2015. Characterization of electron mediated microbial fuel cell by Saccharomyces cerevisiae. Chemical Engineering Transactions, 43, 337–343.

Papers submitted

Rossi, R., 2017. Saccharomyces cerevisiae: exoelectrogenic microorganism for application in microbial fuel cells. Bioelectrochemistry, **submitted**.

Conferences

EU-ISMET 2016, 26-28/09/2016, The 3rd European Meeting of the International Society for Microbial Electrochemistry and Technology. Rome, Italy. Poster.

IBIC 2016, 10/04/2016, Associazione Italiana di Ingegneria Chimica, 5th International Conference on Industrial Biotechnology. Bologna, Italy. Poster.

Enerchem – 1, 18/02/2016, Societa Chimica Italiana , Firenze ENERCHEM – 1 will represent a special event for all chemists interested in the research on renewable energy particularly related to Photovoltaics, Artificial Photosynthesis/Photocatalysis, Hydrogen, Fuel Cells, Battery and Biofuels . Florence, Italy. Oral presentation.

Ecomondo 2015, 03/11/2015, Ecomondo 2015, Le acque di scarico: una risorsa da valorizzare. Rimini, Italy. Poster.

ICheap12, 19/05/2015, Associazione Italiana di Ingegneria Chimica , Milano 12th International Conference on Chemical and Process Engineering. Milano, Italy. Poster.

References

Appels, L., Lauwers, J., Degreve, J., Helsen, L., Lievens, B., Willems, K., Van Impe, J., Dewil, R., 2011. Anaerobic digestion in global bio–energy production: Potential and research challenges. Renew. Sust. Energy Rev., 15(9), 4295–4301.

Babanova, S., Hubenova, Y., Mitov, M., 2011. Influence of artificial mediators on yeast-based fuel cell performance, J. Biosci. Bioeng., 112, 379–387.

Bailey, M.J., Biely, P., Poutanen, K., 1992. Interlaboratory testing of method for assay of xilanase activity, Journal of Biotechnology, 23, 257-270.

Bezerra, C.W., Zhang, L., Lee, K., Liu, H., Marques, A.L., Marques, E.P., Wang, H., Zhang, J., 2008. A review of Fe–N/C and Co–N/C catalysts for the oxygen reduction reaction. Electrochim. Acta, 53, 4937–4951.

Biffinger, J., Ribbens, M., Ringeisen, B., Pietron, J., Finkel, S., Nealson, K., 2008. Characterization of electrochemically active bacteria utilizing a high–throughput voltage–based screening assay. Biotechnol. Bioeng., 102(2), 436–444.

Bond, D.R., Holmes, D.E., Tender, L.M., Lovley, D.R., 2002. Electrode–reducing microorganisms that harvest energy from marine sediments, Science, 295, 483–485.

Bond, D.R., Lovley, D.R., 2003. Electricity production by geobacter sulfurreducens attached to electrodes. Appl.Environ. Microbiol., 69, 1548–1555.

Bond, D.R., 2010. Electrodes as electron acceptors, and the bacteria who love them. Geomicrobiology: Molecular and Environmental Perspectives, 385–399. Springer Netherlands.

Borst–Pauwels, G.W., 1981. Ion transport in yeast. Biochim. Biophys. Acta, 650, 88–127.

Bouallagui, H., Touhami, Y., Cheikh, R. B., Hamdi, M., 2005. Bioreactor performance in anaerobic digestion of fruit and vegetable wastes. Process Biochem., 40(3–4), 989–995.

Brentner, L. B., Peccia, J., and Zimmerman, J. B., 2010. Challenges in developing biohydrogen as a sustainable energy source: Implications for a research agenda. Environ. Sci. Technol., 44(7), 2243–2254.

Buffiere, P., Mirquez, L. D., Steyer, J. P., Bernet, N., Delgenes, J. P., 2008. Anaerobic digestion of solid wastes needs research to face an increasing industrial success. Int. J. Chem. Reactor Eng., 6, A94.

Cabib, E., Roh, D.H., Schmidt, M., Crotti, L.B., Varma, A., 2001. The yeast cell wall and septum as paradigms of cell growth and morphogenesis. J. Biol. Chem., 276, 19679–19682.

Cetinkaya, A.Y., Ozdemirb, O.K., Koroglua, E.O., Hasimogluc, A., Ozkayaa, B., 2015. The development of catalytic performance by coating Pt–Ni on CMI7000 membrane as a cathode of a microbial fuel cell. Bioresour. Technol., 195, 188–193.

Chaudhuri, S. K., Lovley, D. R., 2003. Electricity from direct oxidation of glucose in mediator–less microbial fuel cells. Nature Biotechnol. 21, 1229–1232.

Chen, C. C., Lin, C. Y., and Lin, M. C., 2002. Acid–base enrichment enhances anaerobic hydrogen production process. Appl. Microbiol. Biotechnol., 58(2), 224–228.

Cheng, S., Liu, H., Logan, B.E., 2006. Increased performance of single–chamber microbial fuel cells using an improved cathode structure. Electrochem. Commun. 8, 489–494.

Cheng, S.A., Logan, B.E., 2007. Ammonia treatment of carbon cloth anodes to enhance power generation of microbial fuel cells. Electrochem. Comm., 9(3), 492–496.

Choi, Y., Song, J., Jung, S., Kim, S., 2001. Optimization of the performance of microbial fuel cells containing alkalophilic Bacillus sp.. J. Microbiol. Biotechn., 11, 863–869.

Chong, M. L., Sabaratnam, V., Shirai, Y., and Hassan, M. A., 2009. Biohydrogen production from biomass and industrial wastes by dark fermentation. Int. J. Hydrogen Energy, 34(8), 32773287.

Cohen, B., 1931. The bacterial culture as an electron half–cell. J. Bacteriol., 21, 18–19.

Coppi, M., Leang, C., Lovley, D.R., Sandler, S., 2001. Development of a genetic system for Geobacter sulfurreducens. Appl. Environ. Microbiol. 67, 3180–3187.

Dancis, A., Roman, D. G., Anderson, G. J., Hinnebusch, A. G., Klausner,. R. D., 1992. Ferric reductase of Saccharomyces cerevisiae: molecular characterization, role in iron uptake, and transcriptional control by iron. Proc. Natl. Acad. Sci., 89, 3869–3873.

Das, D., and Veziroglu, T. N., 2008. Advances in biological hydrogen production processes. Int. J. Hydrogen Energy, 33, 6046–6057.

Demirbas, A., 2005. Potential applications of renewable energy sources, biomass combustion problems in boiler power systems and combustion related environmental issues. Prog. Energy Combust. Sci., 31, 171–192.

Deng, Q., Li, X.Y., Zuo, J.E., Ling, A., Logan, B.E., 2010. Power generation using an activated carbon fiber felt cathode in an upflow microbial fuel cell. J. Power Sources, 195, 1130–1135.

Dewan, A., Beyenal, H., Lewandowski, Z., 2008. Scaling up microbial fuel cells. Environ. Sci. Technol., 42(20), 7643–7648.

Dumas, C., Mollica, A., Feron, D., Basseguy, R., Etcheverry, L., Bergel, A., 2008. Checking graphite and stainless anodes with an experimental model of marine microbial fuel cell. Bioresour. Technol., 99, 8887–8894.

Eide, D.J., 1998. The molecular biology of metal ion transport in Saccharomyces cerevisiae. Annu. Rev. Nutr., 18, 1–469.

Eschbach, M., Schreiber, K., Trunk, K., Buer, J., Jahn, D., Schobert, M., 2004. Long–term anaerobic survival of the opportunistic pathogen Pseudomonas aeruginosa via pyruvate fermentation. J. Bacteriol., 186(14), 4596–4604.

Fan, Y., Sharbrough, E., Liu, H., 2008. Quantification of the internal resistance distribution of microbial fuel cells. Environ. Sci. Technol., 42, 8101–8107.

Feng, L., Chen, Y., Chen, L., 2011. Easy–to–operate and low–temperature synthesis of gram–scale nitrogen–doped graphene and its application as cathode catalyst in microbial fuel cells. ACS Nano, 5, 9611–9618.

Fidaleo, M., Charaniya, S., Solheid, C., Diel, U., Laudon, M., Ge, H., Scriven, L.E., Flickinger, M.C., 2006. A model system for increasing the intensity of whole-cell biocatalysis: Investigation of the rate of oxidation of D-sorbitol to L-sorbose by thin bi-layer latex coatings of non-growing Gluconobacter oxydans. Biotechnol. Bioeng., 95,446–458.

Finneran, K. T., Johnsen, C. V., Lovley, D. R., 2003. Rhodoferax ferrireducens gen. nov., sp. nov.; a psychrotolerant, facultatively anaerobic bacterium that oxidizes acetate with the reduction of Fe(III). Int. J. Syst. Evol. Microbiol. 53, 669–673.

Flickinger, M.C., Schottel, J.L., Bond, D.R., Aksan, A., Scriven, L.E., 2007. Painting and printing living bacteria: engineering nanoporous biocatalytic coatings to preserve microbial viability and intensify reactivity. Biotechnol. Prog., 23, 2–17.

François, J., Parrou, J.L., 2001. Reserve carbohydrates metabolism in the yeast Saccharomyces cerevisiae, FEMS Microbiol. Rev., 25, 125–145.

Georgatsou, E., Alexandraki, D.,1994.Two distinctly regulated genes are required for ferric reduction, the first step of iron uptake in Saccharomyces cerevisiae. Mol. Cell. Biol., 14, 3065–3073.

Gorby, Y.A., Yanina, S., McLean, J.,S., Rosso K.,M. Moyles, D., Dohnalkova A., Beveridge, T.J., Chang, I.S., Kim, B.H., Kim, K.S., Culley, D.E., Reed, S.B., Romine, M.F., Saffarini, D.A., Hill, E.A., Shi, L., Elias, D.A., Kennedy, D.W., Pinchuk, G., Watanabe, K., Ishii, S., Logan, B.E., Nealson, K.H., Fredrickson, J.K., 2006. Electrically conductive bacterial nanowires produced by Shewanella oneidensis strain MR–1 and other microorganisms. PNAS, 103(30), 11358 – 11363.

Gosse, J.L., Engel, B.J., Rey, F.E., Harwood, C.S., Scriven, L.E., Flickinger, M.C., 2007. Hydrogen production by photoreactive nanoporous latex coatings of nongrowing Rhodopseudomonas palustris CGA009. Biotechnol. Prog., 23, 124–130.

Gregory, K. B., Sullivian, S. A., Lovley, D. R., 2005. Electricity from swine waste coupled with odor reduction using electrodes. Abstr. Gen. Meet. Am. Soc. Microbiol., Q114.

Gude, V.G., 2016. Wastewater treatment in microbial fuel cells – an overview. J. Clean. Prod., 122(20), 287–307.

Gunawardena, A., Fernando, S., To, F., 2008. Performance of a yeast–mediated biological fuel cell. Int. J. Mol. Sci., 9, 1893–1907.

Holmes, D.E., Bond, D.R., O'Neil, R.A., Reimers, C.E., Tender, L.R., Lovley, D.R., 2004a. Microbial communities associated with electrodes harvesting electricity from a variety of aquatic sediments. Microbial Ecol. 48, 178–190.

Holmes, D. E., Bond, D. R., Lovley, D. R., 2004b. Electron transfer to Fe(III) and graphite electrodes by Desulfobulbus propionicus. Appl. Environ. Microbiol. 70, 1234–1237.

Holmes, D.E., Chaudhuri, S.K., Nevin, K.P., Mehta, T., Methé, B.A., Liu, A., Ward, J.E., Woodard, T.L., Webster, J., Lovley, D.R., 2006. Microarray and genetic analysis of electron transfer to electrodes in Geobacter sulfurreducens. Environ Microbiol., 8(10), 1805–1815.

Hubenova, Y., Mitov, M., 2015. Extracellular electron transfer in yeast–based biofuel cells: a review. Bioelectrochemistry, 106, 177–185.

IPCC (2006) Guidelines for National Greenhouse Gas Inventories, Volume 4 – Agriculture, Forestry and other Land Use. Intergovernmental Panel on Climate Change, Hayama, Japan.

ISPRA, 2015. Rapporto rifiuti urbani. Rapporti n. 230/2015. ISPRA – Istituto Superiore per la protezione e la ricerca ambientale. Via Vitaliano Brancati, 48 – 00144 Roma www.isprambiente.gov.it.

Johansson, T.B., Kelly, H., Reddy, A.K.N., Williams, R.H., 1993. Renewable energy sources for fuels and electricity, Island Press, Suite 300, 1718 Connecticut Avenue NW, Washington, DC, 20009.

Kim, B.H., Park, H. S., Kim, H. J., Kim, G. T., Chang, I. S., Lee, J., Phung, N. T., 2004. Enrichment of microbial community generating electricity using a fuel–cell–type electrochemical cell. Appl. Microbiol. Biotechnol., 63(6), 672–681.

Koopman, B.J., Hindriks, F. A., Lokerse, V. G., Wolthers, B.G., Orverdijk, J. F., 1985. Injurious effect of EDTA contamination on colorimetry of serum iron. Clin. Chem., 31(12), 2030-2032.

Kumar, A., Huan-Hsuan Hsu, L., Kavanagh, P., Barrière, F., Lens, P.N.L., Lapinsonnière, L., Lienhard V, J.H., Schröder, U., Jiang X., Leech, D., 2017. The ins and outs of microorganism-electrode electron transfer reactions. Nat. Rev. Chem. 1, 0024, 1–13.

Lee, H. S., Vermaas, W. F. J., Rittmann, B. E., 2010. Biological hydrogen production: Prospects and challenges. Trends Biotechnol., 28(5), 262–271.

Lesuisse, E., Labbe, P., 1992. Iron reduction and trans plasma membrane electron transfer in the yeast *Saccharomyces cerevisiae*. Plant Physiol., 100, 769–777.

Lesuisse, E., Labbe, P., 1994. Reductive iron assimilation in Saccharomyces cerevisiae. Metal Ions in Fungi, Winkelman, G. and Winge, D.R., Eds., 149–178, Marcel Dekker, NY, 1994.

Li, W. W., Yu, H. Q., 2011. From wastewater to bioenergy and biochemicals via two–stage bioconversion processes: A future paradigm. Biotechnol. Adv., 29(6), 972–982.

Li, D., Liu, J., Qu, Y., Wang, H., Feng, Y., 2016.Analysis of the effect of biofouling distribution on electricity output in microbial fuel cells. RSC Adv., 6, 27494–27500.

Liang, P., Huang, X., Fan, M.Z., Cao, X.X., Wang, C., 2007. Composition and distribution of internal resistance in three types of microbial fuel cells. Appl. Microbiol. Biotechnol., 77, 551–558.

Logan, B.E., Murano, C., Scott, K., Gray, N.D., Head, I.M.,2005. Electricity generation from cysteine in a microbial fuel cell Water Res., 39, 942–952.

Logan, B.E., Regan, J.M., 2006. Electricity–producing bacterial communities in microbial fuel cell. Trends Microbiol., 14(12), 512–518.

Logan, B.E., Cheng, S., Watson, V., Estadt, G., 2007. Graphite fiber brush anodes for increased power production in air–cathode microbial fuel cells. Environ. Sci. Technol., 41, 3341–3346.

Logan, B.E., 2008. Microbial Fuel Cell, John Wiley & Sons, Inc., Hoboken, NJ, 2008.

Logan, B.E., 2009. Exoelectrogenic bacteria that power microbial fuel cells, Nat. Rev. Microbiol., 7, 375–381.

Logan, B. E., 2012. Essential data and techniques for conducting microbial fuel cell and other types of bioelectrochemical system experiments. Chemsuschem, 5, 988–994.

Logan, B. E., Rabaey, K., 2012. Conversion of wastes into bioelectricity and chemicals by using microbial electrochemical technologies. Science, 337, 686–690.

Logan, B.E., Wallack, M.J., Kim, K.Y., He, W., Feng, Y., Saikaly, P.E., 2015. Assessment of microbial fuel cell configurations and power densities, Environ. Sci. Technol. letters, 2, 206−214.

Lovley, D. R., Phillips, E. J. P., 1988. Novel mode of microbial energy metabolism: organic carbon oxidation coupled to dissimilatory reduction of iron or manganese. Appl Environ Microbiol., 54, 1472–1480.

Lovley, D. R., Coates, J. D., Blunt–Harris, E. L., Phillips, E. J. P., Woodward, J. C., 1996. Humic substances as electron acceptors for microbial respiration. Nature 382, 445–448.

Lovley, D. R., Holmes, D. E., Nevin, K. P., 2004. Dissimilatory Fe(III) and Mn(IV) reduction. Adv. Microb. Physiol. 49, 219–286.

Lovley, D.R., 2006. Bug juice: harvesting electricity with microorganisms, Nat. Rev. Microbiol., 4, 497–508

Lyngberg, O.K., Scriven, L.E., Flickinger, M.C., 1998. A multi–layer patch coating method for preparing biocatalytic–coating samples of E–coli in latex copolymer. Abstr. Pap. Am. Chem. Soc., 216, U254–U254.

Lyngberg, O.K., Ng, C.P., Scriven, L.E., Flickinger, M.C., 2000. Engineering permeability of latex-bacterial composite coatings for industrial metabolically active cell biotransformations. Abstr. Pap. Am. Chem. Soc., 219, U170–U170.

Lyngberg, O.K., Ng, C.P., Thiagarajan, V., Scriven, L.E., Flickinger, M.C., 2001. Engineering the microstructure and permeability of thin multilayer latex biocatalytic coatings containing E. coli. Biotechnol. Prog., 17, 1169–1179.

Lyngberg, O.K., Solheid, C., Charaniya, S., Ma, Y., Thiagarajan, V., Scriven, L.E., Flickinger, M.C., 2005. Permeability and reactivity of Thermotoga maritima in latex bimodal blend coatings at 80 degrees C: A model high temperature biocatalytic coating. Extremophiles, 9, 197–207.

Mao, L., Verwoerd, W.S., 2013. Selection of organisms for systems biology study of microbial electricity generation: a review. IJEEE, 4, 1–18.

May, J.M., Qu, Z.C., Cobb, C.E., 2004. Reduction and uptake of methylene blue by human erythrocytes. Am. J. Physiol. Cell. Physiol., 286, C1390–1398.

McKendry, P., 2002. Energy production from biomass (part1): overview of biomass. Bioresour. Technol., 83, 37–46.

McCreery, R.L., 2008. Advanced carbon electrode materials for molecular electrochemistry. Chem. Rev., 108(7), 2646–2687.

Methé, B. A., Nelson, K. E.,. Eisen, J. A,. Paulsen, I. T, Nelson, W., Heidelberg, J. F., Wu, D., Wu, M., Ward, N., Beanan, M. J., Dodson, R. J., Madupu, R., Brinkac, L. M., Daugherty, S. C., DeBoy, R. T., Durkin, A. S., Gwinn, M., Kolonay, J. F., Sullivan, S. A., Haft, D. H., Selengut, J., Davidsen, T. M., Zafar, N., White, O., Tran, B., Romero, C., Forberger, H. A, Weidman, J., Khouri, H., Feldblyum, T. V., Utterback, T. R., Van Aken, S. E., Lovley, D. R., Fraser, C. M. 2003. Genome of Geobacter sulfurreducens: metal reduction in subsurface environments. Science, 302, 1967–1969.

Mowry, S., Ogren, P.J., 1999. Kinetics of methylene blue reduction by ascorbic acid. J. Chem. Educ., 76, 970-973.

Myers, C.R., Myers, J.M., 1992. Localization of Cytochromes to the outer membrane of anaerobically grown Shewanella putrifaciens MR–1, J. Bacteriol., 174, 3429–3438.

Najafpour, G.D., Rahimnejad, M., Mokhtarian, N., Wan Ramli Wan Daud, Ghoreyshi, A.A., 2010. Bioconversion of whey to electrical energy in a biofuel cell using Saccharomyces cerevisiae. World Appl. Sci. J., 8, 01–05.

Nevin, K. P., Lovley, D. R., 2000. Lack of production of electron–shuttling compounds or solubilization of Fe(III) during reduction of insoluble Fe(III) oxide by Geobacter metallireducens. Appl. Environ. Microbiol. 66, 2248–2251.

Nevin, K.P., Richter, H., Covalla, S.F., Johnson, J.P., Woodard, T.L., Orloff, A.L., Jia, H., Zhang, M., Lovley, D.R., 2008. Power output and columbic efficiencies from biofilms of Geobacter sulfurreducens comparable to mixed community microbial fuel cells. Environ. Microbiol., 10(10), 2505–2514.

Pan, Y., Mo, X., Li, X., Pu, L., Liu, D., Yang, T., 2016. Iron–nitrogen–activated carbon as cathode catalyst to improve the power generation of single–chamber air–cathode microbial fuel cells. Bioresour. Technol., 206, 285–289.

Pant, D., Van Bogaert, G., De Smet, M., Diels, L., Vanbroekhoven, K., 2010. Use of novel permeable membrane and air cathodes in acetate microbial fuel cells. Electrochim. Acta, 55, 7710–7716.

Pavan, P., Battistoni, P., Cecchi, F., and Mata–Alvarez, J., 2000. Two–phase anaerobic digestion of source sorted OFMSW (organic fraction of municipal solid waste): Performance and kinetic study. Water Sci. Technol., 41(3), 111–118.

Pham, T. H., Aelterman, P., and Verstraete, W., 2009. Bioanode performance in bioelectrochemical systems: recent improvements and prospects. Trends Biotechnol., 27(3), 168–178.

Potter M.C., 1911. Electrical effects accompanying the decomposition of organic compounds. Proc. R. Soc. London, Ser. B, 84(571), 260–276.

Rabaey, K., Clauwaert, P., Aelterman, P., Verstraete, W., 2005. Tubular microbial fuel cells for efficient electricity generation. Environ. Sci. Technol., 39(20), 8077–8082.

Ramalho, P.A., Paiva, S., Cavaco-Paulo, A., Casal, M., Cardoso, M.H., Ramalho, M.T., 2005. Azo reductase activity of intact Saccharomyces cerevisiae cells is dependent on the Fre1p component of plasma membrane ferric reductase. Appl. Env. Microbiol., 71, 3882–3888.

Reguera, G., McCarthy, K.D., Mehta, T., Nicoll, J.S., Tuominen, M.T., Lovley, D.R., 2005. Extracellular electron transfer via microbial nanowires. Nature 435, 1098–1101.

Reid, G.A., Schatz, G., 1982. Import of proteins into mitochondria. J. Biol. Chem., 257, 13056–13061.

Ren, N. Q., Guo, W. Q., Liu, B. F., Cao, G. L., and Ding, J., 2011. Biological hydrogen production by dark fermentation: Challenges and prospects towards scaled–up production. Curr. Opin. Biotechnol., 22(3), 365–370.

Richter, H., McCarthy, K., Nevin, K.P., Johnson, J.P., Rotello, V.M., Lovley, D.R., 2008. Electricity generation by Geobacter sulfurreducens attached to gold electrodes. Langmuir, 24(8), 4376–4379.

Rossi, R., Yang, W., Setti, L., Logan, B.E., 2017. Assessment of a metal–organic framework catalyst in air cathode microbial fuel cells over time with different buffers and solutions. Bioresour. Technol., 233, 399–405.

Rossi, R., Setti, L., 2016. Effect of methylene blue on electron mediated microbial fuel cell by Saccharomyces cerevisiae. Environ. Eng. Manag. J., 16, 2011–2018.

Rossi, R., Cavina, M., Setti, L., 2016. Characterization of electron transfer mechanism in mediated Microbial Fuel Cell by entrapped electron mediator in Saccharomyces cerevisiae. CET, 49, 559–565.

Rossi, R., Fedrigucci, A., Setti, L., 2015. Characterization of electron mediated microbial fuel cell by Saccharomyces cerevisiae. CET, 43, 337–343.

Rozendal, R.A, Hamelers, H.M.V., Rabaey, K., Keller, J., Buisman, C.J.N., 2008. Towards practical implementation of bioelectrochemical wastewater treatment. Trends Biotechnol., 26, 450–459.

Sasaki, T., Norihide, K., Miyachi, S., 1998. Induction of ferric reductase activity and of iron uptake capacity in Chlorococcum littorale cells under extremely high-CO_2 and iron-deficient conditions. Plant Cell Physiol., 39, 405–410.

Sayed, E.T., Tsujiguchi, T., Nakagawa, N., 2012. Catalytic activity of baker's yeast in a mediatorless microbial fuel cell. Bioelectrochemistry, 97–101.

Schaetzle, O., Barriere, F., Baronian, K., 2008. Bacteria and yeasts as catalysts in microbial fuel cells: electron transfer from micro–organisms to electrodes for green electricity. Energy Environ. Sci., 1, 607–620.

Shena, J., Huanga, L., Zhoub, P., Quana, X., Li Puma, G., 2017. Correlation between circuital current, Cu(II) reduction and cellular electron transfer in EAB isolated from Cu(II)-reduced biocathodes of microbial fuel cells. Bioelectrochemistry, 114, 1–7.

Shi, X., Feng, Y., Wang, X., Lee, H., Liu, J., Qu, Y.,He W.,Kumar, S.M.S, Ren, N., 2012. Application of nitrogen–doped carbon powders as low–cost and durable cathodic catalyst to air–cathode microbial fuel cells. Bioresour. Technol., 108, 89–93.

Schnurer, A., Zellner, G., Svensson, B. H., 1999. Mesophilic syntrophic acetate oxidation during methane formation in biogas reactors. FEMS Microbiol. Ecol., 29, 249–261.

Schröder, U., 2007. Anodic electron transfer mechanisms in microbial fuel cells and their energy efficiency. Phys.Chem.Chem.Phys., 9, 2619–2629.

Schröder, I., Johnson, E., de Vries, S., 2003. Microbial ferric iron reductases. FEMS Microbiol. Rev., 27, 427–447.

Scott, K., Cotlarciuc, I., Head, I., Katuri, K.P., Hall, D., Lakeman, J.B., Browning, D., 2008. Fuel cell power generation from marine sediments, investigation of cathode materials J. Chem. Technol. Biotechnol., 83, 1244–1254.

Stafford, D. A., Wheatley, B. I., Hughes, D. E., 1980. Anaerobic Digestion. Elsevier Science.

Torres, C.I., Kato Marcus, A., Rittmann, B.E. 2008a. Proton transport inside the biofilm limits electrical current generation by anode–respiring bacteria. Biotechnol. Bioeng., 100(5), 872–881

Torres, C.I., Lee, H., Rittmann, B.E., 2008b. Carbonate species as OH^- carriers for decreasing the pH gradient between cathode and anode in biological fuel cells. Environ. Sci. Technol., 42, 8773–8777.

UNFCCC, 2003. Estimating, reporting, and accounting of harvested wood products. Technical paper FCCC/TP2003/7.

Volkov, V., 2015. Quantitative description of ion transport via plasma membrane of yeast and small cells. Front Plant Sci., 6, 425.

Wagner, R.C., Porter–Gill, S., Logan, B.E., 2012. Immobilization of anode-attached microbes in a microbial fuel cell. AMB express, 2, 1–6.

Ward, A. J., Hobbs, P. J., Holliman, P. J., Jones, D. L., 2008. Optimization of the anaerobic digestion of agricultural resources. Bioresour. Technol., 99(17), 7928–7940.

Wartmann, Y., Stephan, U.W., Bube, I., Boer, E., Melzer, M., Manteuffel, R., Stoltenburg, R., Guengerich, L., Gellissen, G., Kunze, G., 2002. Post–translational modifications of the AFET3 gene product – a component of the iron transport system in budding cells and mycelia of the yeast Arxula adeninivorans. Yeast, 19, 849–862.

Wei, J., Liang, P., Huang, X., 2011. Recent progress in electrodes for microbial fuel cells, Bioresour. Technol., 102, 9335–9344.

Yang, Y., Xu, M., Guo J., Sun, G., 2012. Bacterial extracellular electron transfer in bioelectrochemical systems. Process Biochem., 47(12), 1707–1714.

Yang, W., Logan, B.E., 2016. Immobilization of a metal–nitrogen–carbon catalyst on activated carbon with enhanced cathode performance in microbial fuel cells. ChemSusChem, 9, 2226–2232.

Yi, H., Nevin, K.P., Kim, B.C., Franks, A.E., Klimes, A., Tender, L.M., Lovley, D.R., 2009. Selection of a variant of Geobacter sulfurreducens with enhanced capacity for current production in microbial fuel cells. Biosens. Bioelectron., 24(12), 3498–3503.

Yu, E.H., Cheng, S.A., Scott, K., Logan, B.E., 2007. Microbial fuel cell performance with non–Pt cathode catalysts. J. Power Sources, 171, 275–281.

Yuan, Y. Ahmedb, J., Zhouc, L., Zhaoa, B., Kim, S., 2011. Carbon nanoparticles–assisted mediator–less microbial fuel cells using Proteus vulgaris. Biosens. Bioelectron., 27, 106–112.

Zhang, B., Zhang, L. L., Zhang, S. C., Shi, H. Z., Cai, W. M., 2005. The influence of pH on hydrolysis and acidogenesis of kitchen wastes in two–phase anaerobic digestion. Environ. Technol., 26(3), 329–339.

Zhang, F., Cheng, S.A., Pant, D., Van Bogaert, G., Logan, B.E., 2009. Power generation using an activated carbon and metal mesh cathode in a microbial fuel cell. Electrochem. Commun., 11, 2177–2179.

Zhang, X., Shi, J., Liang, P., Wei, J., Huang, X., Zhang, C., Logan, B.E., 2013. Power generation by packed–bed air–cathode microbial fuel cells. Bioresour. Technol., 142, 109–114.

Zhang, X., Pant, D., Zhang, F., Liu, J., He, W., Logan, B.E., 2014. Long–term performance of chemically and physically modified activated carbons in air cathodes of microbial fuel cells. ChemElectroChem 1, 1859–1866.

Zuo, Y., Cheng, S., Logan, B.E., 2008a. Ion exchange membrane cathodes for scalable microbial fuel cells. Environ. Sci. Technol., 42(18), 6967–6972.

Appendix A

During the last year of my Ph. D., I've spent six months at the Pennsylvania State University (PSU), under the supervision of prof. Bruce E. Logan, working on microbial fuel cell. Here are the results of the experiments conducted during that period. Part of these experiment has been published into the peer–reviewed journal Bioresource Technology.

Assessment of a metal–organic framework catalyst in air cathode microbial fuel cells over time with different buffers and solutions

Abstract

Activated carbon (AC) cathode performance is enhanced by using a metal–organic framework (MOF) but longevity needs to be considered in the presence of metal chelators or ligands, such as phosphate, commonly present in wastewaters. MOF catalysts on AC initially produced 2.78 ± 0.08 W m^{-2}, but power decreased by 26% after eight weeks in MFCs using a 50 mM phosphate buffer (PBS) and acetate due to decreased cathode performance. However, power was still 41% larger than that of the control AC (no MOF). Power generation using domestic wastewater was initially 0.73 ± 0.01 W m^{-2}, and decreased by 21% over eight weeks, with final power 53% larger than previous reports, although changes in wastewater composition were a factor in performance. Adding phosphate salts, EDTA or TWEEN 80 to the wastewater did not affect the catalyst performance over time. While MOF catalysts are therefore initially adversely affected by chelators, performance remains enhanced compared to plain AC.

Introduction

In this study, the longevity of MOF catalyst added onto AC (Fe–N–C/AC) and plain AC cathodes (control) were examined over eight weeks using acetate and two different buffers, or domestic wastewater. One concern with using a phosphate as a buffer, or with wastewater, is that phosphate in these solutions could cause the deactivation of the catalytic activity of iron through the formation of iron–phosphate complexes or through precipitation of salts on the catalyst. To examine the potential impact of phosphate on iron, the performance of MFCs over time with an inorganic phosphate buffer solution (PBS) was compared to that obtained using an organic buffer (piperazine–N,N′–bis(2–ethanesulfonic acid, PIPES) that did not contain phosphate. In addition, MFCs were also examined using domestic wastewater, which contain a complex organic matter as the fuel and inorganic and organic forms of phosphorus. Additional experiments were conducted with phosphate salts added to the wastewater to evaluate if the presence of higher concentrations of inorganic phosphorus would affect power generation over time. The effect of adding EDTA as not phosphoric ligand was evaluated in MFCs using wastewater and parallel experiments were conducted using wastewater amended with TWEEN 80, to evaluate if the addition of a non-ionic surfactant could help keeping clean the solution side of the cathode surface. Wen et al. (2011) reported higher performance of MFCs after the addition of TWEEN 80 to the anodic solution (Wen et al., 2011).

Materials and methods

Catalyst synthesis and cathode fabrication

Cathodes with the Fe–N–C/AC catalyst were synthetized as previously described (Yang and Logan, 2016). Briefly, 6 g of AC powder (Norit SX plus, Norit Americas Inc.,TX) was dispersed in water containing 1 g of iron chloride (anhydrous, Sigma Aldrich, USA) and 1 g of 1,10–phenanthroline (Sigma Aldrich,

USA) at 60 °C. The mixture was stirred until dryness under a fume hood at 60 °C, and then pyrolyzed at 800 °C for 15 min in an N_2 atmosphere. The resulting powder was dispersed in 10 mM hydrochloric acid (HCl), filtered, and dried at room temperature for 48 h. AC–based cathodes were fabricated by placing the catalyst layer between stainless steel mesh (42 mesh size, type 304, McMaster–Carr, USA) and the hydrophobic PVDF membrane diffusion layer (0.45 μm, MILLIPORE, USA). The material was then rinsed with ethanol, pressed at 3×10^7 Pa for at least 15 s at 60 °C (Model 4388, CARVER, INC., USA), and dried in a fume hood at room temperature. The AC catalyst layer was prepared by mixing and then drying 6 g of the AC catalyst and 0.67 mL of a 60% PTFE (polytetrafluoroethylene) emulsion (Sigma Aldrich, USA) in ethanol on a hot plate at 60 °C.

MFC construction and operation

MFCs were single–chamber, cubic reactors constructed from a polycarbonate block 4 cm in length, with an inside cylindrical chamber having a diameter of 3 cm (Zhang et al., 2011). The anodes were graphite fiber brushes (2.5 cm in both diameter and length), heat treated at 450 °C in air for 30 min, and placed horizontally in the middle of MFC chambers (Logan et al., 2007, Vargas et al., 2013, Shi et al., 2012). Anodes were fully pre–acclimated in MFCs for over four months at a fixed external resistance of 1000 Ω, at a constant temperature (30 °C). The medium contained 1 g L^{-1} sodium acetate dissolved in 50 mM PBS (Na_2HPO_4, 4.58 g L^{-1}; $NaH_2PO_4 \cdot H_2O$, 2.45 g L^{-1}; NH_4Cl, 0.31 g L^{-1}; KCl, 0.13 g L^{-1}; pH 7.0; conductivity of σ = 6.2 mS cm^{-1}) or a PIPES buffer (15.12 g L^{-1}, pH adjusted to 7 using NaOH) that was amended with 12.5 mL L^{-1} minerals and 5 mL L^{-1} vitamins (Cheng et al., 2009). Previous studies have suggested that the conductivity of the solution is more important to performance than the buffer concentration

(Nam et al., 2010). Therefore, NaCl was added to adjust the conductivity of the PIPES buffer to match that of the PBS solution (6.2 mS cm^{-1}).

Domestic wastewater was collected once a week from the primary clarifier of the Pennsylvania State University Waste Water Treatment Plant, and stored at 4 °C prior to use. For some tests, wastewater was amended with the same phosphate concentration used for acetate fueled MFCs (Na_2HPO_4, 4.58 g L^{-1}; $NaH_2PO_4 \cdot H_2O$, 2.45 g L^{-1}). Control reactors were operated with NaCl amended wastewater with the same conductivity as that of phosphate amended wastewater. The experiments conducted with wastewater amended with EDTA were conducted adding 0.5 mL EDTA disodium salt hydrate (0.2 M) to 0.1 L of wastewater (final concentration 1 mM), while Tween 80 was prepared in distilled water and added to a final concentration of 20 mg L^{-1} in the wastewater. All reactors were operated in batch mode at 30 °C.

Single cycle polarization tests were conducted by varying the external resistance from 1000, 500, 200, 100, 75, 50, to 20 Ω at a 20 min interval after open circuiting for 2 h with a total test duration of 4 h, in a constant temperature room (30 °C) (Yang et al., 2015). The voltage drop (U) across an external resistor was recorded by a computer based data acquisition system (2700, Keithley Instrument, OH). Current densities (i) and power densities (P) were normalized to the exposed projected cathode area (A = 7 cm^2), and calculated as $i = U/RA$ and $P = iU/A$, where R is the external resistance. The high conductivity combined with low COD of the solutions with wastewater and salts led to power overshoot in single cycle polarization tests, so the multiple cycle polarization test was used for power tests in wastewater to avoid power overshoot (Watson and Logan, 2011). The external resistance was gradually changed from 1000 to 50 Ω and the reactors were operated for at least two fed–batch cycles at each resistance to allow the biofilm to adapt and ensure reproducible power output. At each cycle, the voltages were

measured for 1 h after the MFC produced the peak voltage and were averaged for the final reported value.

Electrochemical analysis

The ohmic and charge transfer resistances were measured using electrochemical impedance spectroscopy (EIS). A potentiostat (VMP3 Multichannel Workstation, Biologic Science Instruments, USA) was used for all measurements, with all electrochemical tests conducted in a constant temperature room (30 °C). EIS was performed under open circuit voltage (OCV) conditions over a frequency range of 100 KHz to 100 mHz with sinusoidal perturbation of 10 mV amplitude. Ohmic resistance was obtained from a Nyquist plot as the first x–intercept (lower value of x) at high frequency range, while the diameter of the fitted semicircle was the charge transfer resistance (Sekar and Ramasamy, 2013).

Surface characterization

Environmental scanning electron microscopic (ESEM) images were produced using a FEI Quanta 200 instrument (FEI company, Hillsboro, OR, USA). A quick XPS (Axis Ultra XPS, Kratos Analytical, UK, monochrome AlKa source, 1486 eV) scan was conducted on the cathode to identify the elements present initially and after eight weeks of operation with a high generation energy, and short dwell time. CASA XPS software was used for the elemental analysis.

Results and discussion

MFC performance in PBS or PIPES over time

MFCs with the MOF catalyst and 50 mM PBS initially (week 1) produced 2.78 ± 0.08 W m^{-2}, which was 54% higher than the power initially generated by the plain AC catalyst in the same buffer (1.80 ± 0.03 W m^{-2}) (**Fig. A.1**). This initial increase was consistent with that previously reported for these MOF AC-treated

cathodes in MFCs. The behavior of the MOF catalyst was also examined in an organic buffer lacking phosphate to avoid possible ligation of phosphorus with iron. The power generation in the first week in using the PIPES buffer was 2.19 ± 0.01 W m^{-2}, which was 21% lower of that obtained using PBS (**Fig. A.2**). This impact of the buffer on MFCs performance was different from that previously shown by Nam et al. (2010) using PBS, PIPES or other buffers in single–chambered MFCs with a different architecture (bottles, with relatively small cathodes compared to the anode size) and Pt catalysts. It is likely that differences in the buffers were due to the different catalysts and the much higher internal resistances, and therefore lower power densities, which may have precluded observing an impact of the buffer.

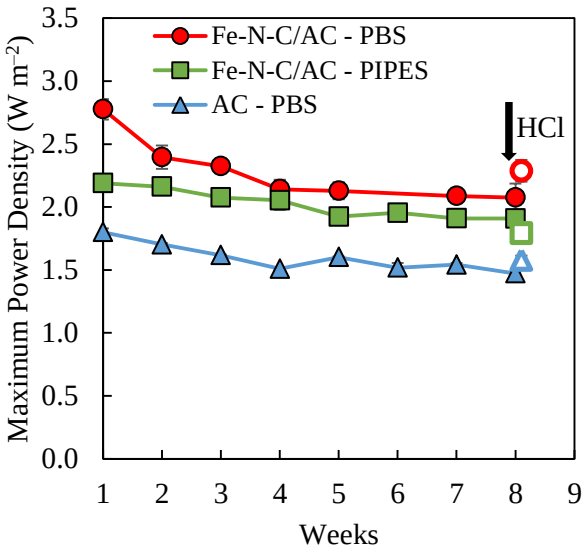

Fig. A.1. Maximum power production over time using Fe–N–C/AC catalyst in PBS and PIPES and plain AC in PBS. After the eight weeks the cathodes were treated with hydrochloric acid (arrow) and tested again for the maximum power density (open symbols).

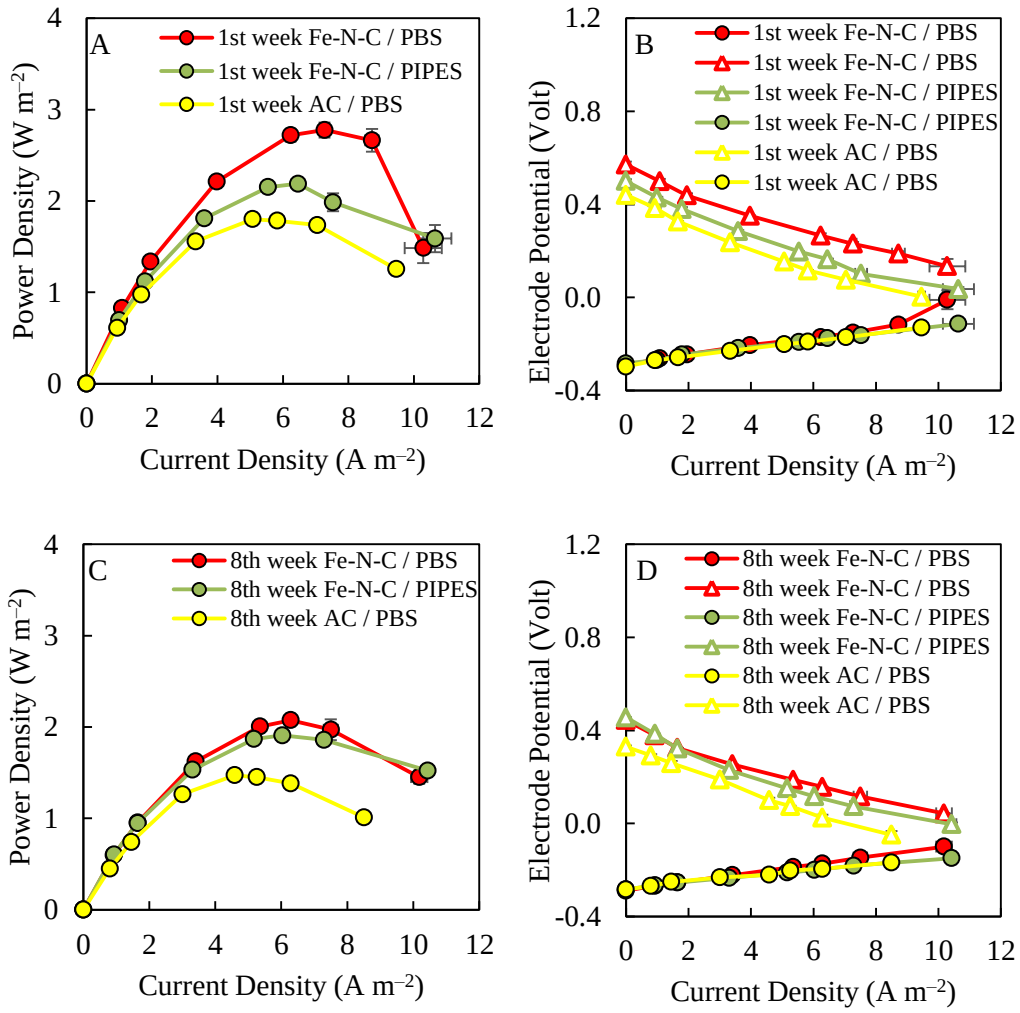

Fig. A.2. Comparison of (A, C) power density curves and (B, D) corresponding electrode potentials for MFCs using Fe-N-C/AC or AC catalyst in PBS and PIPES in 1st and 8th week.

The maximum power density of Fe–N–C/AC cathodes in PBS decreased by 23% in the first four weeks to 2.14 ± 0.07 W m^{-2} and then remained constant through the rest of the experiment with a final maximum power density of 2.07 ± 0.01 W m^{-2} (F_{test} = 3.00; α = 0.05). The power generation using the MOF–AC cathodes in the PIPES buffer was lower but relatively more stable than results with PBS, decreasing by only 13% over the eight weeks to a final maximum power

density of 1.91 ± 0.03 W m^{-2}. This final power density with PIPES buffer was only slightly lower than that of 2.07 ± 0.01 W m^{-2} obtained with PBS in the last week. The performance obtained with the plain AC cathodes also declined slowly over time, with an 18% decrease in power over eight weeks, from 1.80 ± 0.03 W m^{-2} to 1.47 ± 0.02 W m^{-2}. The relatively rapid decrease in the MOF–AC catalyst indicated that the high initial power density of the MOF catalyst could not be maintained over time. As a rapid decrease in power was not observed in tests with the plain AC catalyst or using the PIPES media with the MOF–AC catalyst, it was concluded that the rapid initial decrease was due to the interactions of the inorganic phosphate salts with the iron catalyst. However, despite this rapid decrease in power, relatively stable power generation was obtained in weeks 4–8 (average 2.11 ± 0.03 W m^{-2}) at a power density that was 38% higher than that of plain AC over weeks 4 to 8 and 41% greater at week 8.

To examine if the decrease in the maximum power densities could be restored, after eight weeks of operation the cathodes were cleaned by gently removing the biofilm and soaking them in weak hydrochloric acid (Zhang et al., 2014). The acid cleaning partially restored the performance of the MOF cathodes tested in PBS to 2.29 ± 0.09 W m^{-2} (82% of the initial value) compared to the last value of 2.07 ± 0.01 W m^{-2}. However, the performance of the MFCs with the MOF cathodes in PIPES was negatively affected by the cleaning procedure, as cleaning resulted in slightly lower power density value of 1.79 ± 0.02 W m^{-2} compared to 1.91 ± 0.03 W m^{-2} before the acid cleaning. The recovery for plain AC was 88% of the initial value, with 1.58 ± 0.03 W m^{-2} after eight weeks with cleaning, compared to the initial power density of 1.47 ± 0.02 W m^{-2}. These results showing improved performance with the PBS electrolyte were consistent with previous results, where 85% of performance was restored by acid cleaning, although those tests compared power after 17 months to 1 month (Zhang et al., 2014).

To demonstrate that the changes in power generation were due to the cathode performance, the electrode potentials were examined during polarization tests (**Fig. A.3**). The cathode potential of the MOF catalyst at its maximum power in PBS was 0.23 ± 0.01 V in the first week, with a decrease to 0.16 V after eight weeks. In PIPES the cathode shifted from 0.16 V to 0.12 V, while with plain AC it decreased from 0.15 V to 0.10 (**Fig A.3B, D** and **F**). In all tests, the anode potentials were stable and constant over time (**Fig A.3B, D** and **F**). These changes in the cathode potentials to more negative potentials for both cathodes when using PBS, with no changes in the anode potentials over time, demonstrated that the reductions in power production were due to changes in the cathodes and not the anodes.

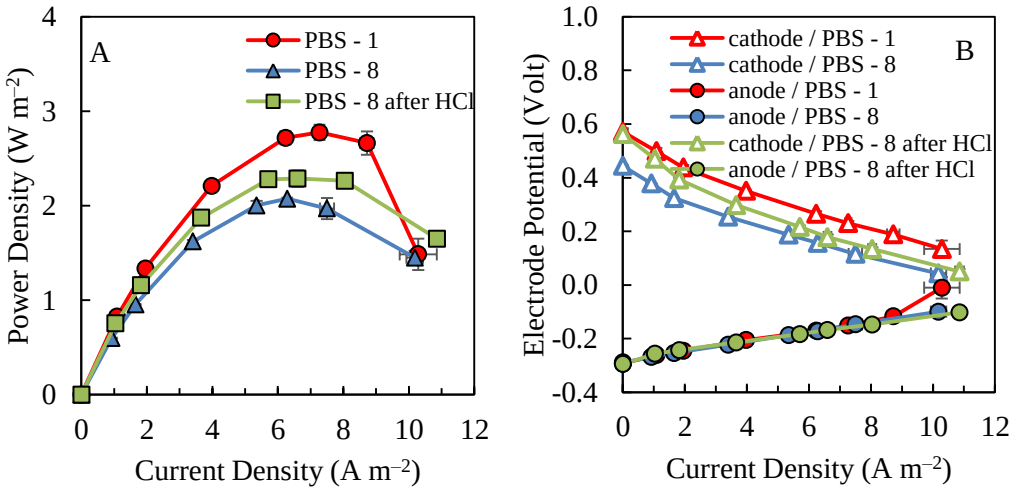

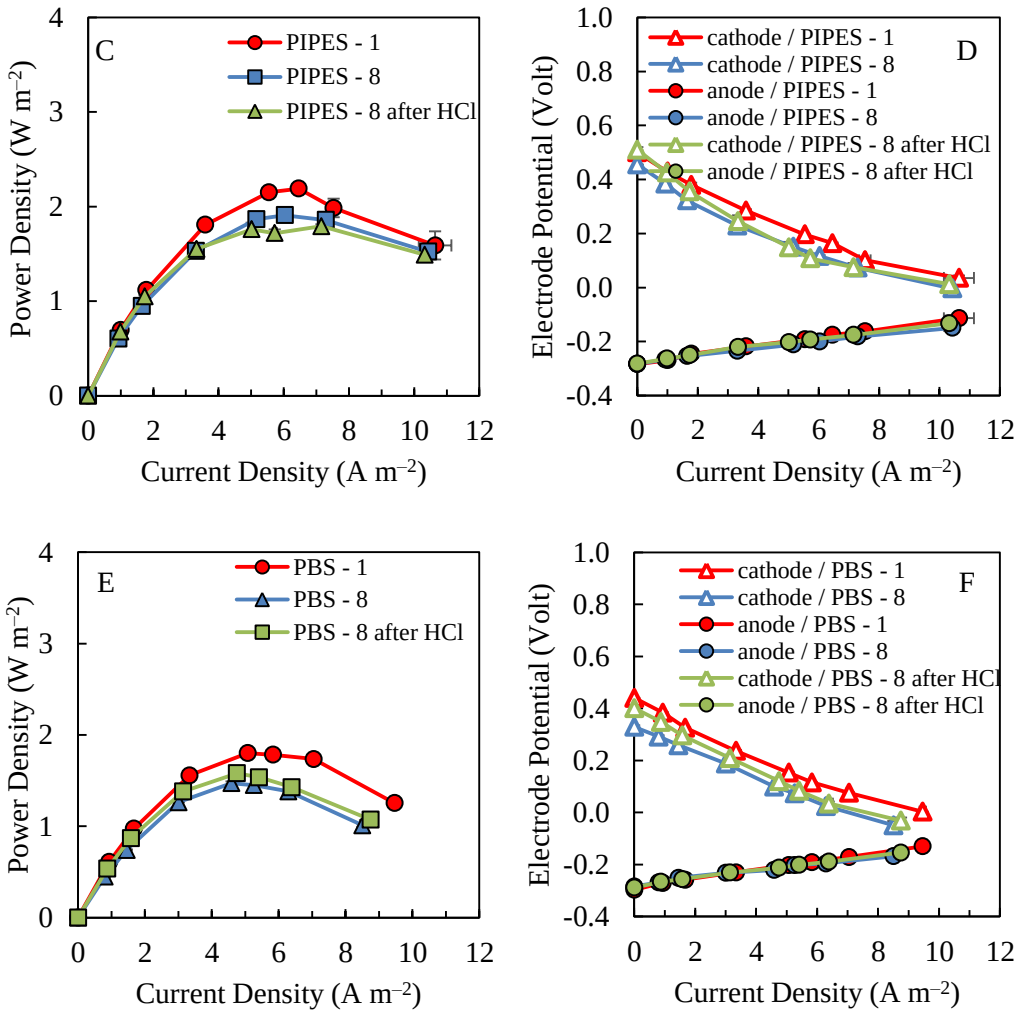

Fig. A.3. Comparison of power density curves of (A) Fe–N–C/AC catalyst in 50 mM PBS and corresponding electrode potentials (B). Power density curves of (C) Fe–N–C/AC catalyst in 50 mM PIPES and corresponding electrode potentials (D). Power density curves of (E) AC catalyst in 50 mM PBS and corresponding electrode potentials (F) during the 1st, 8th week and after the acid cleaning.

The cathode potentials at open circuit voltage (OCV) of the MOF catalyst in PBS dropped from 0.57 ± 0.01 V at week 1 to 0.44 V at week 8. This suggested a reduction in the catalyst conductivity, which could be due to deposition of salts on the solution side of the cathode (Winfield et al., 2011). In contrast, the cathode potential at OCV in PIPES was relatively stable over time and decreased only

slightly from 0.50 ± 0.01 V to 0.47 V. Acid cleaning partially restored the initial cathode potentials. The initial OCVs of the MOF cathodes tested in PBS were recovered after acid cleaning (from 0.44 to 0.52 ± 0.02 V) while cathode potentials at OCV in PIPES showed no change, suggesting that cathode potential drop was due to the deposition of phosphate salts on the cathodes which could be reversed by acid treatment. The salts precipitation could potentially lower the cathode performance by affecting the conductivity of the catalyst. Although the acid treatment was effective in restoring the initial open circuit potentials, it did not completely restore cathode performance at higher current densities indicating other irreversible changes in the oxygen reduction reaction, as observed for the plain AC catalyst following cleaning.

Electrochemical analysis

EIS was performed on new and used cathodes in an abiotic electrochemical cell to evaluate changes in performance of the cathodes in the absence of bacteria (**Fig. A.4**). The new MOF cathodes showed the same solution resistance of R_s = 19.9 **Ω**, and a similar charge transfer resistance in both PBS (R_{ct} = 0.90 **Ω**) and PIPES (R_{ct} = 0.99 **Ω**). After eight weeks operation, the charge transfer resistance of the MOF cathode increased to R_{ct} = 3.85 **Ω** (PBS) and R_{ct} = 5.24 **Ω** (PIPES), mainly due to the deterioration of the catalyst, consistent with the lower performance of the cathodes at the end of the experiment (**Fig. A.5**).

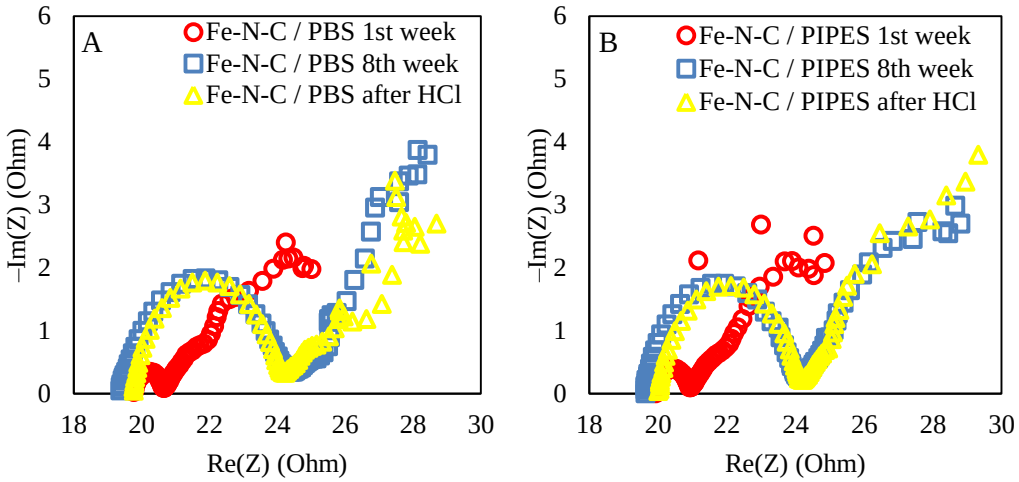

Fig. A.4. Nyquist plots of EIS spectra of by two types of Fe–N–C/AC catalyst under new and used conditions in PBS (A) and PIPES (B).

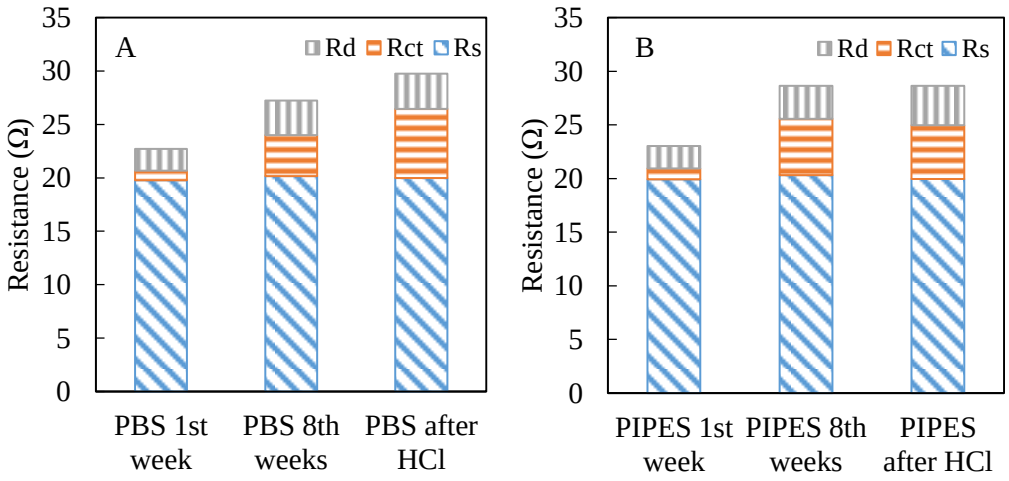

Fig. A.5. Component analysis of internal resistance for the Fe–N–C/AC catalyst under both new and used conditions in (A) PBS and (B) PIPES.

Cleaning the cathodes with hydrochloric acid did not restore the initial charge transfer resistance, which suggested an alternative cleaning method or another type of chemical treatment might be needed to fully restore cathode performance. The R_{ct} after the acid cleaning procedure was 5.02 Ω in PIPES and 6.48 Ω in PBS, which were higher than the resistance registered before the treatment (3.85 Ω).

Surface characterization

SEM images (**Fig. A.6**) clearly showed the effectiveness of the cathode cleaning procedure on removing material from the cathode. After eight weeks of operation the catalyst on the solution side of the cathode was completely covered by the microorganisms but the cleaning procedure was effective in restoring the initial appearance of the solution side of the cathode. XPS analysis of new cathodes confirmed the addition of iron due to the MOF treatment of the AC cathodes, based on Fe peaks in the new cathodes. However, after eight weeks operation no iron peaks were detected in the catalyst (**Table A.1**). The loss of iron from the MOF catalyst likely explains the large decrease in the power density performance in the initial weeks of operation. Moreover, the iron content of the new samples was four times higher than previously reported (Yang and Logan, 2016), showing a large variability on the effectiveness of the immobilization.

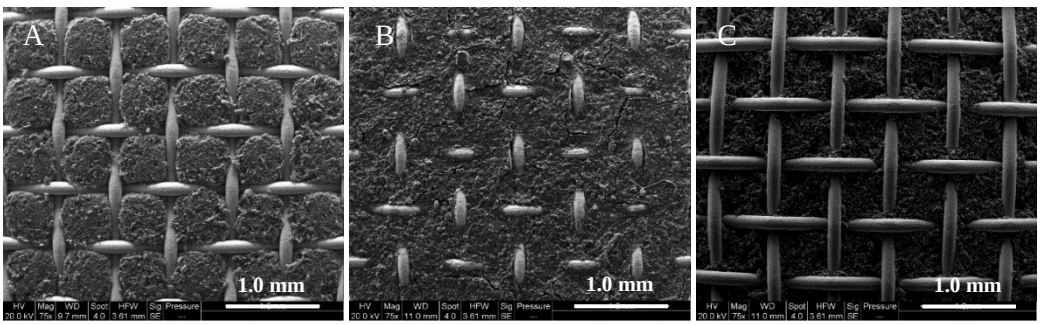

Fig. A.6. SEM images of the solution side of new (A) cathode, after removal of biofilm (B) and after cleaning procedure (C).

Table A.1. Elemental composition of Fe–N–C / AC cathodes under new, used, and cleaned conditions.

Sample	C [%]	O [%]	N [%]	Fe [%]
Fe–N–C/AC 1st week	73.1	8.4	0.3	5.6
Fe–N–C/AC 8th week	57.6	24.2	6.4	–
Fe–N–C/AC 8th week after HCl cleaning	78.1	4.8	1.0	–

MFCs performance in wastewater over time

To better examine the longevity of the MOF catalyst in more complex medium, the performance of the Fe–N–C/AC modified cathodes was evaluated in MFCs fed with domestic wastewater (**Fig. A.7A**). The initial maximum power density of the MOF–AC cathodes in raw wastewater was 0.73 ± 0.01 W m^{-2}, consistent with power densities previously obtained using new MOF cathodes and domestic wastewater (Yang and Logan, 2016). After an initial decrease in power production after week 1 (from 0.73 ± 0.01 W m^{-2} to 0.61 ± 0.01 W m^{-2}), there was no observable change in the maximum power densities due to the high variability of the different wastewater samples (**Fig. A.7B**). While the maximum power density decreased by 25% from the initial value (0.73 ± 0.01 W m^{-2}) to that obtained after eight weeks (0.58 ± 0.07 W m^{-2}) (**Fig. A.8A**), the decline in power was not associated with changes in cathode potentials in this case, as the anode potentials changed likely due to the use of the different wastewater samples, particularly at high current densities (**Fig. A.8B**). The average power density for the raw wastewater reactors was 0.61 ± 0.05 W m^{-2} over either weeks, which was 53 % higher than that previously reported (0.40 ± 0.03 W m^{-2}) for new Pt based carbon cloth (Pt/C) cathodes and domestic wastewater from the same treatment plant (Yang and Logan, 2016).

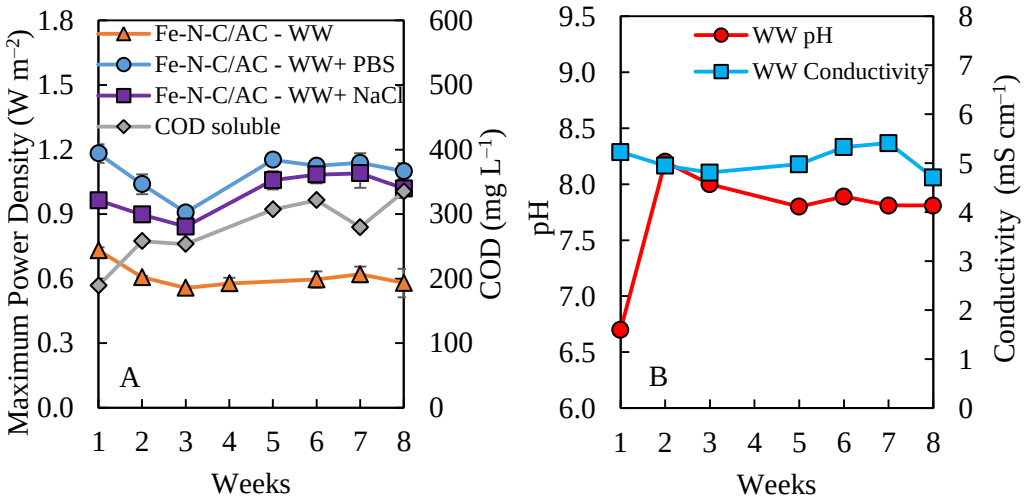

Fig. A.7. (A) Maximum power production and COD level over time using Fe–N–C / AC catalyst in wastewater, wastewater added with PBS and wastewater added with sodium chloride (same conductivity of wastewater with PBS). (B) Wastewater pH and conductivity after the addition of NaCl.

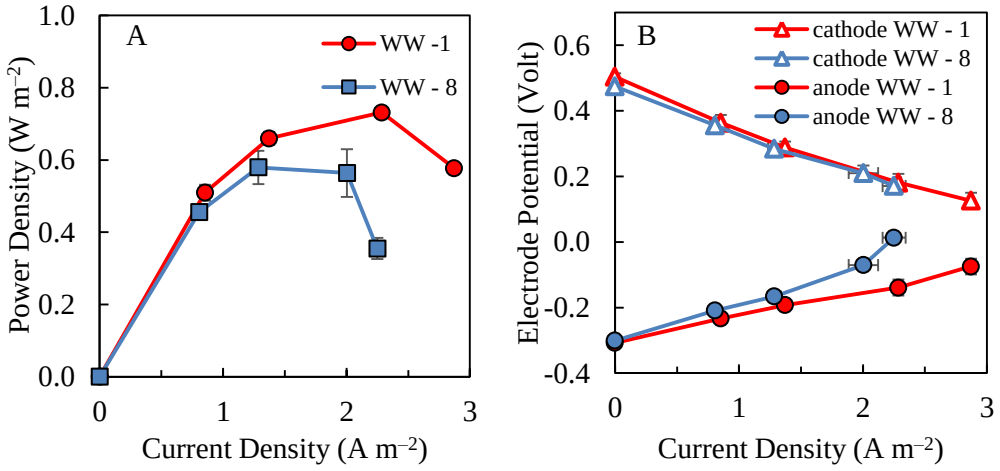

Fig. A.8. Comparison of (A) power density curves and (B) corresponding electrode potentials for MFCs using Fe–N–C/AC catalyst in wastewater in 1st and 8th week.

To further evaluate if phosphate salts in solution could affect the performance of the catalyst, MFCs were tested using wastewater amended with phosphate (50 mM

PB) (**Fig. A.7**). Adding salts to the wastewater increased the solution conductivity and consequently the power densities. The initial power density using wastewater with PBS was 1.18 ± 0.04 W m^{-2}. The power generation decreased to 0.91 ± 0.03 W m^{-2} at week 3 followed by increases to 1.15 ± 0.01 W m^{-2} in week 5. The last four weeks showed relatively stable values of the maximum power densities with a final value of 1.10 ± 0.04 W m^{-2} at week 8. The increases and decreases in maximum power densities generally followed the same trend as the changes conductivity of the solution. The variability of the wastewater parameters (**Fig. A.7B**) caused small changes in both the anode and the cathode potentials and affected the final power output (**Fig. A.9** and **Fig. A.10**).

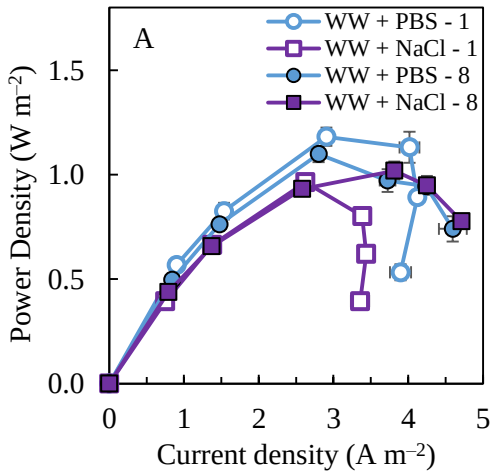

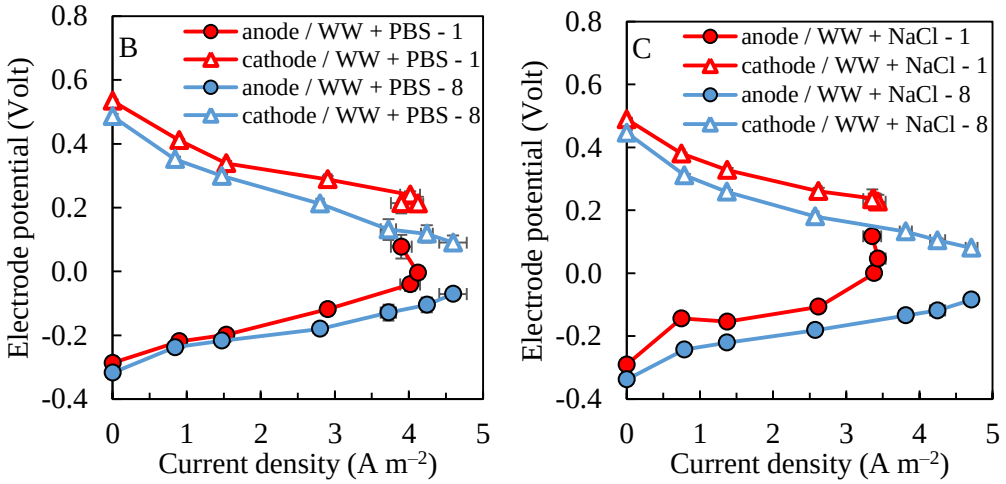

Fig. A.9. Comparison of power density curves (A) and corresponding electrode potentials (B, C) for MFCs using cathodes with Fe–N–C/AC catalyst in wastewater added with PBS and NaCl in 1st and 8th week.

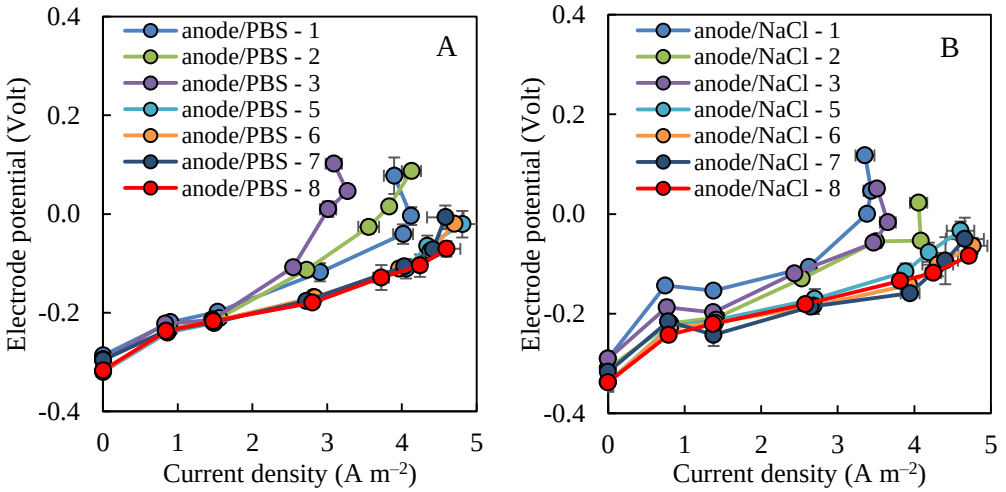

Fig. A.10. Anode potentials for MFCs using Fe-N-C/AC catalyst in (A) PBS and (B) NaCl during the eight weeks.

The control reactors with wastewater amended with NaCl showed the same behavior of the wastewater amended with PBS over time. The initial power generation was 0.96 ± 0.03 W m^{-2} with a decrease to 0.84 ± 0.03 W m^{-2} at week 3,

before increasing to 1.06 ± 0.04 W m^{-2} in the fifth week. In the last three weeks, the power density generated by the MFCs was stable and comparable with the values obtained with wastewater amended with PBS, with the maximum power density at week 8 of 1.02 ± 0.04 W m^{-2}. The anode and the cathode potentials of the controls reactors showed the same variability of the reactors with wastewater amended with PBS (**Fig. A.9** and **Fig. A.10**). The small decrease of the cathode potential after eight weeks could not be concluded to be due to deterioration of the catalyst due to the larger changes in power associated with changes in batches of wastewater. Thus, the addition of phosphate into the wastewater did not allow evaluation of the impact of the phosphate on power generation with the wastewater over time due to changes in COD, pH and conductivity.

Parallel experiments were conducted using wastewater amended with EDTA and Tween 80. At present, ethylenediaminetetraacetic acid (EDTA) is the cheapest and most suitable complexing compound for many technical purposes, and is used in large quantities as cleaning additive in the detergent industry. EDTA possess antimicrobial properties and could consequently affects the stability of the anode biofilm, however, in our view, could limit the deposition of salts on the solution side of the cathode in air–cathode MFCs. Tween 80 was evaluated as a chemical able to increase the current density of the MFCs affecting the anodic biofilm (Van Hamme et al., 2006, Singh et al., 2007). The main application of Tween 80 is in the food and cosmetic industry, the hydrophobic heads solubilize the hydrophobic chemicals dispersed in the matrix incorporating in micelles with the hydrophilic tales oriented toward the matrix. The addition of this chemicals to the MFC could potentially keep the cathode clean from the biomass deposition and consequently limit the fouling of the electrode (Pasternak et al., 2016)

The addition of Tween 80 to the wastewater did not cause any appreciable alteration to the maximum power output of the MFCs (**Fig. A.11**). The maximum power generated in the first week was 0.75 ± 0.01 W m^{-2}, comparable with that

obtained in the presence of raw wastewater (0.73 ± 0.01 W m^{-2}). The performance decrease during the second and third weeks to 0.63 W m^{-2} and 0.55 W m^{-2}. The performance of the MFCs in the presence of Tween 80 was then stable up to the seventh week (0.56 ± 0.02 W m^{-2}) showing small oscillations due to some changes in the wastewater parameters.

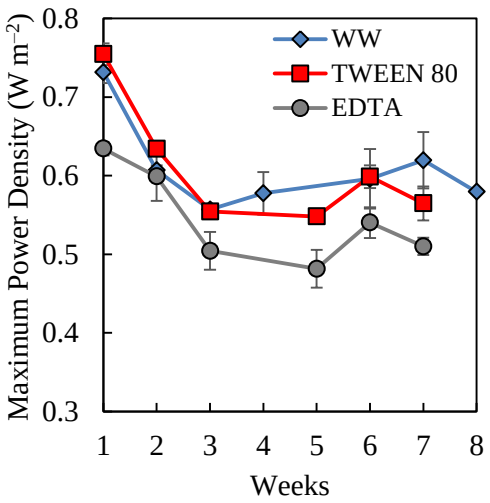

Fig. A.11. Maximum power production over time using Fe–N–C / AC catalyst in wastewater, wastewater amended with Tween 80 and EDTA.

Adding EDTA disodium salts to the wastewater caused a decrease in the maximum power produced by the MFCs over the entire length of the experiment. The power initially produced was 0.63 ± 0.01 W m^{-2}, 86% of the power registered with raw wastewater and decrease to 0.50 ± 0.02 W m^{-2} after three weeks, the performance was then stable and the final 0.51 ± 0.01 W m^{-2} was registered after seven weeks.

The anode and the cathode potentials of the MFCs under different operative conditions showed similar behavior (**Fig. A.12**). The cathode potentials were comparable both at the first and last week while the anode potential showed some variability related to the different wastewater composition. The presence of EDTA

in solution decrease the anode potential, in the first week this phenomenon was observed just at higher current density while in the week 7 the adverse effect of EDTA affected the anode potential also at low current density decreasing the anode potential at OCV from –0.30 ± 0.02 V obtained with raw wastewater to –0.23 V.

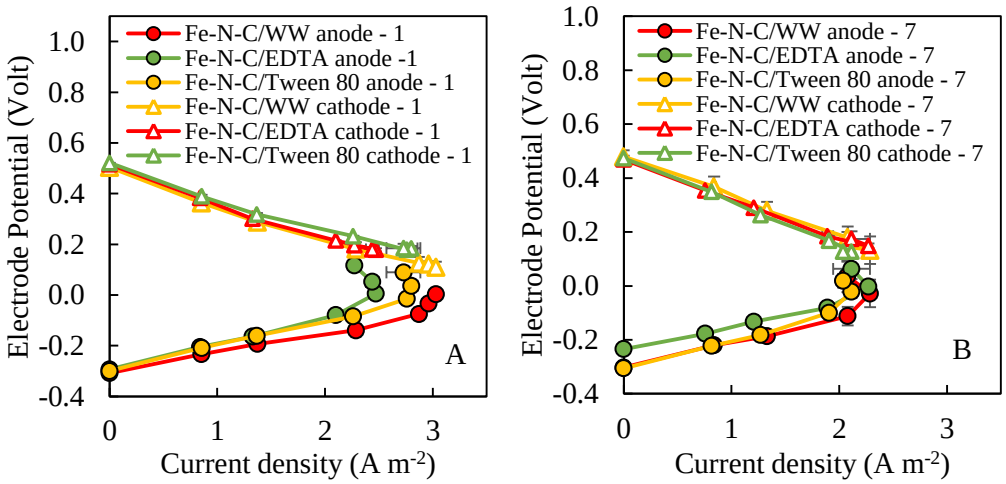

Fig. A.12. Comparison of (A) electrode potentials for MFCs fed with WW (wastewater), EDTA (wastewater amended with EDTA) or Tween 80 (wastewater amended with Tween 80) in 1st and 7th week.

As observed with the addition of phosphate, also with other amendments such as EDTA or Tween 80, our results did not permit an evaluation of the impact of these chemicals on power generation with the wastewater over time, mainly due to changes in COD, pH and conductivity.

Conclusions

Power densities generated using MOF catalyst cathodes and phosphate buffer decreased over time, but they were still 41% greater than plain AC after 8 weeks, consistent with a loss of iron from the framework. Power with wastewater also declined over time, but it remained higher than the plain AC and 53% higher than

maximum power densities previously reported for Pt catalysed cathodes. These results show that the performance of MFC AC cathodes can decrease over time, but because power remains higher than untreated AC cathodes, MOF treatment is useful for improving MFC power generation from solutions or wastewaters containing phosphate.

References

Cetinkaya, A.Y., Ozdemirb, O.K., Koroglua, E.O., Hasimogluc, A., Ozkayaa, B., 2015. The development of catalytic performance by coating Pt–Ni on CMI7000 membrane as a cathode of a microbial fuel cell. Bioresour. Technol., 195, 188–193.

Rozendal, R.A, Hamelers, H.M.V., Rabaey, K., Keller, J., Buisman, C.J.N., 2008. Towards practical implementation of bioelectrochemical wastewater treatment. Trends Biotechnol., 26, 450–459.

Li, D., Liu, J., Qu, Y., Wang, H., Feng, Y., 2016.Analysis of the effect of biofouling distribution on electricity output in microbial fuel cells. RSC Adv., 6, 27494–27500.

Zhang, X., Pant, D., Zhang, F., Liu, J., He, W., Logan, B.E., 2014. Long–term performance of chemically and physically modified activated carbons in air cathodes of microbial fuel cells. ChemElectroChem 1, 1859–1866.

Zhang, X., Shi, J., Liang, P., Wei, J., Huang, X., Zhang, C., Logan, B.E., 2013. Power generation by packed-bed air-cathode microbial fuel cells. Bioresour. Technol., 142, 109–114.

Pan, Y., Mo, X., Li, X., Pu, L., Liu, D., Yang, T., 2016. Iron–nitrogen–activated carbon as cathode catalyst to improve the power generation of single–chamber air–cathode microbial fuel cells. Bioresour. Technol., 206, 285–289.

Shi, X., Feng, Y., Wang, X., Lee, H., Liu, J., Qu, Y.,He W.,Kumar, S.M.S, Ren, N., 2012. Application of nitrogen–doped carbon powders as low–cost and durable cathodic catalyst to air–cathode microbial fuel cells. Bioresour. Technol., 108, 89–93.

Feng, L., Chen, Y., Chen, L., 2011. Easy–to–operate and low–temperature synthesis of gram–scale nitrogen–doped graphene and its application as cathode catalyst in microbial fuel cells. ACS Nano, 5, 9611–9618.

Bezerra, C.W., Zhang, L., Lee, K., Liu, H., Marques, A.L., Marques, E.P., Wang, H., Zhang, J., 2008. A review of Fe–N/C and Co–N/C catalysts for the oxygen reduction reaction. Electrochim. Acta, 53, 4937–4951.

Yang, W., Logan, B.E., 2016. Immobilization of a metal–nitrogen–carbon catalyst on activated carbon with enhanced cathode performance in microbial fuel cells. ChemSusChem, 9, 2226–2232.

Wen, Q., Kong, F., Ma, F., Ren, Y., Pan, Z., 2011. Improved performance of air-cathode microbial fuel cell through additional Tween 80. Journal of Power Sources 196, 899-904.

Zhang, F., Merrill, M.D., Tokash, J.C., Saito, T., Cheng, S., Hickner, M.A., Logan, B.E., 2011. Mesh optimization for microbial fuel cell cathodes constructed around stainless steel mesh current collectors. J. Power Sources, 196, 1097–1102.

Vargas, T.I., Albert, I.U., Regan J.M., 2013. Spatial distribution of bacterial communities on volumetric and planar anodes in single–chamber air–cathode microbial fuel cells. Biotechnol. Bioeng., 110, 3059–3062.

Logan, B.E., Cheng, S., Watson, V., Estadt, G., 2007. Graphite fiber brush anodes for increased power production in air–cathode microbial fuel cells. Environ. Sci. Technol., 41, 3341–3346.

Cheng, S., Xing, D., Call, D. F., Logan, B. E., 2009. Direct biological conversion of electrical current into methane by electromethanogenesis. Environ. Sci. Technol.,43, 3953–3958.

Nam, J.Y., Kim, H.W., Lim, K.H., Shin, H.S., Logan, B. E., 2010. Variation of power generation at different buffer types and conductivities in single chamber microbial fuel cells. Biosens. Bioelectron., 25, 1155–1159.

Yang, W., Kim, K.–Y., Logan, B. E, 2015. Development of carbon free diffusion layer for activated carbon air cathode of microbial fuel cells. Bioresour. Technol., 197, 318–322.

Watson, V.J., Nieto Delgado, C., Logan, B.E., 2013. Influence of chemical and physical properties of activated carbon powders on oxygen reduction and microbial fuel cell performance. Environ. Sci. Technol., 47, 6704–6710.

Sekar, N., Ramasamy, R.P., 2013. Electrochemical impedance spectroscopy for microbial fuel cell characterization. J. Microb. Biochem. Technol., S6, 1–14.

Winfield, J., Ieropolous, I., Greeman, J., Dennis, J., 2011. Investigating the effects of fluidic connection between microbial fuel cells. Bioprocess Biosyst. Eng., 34, 477–484.

Van Hamme, J.D., Singh, A., Ward, O.P., 2006. Physiological aspects – part 1 in a series of papers devoted to surfactants in microbiology and biotechnology. Biotechnol. Adv., 24(6), 604 – 620.

Singh, A., Van Hamme, J.D., Ward, O.P., 2007. Surfactants in microbiology and biotechnology: part 2. Application aspects. Biotechnol. Adv., 25(1), 99 – 121.

Pasternak, G., Greenman, J., Ieropoulos, I., 2016. Regeneration of the power performance of cathodes affected by biofouling. Applied energy, 173, 431–437.